

NASA Technical Memorandum 4004

**Operational Performance of
Vapor-Screen Systems for
In-Flight Visualization of
Leading-Edge Vortices on
the F-106B Aircraft**

**John E. Lamar, Philip W. Brown, Robert A. Bruce,
Joseph D. Pride, Jr., Ronald H. Smith,
and Thomas D. Johnson, Jr.**

SEPTEMBER 1987

NASA

Operational Performance of
Vapor-Screen Systems for
In-Flight Visualization of
Leading-Edge Vortices on
the F-106B Aircraft

John E. Lamar, Philip W. Brown, Robert A. Bruce,
Joseph D. Pride, Jr., and Ronald H. Smith

*Langley Research Center
Hampton, Virginia*

Thomas D. Johnson, Jr.

*PRC Kentron, Inc.
Hampton, Virginia*



National Aeronautics
and Space Administration

Scientific and Technical
Information Office

Abstract

A flight research program was undertaken at the NASA Langley Research Center to apply the vapor-screen technique, widely used in wind tunnels, to an aircraft. The purpose was to obtain qualitative and quantitative information about near-field vortex flows above the wings of fighter aircraft and ascertain the effects of Reynolds and Mach numbers over an angle-of-attack range.

The hardware for the systems required for flight application of the vapor-screen technique was successfully developed and integrated. Details of each system, its operational performance on the F-106B aircraft, and pertinent aircraft and environmental data collected are presented.

Introduction

Current and future military aircraft do and will use vortical flows to gain high- g maneuver performance, especially at transonic speeds. Though these configurations are backed up with much design effort and wind-tunnel testing, the airframe designer may not know whether the vortex system behaved in flight the same as in the design assumptions or in the wind-tunnel tests. Therefore, a need exists to actively observe the vortex system in terms of the core location and extent of the vortex as functions of Reynolds number and Mach number in order to further optimize a configuration.

The vapor-screen technique is a proven method to visualize the flow about models in wind tunnels for which the ambient light level is low. This technique is a logical choice for examining vortical flows in flight since only a thin cross section of the flow is illuminated; and furthermore, only three basic systems are involved: seeding, light-sheet generation, and image recording. Since a light sheet is used to illuminate the vortex flow, better contrast with ambient light occurs by flying at night. In order to record the resulting images, one can imagine using techniques employed by others, that is, a chase plane or ground-based photography. However, the first is not safe for high- g maneuvers, and the second is unacceptable from a logistical point of view, in particular, if the target was shielded by the wing. Hence, the visual recording equipment must be located on the vortex-generating aircraft.

In the late 1970's, the Soviets made a successful flight application of the vapor-screen technique where they used atmospheric water vapor for seeding, a ruby laser for the light-sheet generation, and a camera mounted to the aircraft to record the events (ref. 1).

At the start of the present work, such capability was not available in the United States, so hardware had to be developed. Because of the variety of maneuvers to be flown with this application of the vapor-screen technique, an initial constraint was imposed for the seeding to be weather independent. This disallowed total dependence on atmospheric water vapor and created the need for an onboard seeding system, which was satisfied by vaporizing propylene glycol. The other two systems are a mercury-arc lamp with appropriate optics for light-sheet generation and a low-light-level video camera with a video cassette recorder (VCR) for image recording. Each of these has an associated onboard control system and hardware.

Developmental testing was done on the individual systems alone and then together during a complete-integration test on a full-scale semispan F-106B model (half-airplane) in the Langley 30- by 60-Foot Tunnel, prior to flight. That test program and its results are discussed in reference 2.

In the present report, details of the flight project, including types of data taken, the various systems, and their operational performance, are given. Furthermore, selected flight records for the aircraft and environmental data are included. A summary of this work and of the scientific results obtained is given in reference 3.

Symbols and Abbreviations

AIS	aircraft instrumentation system
ASRB	Airworthiness and Safety Review Board
BL	butt line on aircraft, in. (see fig. 1)
d	distance along leading edge to probe tip from wing-fuselage juncture, in.
FS	fuselage station on aircraft, in. (see fig. 1)
g	load factor normal to longitudinal axis of aircraft
LCO ₂	liquid carbon dioxide
LE	leading edge
ℓ	reference wing chord, 23.75 ft
M	Mach number
O.D.	outside diameter
p	free-stream static pressure, lb/ft ²
P_1	CO ₂ tank pressure, 0 to 1000 lb/in ² absolute
P_3	line pressure, 0 to 200 lb/in ² absolute

R_n	Reynolds number, $1.232\rho M[(T + 216)/T^2]10^6$ (ref. 4, eq. (24))
r	perpendicular distance from leading edge to probe tip, in.
S_1	pump speed voltage, 0 to 30 VDC
s	distance from center of probe tip to wing surface, in.
T	absolute temperature, °R
TAS	true airspeed, ft/sec
TE	trailing edge
T_1	liquid CO ₂ temperature, 0 to 100°F
T_2	vaporizer temperature on pallet, 0 to 450°F
T_3	line temperature, 0 to 450°F
T_4	probe temperature, -300 to +450°F
VAC	volts alternating current
VDC	volts direct current
VCR	video cassette recorder
VHS	one video industry standard for tape formatting
WL	waterline on aircraft, in. (see fig. 1)
α	angle of attack, deg

Test Vehicle

The test vehicle is an F-106B aircraft. It is a Mach 2 two-place fighter interceptor that has a 60° delta planform with highly cambered leading edges. This amount of wing sweep was determined in reference 5 to be sufficiently high to develop leading-edge vortical flows. The F-106B uses trailing-edge elevons for control in lieu of a conventional aileron-elevator arrangement. A three-view sketch of the aircraft with pertinent dimensions is presented in figure 1. The particular aircraft chosen for this flight program has the number NASA 816.

Systems

Figure 2 shows the major systems and where they were positioned on the aircraft. Figure 3 identifies portions of the seeding and light-sheet generation systems, mounted on the missile bay pallet, and routes for the seeding tubes. (Details are given on NASA Langley drawing LE-317229.) Figure 4 contains corresponding photographs of all equipment mounted on the pallet.

Seeding Systems

Two seeding systems were designed and fabricated for this project. The one tested in flight used propylene glycol and the other employed liquid carbon dioxide to develop seeding particles. The primary difference between these two systems is that they function at opposite temperature extremes. Details of each follow.

Propylene Glycol

This seeding system consists of a supply tank, pump, vaporizer, heated hose, and unheated probe tips, along with associated aft-cockpit manual and automatic controls. Figure 5 shows a system schematic. The seeding material was produced by vaporizing propylene glycol, an inert fluid, as it flowed through the vaporizer unit. It was kept in vapor form by the heated hose until it exited the seeding probe tip.

Pump. The variable-speed pump moved liquid propylene glycol from a 3-gallon tank to the vaporizer. Flow rate was controlled from the rear cockpit via a rheostat with a range of 10 to 28 VDC. At 28 VDC the pump delivered 4.1 gallons per hour, and at a nominal operational setting of 18 VDC the pump delivered 2.8 gallons per hour to the vaporizer at a head pressure of 30 psi.

Vaporizer. The vaporizer assembly (see fig. 6) was developed at the Langley Research Center for this project. It is basically a 4-inch-diameter steel cylinder, 12-inches long, containing six cartridge heaters (in tubes) and three closely wound tubing coils all held together in a thermal mass. Each heater has a diameter of 0.625 inch, draws 1000 watts (3 phase, 115 volts, 400 hertz), and is the same length as the vaporizer assembly. The 0.25-inch-O.D. tubing coils surround the heaters and have their ends connected so that the fluid makes three complete passes through the vaporizer before making a final exit. This assembly was contained within an insulated box on the pallet. Internal temperature was set and maintained by an automatic temperature controller with a temperature sensor in the thermal mass. The maximum allowable value was 450 degrees Fahrenheit, as larger values would cause the glycol to start decomposing and could produce unwanted products.

Hose and probe tips. From the vaporizer (see fig. 4(a)), the glycol vapor passed through a rigid insulated tube on the pallet to a flexible insulated and heated hose that terminated at one of two external coupling junctures. Each juncture was part

of housing located beneath the left wing (fig. 7). The housing shielded the flexible hose outside the aircraft, and the coupling juncture provided a hard point to secure the uninsulated probe tip. The hose was 12 feet long and was contained within a 1.50-inch-diameter protective jacket. The vapor flowed through a 0.50-inch-O.D. pipe surrounded by heater elements (20 watts per foot), several layers of insulation, and then the protective jacket. The heater elements were set and controlled automatically by a separate temperature controller.

In order to determine the best position to introduce the vapor during the flight conditions of interest, a total of six probe-tip locations were utilized during the flight program. Positions 1 through 4 were associated with the aft housing and positions 5 and 6 with the forward housing. All were uninsulated, composed of 0.50-inch-O.D. tubing of various lengths, and contoured to position the probe tip near the wing leading edge. Figure 8 gives their placements both pictorially and numerically.

Carbon Dioxide

The CO₂ seeding system, also under development, was not ready during the flight-test period. This system, which uses liquid carbon dioxide (LCO₂), is shown schematically in figure 9. It had the capability to generate three different flow rates on a given flight by using different size orifices in each of the two entering tubes in the second Y-connector (Langley drawing LC-317211) in figure 9.

This system produces particles by two processes. As the LCO₂ expands through an orifice, it flashes into a mixture of cold gas and solid CO₂ particles. These solid particles emerge from the probe tip and provide reflection immediately at the probe exit. Mixing of the cold CO₂ gas with the atmosphere condenses water vapor to produce additional particles, as demonstrated in a preliminary ground test. At flight altitudes approximately 10 to 25 percent by weight of the CO₂ may be discharged as solid particles.

The same flexible hose used with the glycol system was to be used for transporting the products of LCO₂ expansion from the outlet of the Y-connector to the probe tip. Naturally, the heaters were not to be activated during the CO₂ operation.

Light-Sheet System

The fixed-position light-sheet system consisted of a 1-kilowatt transformer, a mercury-arc lamp, a slit-lens-mirror optical system, and a compressor to supply cooling air for the lamp. The light passed through an adjustable slit, a lens housing containing

a positive cylindrical lens, and a mirror to rotate the vertically oriented light sheet 90° (see fig. 10). The light sheet was projected at an angle of 11.2° forward of perpendicular to the aircraft longitudinal axis. At the intersection of the light sheet and the wing leading edge, the sheet had a vertical height of approximately 34 inches above the wing surface and widths of 1.50, 0.75, and 0.18 inch for slit widths of 0.041, 0.012, and 0.003 inch, respectively.

The compressor produced an insufficient flow of air, so a baffled air-scoop and dump system was incorporated into the protective shield to provide additional forced air cooling. This shield surrounded the light-sheet assembly in order that it carry no airload and be protected from the weather (see figs. 2 and 10).

Image Recording System

The images were recorded with a video system consisting of a miniature black-and-white camera, 5-inch monitor, and VHS formatted VCR. The camera used a 16-mm, f1.4, manual focus/manual iris lens, was located on the top of the fuselage (see fig. 2—just aft of the rear cockpit inside its own protective shield), and pointed aft and down onto the left wing panel. (Drawing number LD-315729 shows the camera orientation and its assembly in the windscreen. The centerline of the lens is at FS 289, BL 3, WL 44.) The monitor was located in the aft cockpit (fig. 11), whereas the VCR was in the instrument bay and there recorded audio, video, and time code signals from takeoff to landing.

Control and Display Systems

The flight-test pilot had a precision angle-of-attack system comprised of a boom-mounted alpha-vane, a control and display panel, and a heads-up display on the glare shield (fig. 12). The color-coded indexer lights in the heads-up display would indicate "off angle" with deviations of over $\pm 0.25^\circ$ from the preset angle of attack.

A flow-visualization control panel located on the left forward console in the rear cockpit contained most of the flow-visualization controls. It had six toggle switches as shown in figure 11: the switch for the air compressor interlocked with the mercury-arc lamp switch; two switches for the solenoid valves in the CO₂ system; one switch to energize both the vaporizer and the hose heater elements; and one switch to activate the glycol pump. The panel also contained two red lights to indicate power to the vaporizer and hose heaters and two blue lights to indicate CO₂ valve position. The instrument panel incorporated a 28-VDC meter that showed pump

voltage, the pump speed control rheostat, and the monitor. A remote VCR controller was located on the left canopy rail and fixed in a "record only" mode. The temperature at the end of the heated hose was displayed via a digital indicator which was positioned on a camera mount over the rear cockpit glare shield.

Safety Considerations

For a flight program to be conducted at the NASA Langley Research Center, there is an emphasis on safety, which is ensured by the local Airworthiness and Safety Review Board (ASRB). It may require that any new project successfully pass a maximum of four safety reviews (introductory, preliminary, design, and operational). These reviews are in addition to the Critical Design Review for the hardware and systems held by a duly authorized board. There were two types of issues raised by the ASRB: one dealt with the research hardware and the other with its impact on the aircraft flight characteristics.

Regarding hardware, the concerns were with the seeding and light-sheet systems, in particular, (1) whether the plumbing for the CO₂ system could rupture, (2) whether the CO₂ and propylene glycol seeding systems could be operated sequentially, and safely, on a given flight with only a switch to select one system or the other, and (3) whether the light system would interfere with the radio and navigational equipment. Each issue was resolved as follows: (1) through design, (2) by operating only one seeding system on a given flight, and (3) through shielding of the wire from the transformer to the light and ground-based verification testing on the aircraft.

Regarding the flight characteristics, the issue was whether the departure tendency of the airplane at high angles of attack would change detrimentally (that is, whether departure would occur at a lower angle of attack) because of mounting a seeding probe underneath the left wing. A flight investigation was required (supported by wind-tunnel data) prior to the start of the research program to address this issue. The result was that the probe had essentially no effect on the departure tendency of the aircraft. In fact, during the functional check flight with all the externally mounted research hardware in place (light sheet, video camera, and seeding probe), the only resultant changes detectable in the flight characteristics were slight changes in directional and lateral trim. Consequently, the ASRB determined that this project could be undertaken in a safe manner with proper attention to the details spelled out in both the ground and flight procedures.

Data

During each of the 14 flights, visual data were taken continuously. In addition, time-history recordings were made of the test (aircraft and environmental) parameters, as well as those associated with the vapor-screen systems, using the existing Aircraft Instrumentation System (AIS) available on the NASA 816 airplane. Portions of the data recorded on the AIS, deemed critical to the flight experiment, were telemetered to the ground station for monitoring. These included pitch and roll attitudes; angles of attack and sideslip; pitch, roll, and yaw rates; Central Air Data Computer Mach number and altitude; right and left elevon and rudder deflections; temperatures T_2 , T_3 , and T_4 ; pump speed voltage S_1 ; and pressure P_3 . The following sections discuss the manner in which the data were developed.

Aircrew Involvement

Regarding the video data recording, the Flight Test Engineer (FTE) had the monitor in his cockpit so that he could visually ascertain whether sufficient vapor was being produced to make the vortex system visible. Comments made by the crew to each other and to the ground were recorded on one of the VCR audio channels for later transcription and correlation with the other data. The pilot called out initial altitude, initial Mach number, and angle of attack as the test proceeded. The FTE noted the operation of the light, its cycling on and off due either to manual control or electrical fault, probe-tip and coupling-juncture temperature, pump voltage, and the characteristics of the vortex systems. Channel 2 of the VCR audio record contained Greenwich Mean Time for cross referencing with the AIS data.

Video

The left-hand portion of figure 13 shows the arrangement of the light sheet, camera, and seeding-probe tip on a plan-view sketch of the aircraft. (Note that the probe tips were all on the lower surface of the wing except for no. 4.) In the right-hand portion of this figure, the monitor image indicates the camera field of view. Toward the top is the wing trailing edge, intersecting the right side is the wing leading edge, and across the left corner is a portion of the fuselage. In the middle of the screen, parallel to the trailing edge, is a line depicting the light-sheet footprint. Note that it does not extend to the leading edge because of wing camber. The wing outline was not visible at night (except with afterburner on); nevertheless the vortex system could be seen above the wing upper surface since the concentrated vapor reflected the light provided by the sheet. Examples

of the video data are shown in figure 14 with the associated test conditions.

Immediately following each flight, the video tape was reviewed for content. This allowed for adjustments in the test parameters for the next flight.

Seeding System and Flight Parameters

The AIS measured and recorded the parameters for both seeding and flight. The seeding system was instrumented to monitor operations, as previously described, and to evaluate performance during post-flight analysis. Sketch A shows a schematic of various systems and the location of each parameter measured. The associated function and range of each is given in the symbol list. The measured flight parameters included Greenwich Mean Time, pitch and roll attitudes, normal, lateral, and longitudinal accelerations, angles of attack and sideslip, pitch, roll, and yaw rates, and Central Aircraft Data Computer values of altitude and Mach number.

System and flight parameters, in the form of time-coded strip charts, were available the next day. Two days were required to obtain initial computer-generated time-history plots. Final plots for 12 flight parameters are given in figures 15 to 42. These plots are graphed from data sets for the 28 flight segments of interest listed in table 1. These data, 2 points per second, were generated by averaging the measured data gathered at 80 samples per second over 40 consecutive samples.

For the various vapor-screen systems, the time histories over a flight are not presented herein because they were mostly constant throughout a serial; hence, their operational performance is only summarized near the end of the paper. However, table 2 has been prepared to highlight the significant variables and purpose of each flight.

Flight Program

The purpose of the flight program was to examine the effects of Reynolds and Mach numbers on vortex systems. To accomplish this, two kinds of maneuvers were flown: $1g$ decelerations at subsonic speeds and selected constant altitudes (R_n effects) and high- g transonic spiral descents (M effects).

Test Environment

Restricted airspace over the Chesapeake Bay, 65 n.mi. from the NASA Langley Research Center, was selected for the test. Flights were performed on winter nights when the moon was down and in Visual Flight Rules (VFR) conditions, though sometimes over a cloud layer. The test was supported by the ground station.

Procedures

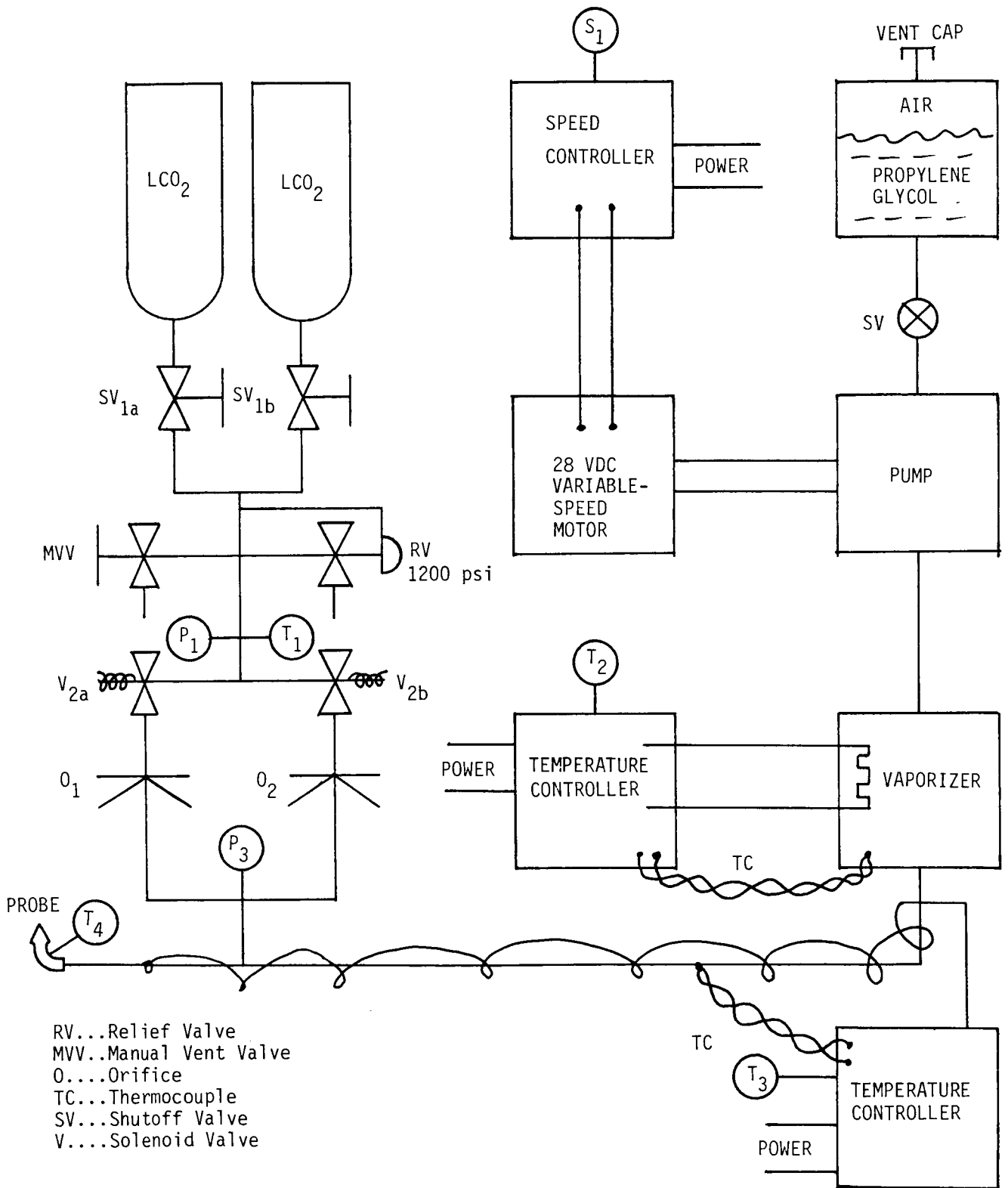
After engine start, the glycol system heaters and vaporizer were turned on and an operational system check was performed prior to taxiing. All recorders and the video system were turned on prior to takeoff. At an altitude of 2000 feet, the mercury-arc lamp and glycol pump were activated and the AIS and voice recorder deactivated. The voice recorder was turned on approaching the test area and the AIS was turned on during each run. The $1g$ decelerations were performed first so that airplane gross weight would not be a limiting factor during the high- g maneuvers. The fuel load normally allowed decelerations at five altitudes and two high- g descents. Prior to each run, the tapes were annotated with the pertinent data for later review and run verification. Commentary on observations was also recorded during each run. On departing the test area, all systems were turned off except for the voice recorder, video system, and air compressor.

Maneuvers

The $1g$ decelerations were performed in 5000-foot increments from 15 000 to 35 000 feet over angles of attack of 15° to 23° in 1° increments. Shallow descents were often required to perform these maneuvers because the thrust available at the military-power setting was insufficient for some high-altitude, high-angle-of-attack flight points. The afterburner was not used during these maneuvers because of its ineffectiveness at slow speeds and the high fuel consumption rate.

All high- g flight points were obtained using maximum afterburner thrust during spiral descents. These maneuvers had as their target test conditions either $M = 0.8$ ($\alpha = 19^\circ$) or $M = 0.9$ ($\alpha = 16^\circ$) and required a pitch attitude of -30° and a peak descent rate of about 25 000 feet per minute. These spiraling maneuvers were started at about 39 000 feet and were recovered by 23 000 feet. The intent was to maintain a nearly steady-state condition between 30 000 and 27 000 feet. Both left and right spirals were performed. The g levels during these maneuvers were normally between $4.5g$ and $5.5g$.

Precision of setting the Mach number and angle of attack was good for the $1g$ maneuvers. However, it was much more difficult to fly the high- g maneuvers, and the precision of setting and maintaining the test conditions was much lower. Once the near 90° bank angle and approximately -30° pitch attitude were established, it was possible to correct for an increasing or decreasing Mach trend only by controlling bank angle, since zero sideslip was needed and rudders could not be used to raise or lower the



Sketch A. Seeding system parameters and measurement locations.

nose. (An alternate way to more precisely control the Mach number may be to employ the speed brake incrementally, its position being displayed in the cockpit.)

Operational Performance

Seeding System

The operational characteristics for the propylene glycol seeding system are summarized as follows:

1. The vapor is clear as it leaves the vaporizer but condenses forming a white smoke upon exposure to air. The smoke persists far enough to be captured by the light sheet and even extends several airplane lengths behind the trailing edge. (See fig. 43.)
2. The vapor is of sufficient density to make the vortex system visible with the light sheet at night and at high angles of attack during daylight.
3. The seeding-probe tip works better on the lower surface about 7 to 8 inches inboard perpendicular to the leading edge, as shown in reference 3. (Fig. 8 gives the locations of the six probe tips in terms of distance perpendicular to the leading edge and along it from the wing-fuselage juncture.)
4. Moving the probe tip to a forward location gave the most vortex system detail for both the $1g$ level deceleration and high- g spiral descent. The best overall probe position was no. 6, and it was suggested from an unpublished water-tunnel study by Mr. John Del Frate of the NASA Dryden Flight Research Facility.
5. The best probe-tip location found on the half-airplane (see ref. 2) was near the no. 1 position for flight; that position produced the best vortex seeding results for the $1g$ decelerations.
6. Pump voltage of 20 volts worked best in flight, just as in the wind tunnel. It corresponds to a liquid flow rate of about 3 gallons per hour, and that was sufficient to generate continuous vapor for about 1 hour.
7. The propylene glycol vapor was maintained in a superheated condition in the insulated heated flexible hose from the pallet to the probe tip, so that the loss of vapor by condensation in the unheated coupling juncture and probe tip would not be significant.

Light-Sheet System

This system has been used extensively in wind tunnels, but its application to flight is new. The characteristics identified and the information learned

about the operation of this system are summarized as follows:

1. The mercury-arc light-sheet system can function at test altitudes while sustaining aircraft maneuver loads and vibrations. These conditions were well simulated by cold soak, reduced pressures, and multiaxis vibration testing on the ground.
2. The light-sheet system did not overheat with the combination of cooling ram air and pumped air.
3. The light-sheet intensity is greatest when the system is first switched on.
4. Slit widths of 0.041 and 0.012 inch produced light sheets of sufficient widths for vortex system visualization. In addition, these widths produced light-sheet thicknesses of approximately 1.50 and 0.75 inch, respectively, at the leading edge. In comparison to typical wind-tunnel light-sheet thicknesses, which vary from 0.50 to 1.00 inch (see ref. 6), the flight values are, relatively, at least an order of magnitude thinner because of the size difference between models and aircraft.
5. An optically uncentered slit width of 0.003 inch was insufficient to perform the visualization function. However, an optically centered slit of this width may yet prove to be acceptable.
6. The light-sheet system cycled off and on by itself (typically 5 to 10 seconds/cycle), indicating the presence of an intermittent electrical circuit fault. Attempts to identify the source of the fault were unsuccessful.
7. No radio or navigational system interference was noted on the aircraft due to operating the light-sheet system.

Video System

Features of the video system include the following:

1. The camera functioned well at night and also in daylight when a "neutral density" filter was put behind the lens.
2. The forward placement of the camera and its orientation with respect to the light sheet captured the vortex system details. This camera light-source arrangement is similar to that of reference 1, where a film camera and a laser light sheet were used in flight.
3. The camera was well matched to the frequency of visible light produced by the mercury-arc lamp.
4. The monitor in the aft cockpit did not always yield indications of the vortex in daylight, primarily because of insufficient color contrast between the wing and smoke under ambient light.

5. The VCR worked well during the high-*g* maneuver. The most noticeable degradation was in the crew audio channel, which may be due to the video tape losing good contact with the recording heads.
6. Recording of the vortex system details worked well even with some reflection off the unpainted aluminum wing upper surface. Painting the wing surface flat black may have resulted in an improvement in the recordings. It is, therefore, recommended that this be done for future vapor-screen flight projects.

Flow-Visualization Cockpit Controls

In general, the cockpit controls for the various systems functioned as designed. The only recommended change would be to relocate the power switch for the light sheet on the control panel, since cycling the switch required that the arm be in physical contact with the throttle during afterburner operation. (The afterburner was needed for the high-*g* transonic maneuver.)

Concluding Remarks

The flight hardware necessary to apply the vapor-screen technique, long used in wind tunnels for flow visualization, has been successfully developed and implemented on the F-106B aircraft. With this hardware it was possible to observe the vortex system

features under a variety of test conditions, including transonic high-*g* maneuvers.

References

1. Burdin, I. Yu.; Zhirnov, A. V.; Kulesh, V. P.; Orlov, A. A.; Pesetskiy, V. A.; and Fonov, S. D. (Foreign Technol. Div., Wright-Patterson Air Force Base, transl.): *Use of Laser Methods for the Study of Detached Flows in a Wind Tunnel and in Flight*. FTD-ID(RS)T-1053-82, U.S. Air Force, Oct. 20, 1982, pp. 2-19. (Available from DTIC as AD B069 459.)
2. Lamar, John E.: In-Flight and Wind Tunnel Leading-Edge Vortex Study on the F-106B Airplane. *Vortex Flow Aerodynamics, Volume I*, James F. Campbell, Russell F. Osborn, and Jerome T. Foughner, Jr., eds., NASA CP-2416, 1986, pp. 187-201.
3. Lamar, J. E.; Bruce, R. A.; Pride, J. D., Jr.; Smith, R. H.; Brown, P. W.; and Johnson, T. D., Jr.: In-Flight Flow Visualization of F-106B Leading-Edge Vortex Using the Vapor-Screen Technique. AIAA-86-9785, Apr. 1986.
4. Aiken, William S., Jr.: *Standard Nomenclature for Airspeeds With Tables and Charts for Use in Calculation of Airspeed*. NACA Rep. 837, 1946. (Supersedes NACA TN 1120.)
5. Chamberlin, Roger: *Flight Investigation of 24° Boat-tail Nozzle Drag at Varying Subsonic Flight Conditions*. NASA TM X-2626, 1972.
6. Snow, Walter L.; and Morris, Odell A.: *Investigation of Light Source and Scattering Medium Related to Vapor-Screen Flow Visualization in a Supersonic Wind Tunnel*. NASA TM-86290, 1984.

Table 1. Flight Summary

Flight/serial	Maneuver (<i>a</i>)	Altitude, 10 ³ ft	Time interval, Greenwich Mean Time	Mach number	Figure
85-007/06	1 <i>g</i>	25	23:26:32-23:28:42	0.4	15
07	1 <i>g</i>	35	23:35:22-23:37:17	.5	16
08	1 <i>g</i>	30	23:42:13-23:46:25	.5	17
10	High- <i>g</i> LS	30-23	23:52:06-23:52:57	.7	18
85-009/04	1 <i>g</i>	35	00:07:26-00:09:53	.5	19
05	1 <i>g</i>	30	00:12:39-00:14:00	.4	20
06a	1 <i>g</i>	25	00:15:41-00:17:15	.4	21
06b	1 <i>g</i>	20	00:19:25-00:21:26	.4	22
07	1 <i>g</i>	15	00:24:21-00:26:11	.3	23
09	1 <i>g</i>	25	00:29:41-00:30:51	.4	24
10	High- <i>g</i> LS	30-24	00:35:15-00:35:29	.8	25
11	High- <i>g</i> RS	35-25	00:39:50-00:40:24	.8	26
85-010/04	1 <i>g</i>	35	00:27:37-00:29:31	.5	27
05	1 <i>g</i>	30	00:32:06-00:33:56	.4	28
06	1 <i>g</i>	25	00:36:59-00:38:41	.4	29
07	1 <i>g</i>	20	00:40:21-00:41:57	.3	30
08	High- <i>g</i> LS	37-20	00:50:03-00:50:40	.8	31
85-011/03	1 <i>g</i>	35	00:45:08-00:46:50	.5	32
04	1 <i>g</i>	30	00:49:04-00:50:51	.4	33
05	1 <i>g</i>	25	00:52:43-00:55:33	.4	34
06	1 <i>g</i>	20	00:58:04-00:59:47	.3	35
08	High- <i>g</i> LS	40-20	01:10:15-01:11:20	.8	36
09	High- <i>g</i> RS	35-21	01:16:30-01:17:02	.7	37
85-012/04	1 <i>g</i>	35	00:31:12-00:36:00	.5	38
05	1 <i>g</i>	30	00:38:55-00:40:36	.4	39
06	1 <i>g</i>	25	00:42:27-00:44:46	.4	40
07	1 <i>g</i>	20	00:47:27-00:49:17	.3	41
09	High- <i>g</i> LS	39-22	01:04:02-01:04:41	.8	42

^aLS = Left spiral; RS = Right spiral.

Table 2. Significant Vapor-Screen Parameters and Flight Purpose

Flight	Time	Probe-tip position	Slit width, inches	Purpose of flight
85-001	Day	1	0.041	Functional check flight (FCF)
85-002	Day	1	.041	Complete FCF and instrument CF
85-003	Day	2	.041	Photo chase/check vapor in vortex
85-004	Day	3	.041	Check vapor location
85-005	Night	3	.041	Check vapor entrainment in vortex
85-006	Night	4	.041	Check vapor entrainment in vortex
85-007	Night	4	.041	See effect of cycling light
85-008	Night	4	.041	Complete flight 85-007
85-009	Night	1	.041	Check vapor entrainment in vortex
85-010	Night	5	.041	Check vapor entrainment in vortex
85-011	Night	6	.041	Check vapor entrainment in vortex
85-012	Night	6	.012	See effect of thinner light sheet
85-013	Day	6	.003	Parameter identification
85-014	Night	6	.003	See effect of thinner light sheet

Wing reference area 697.83 ft²

Wing reference chord 23.75 ft

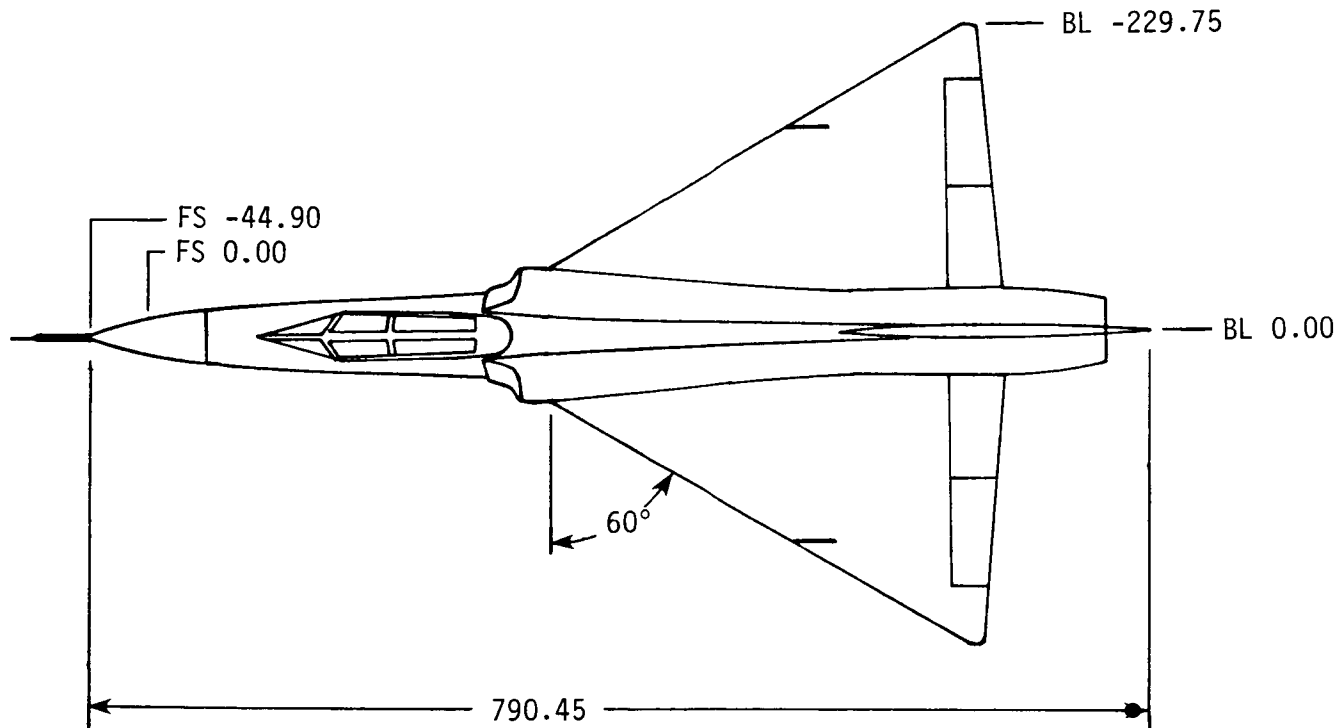
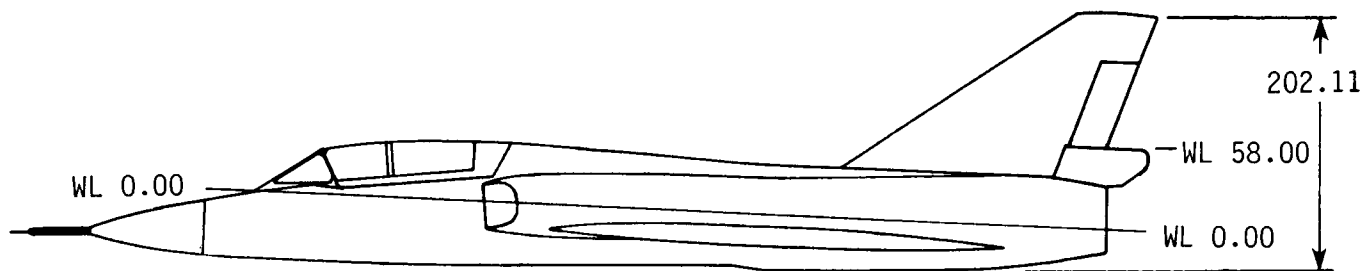
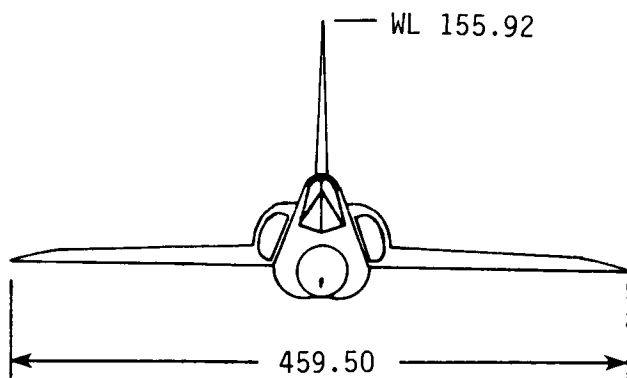
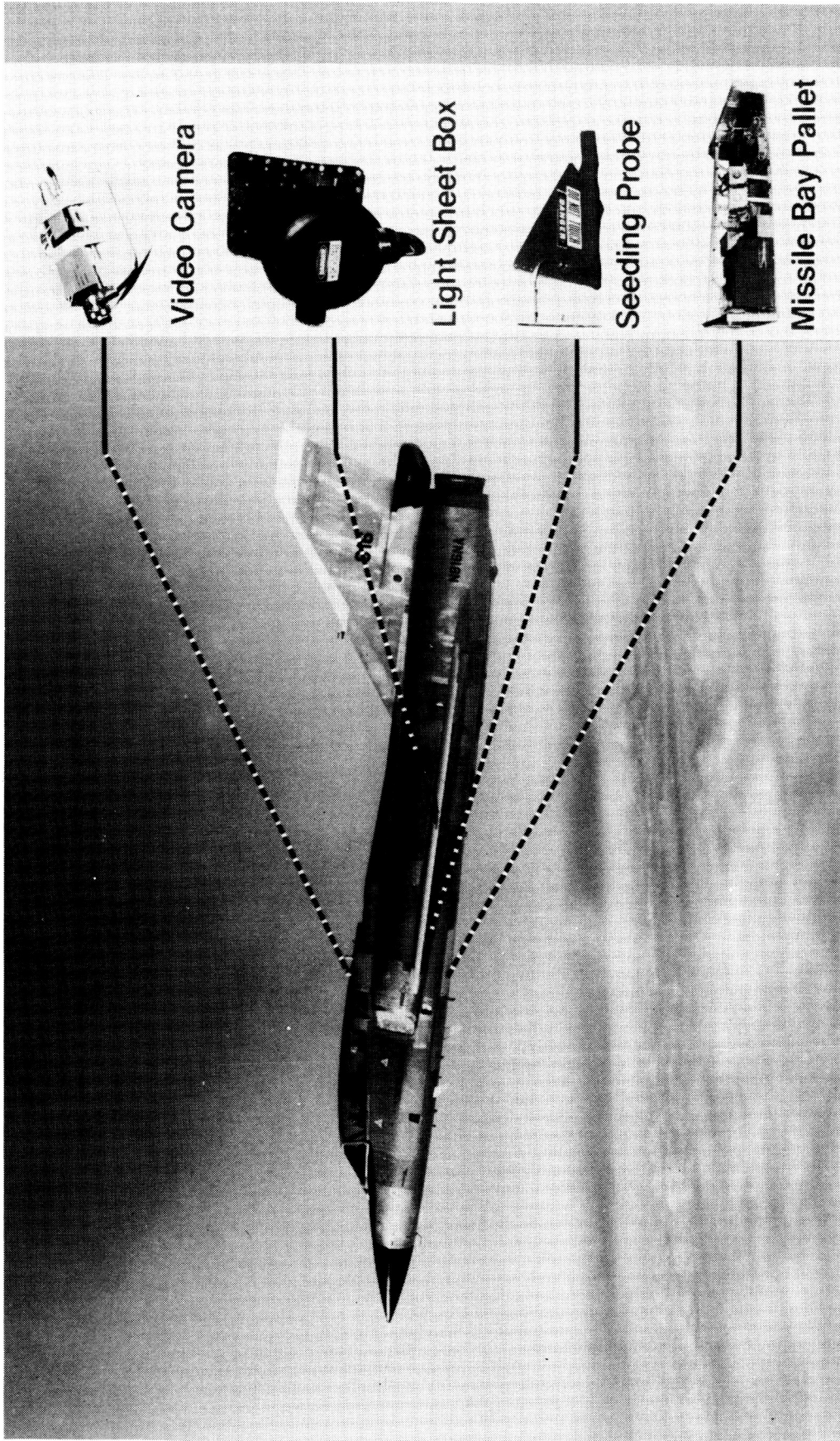


Figure 1. Three-view sketch of the F-106B aircraft. Dimensions are in inches.



L-87-6582

Figure 2. F-106 flow-visualization elements.

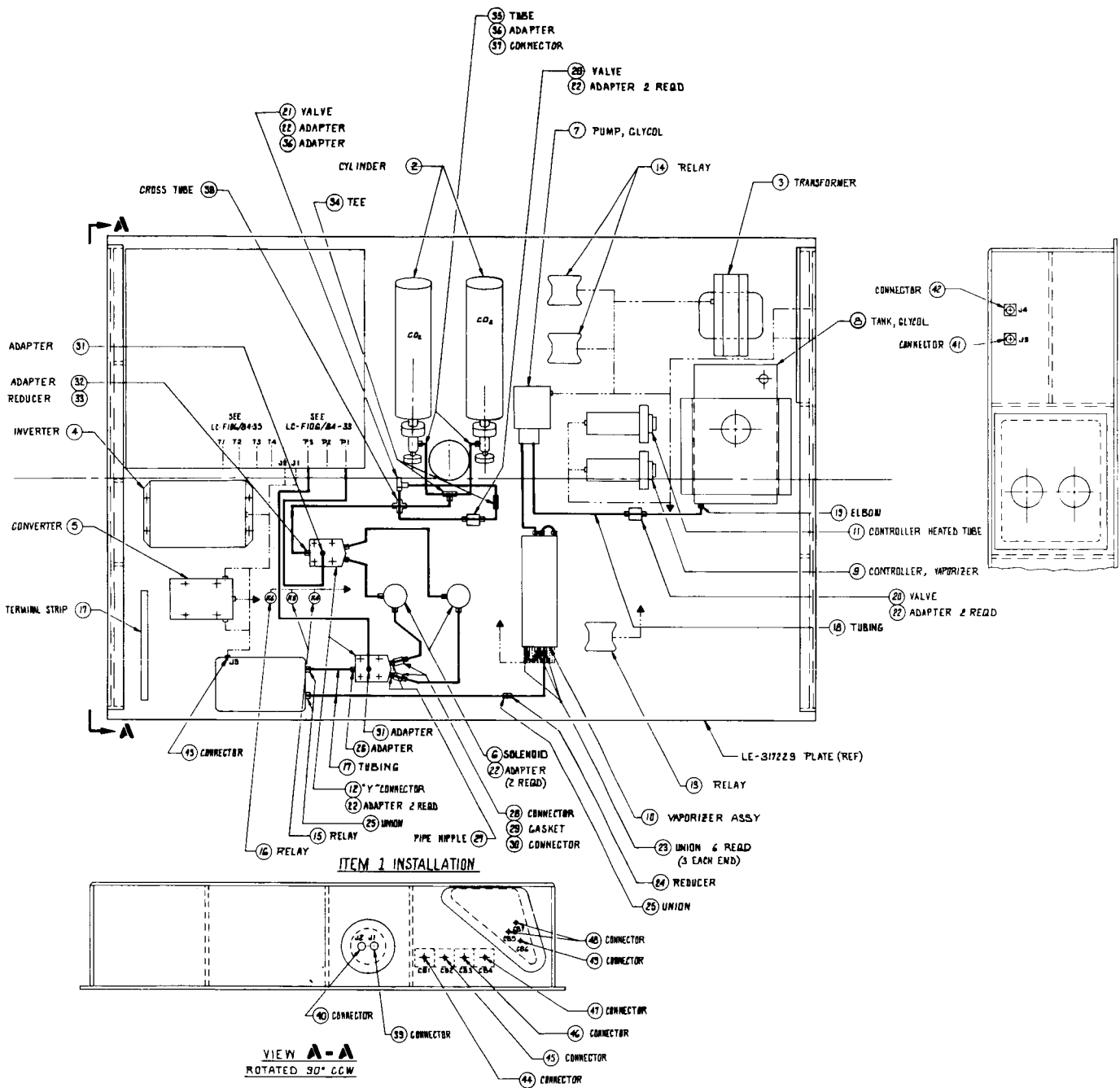
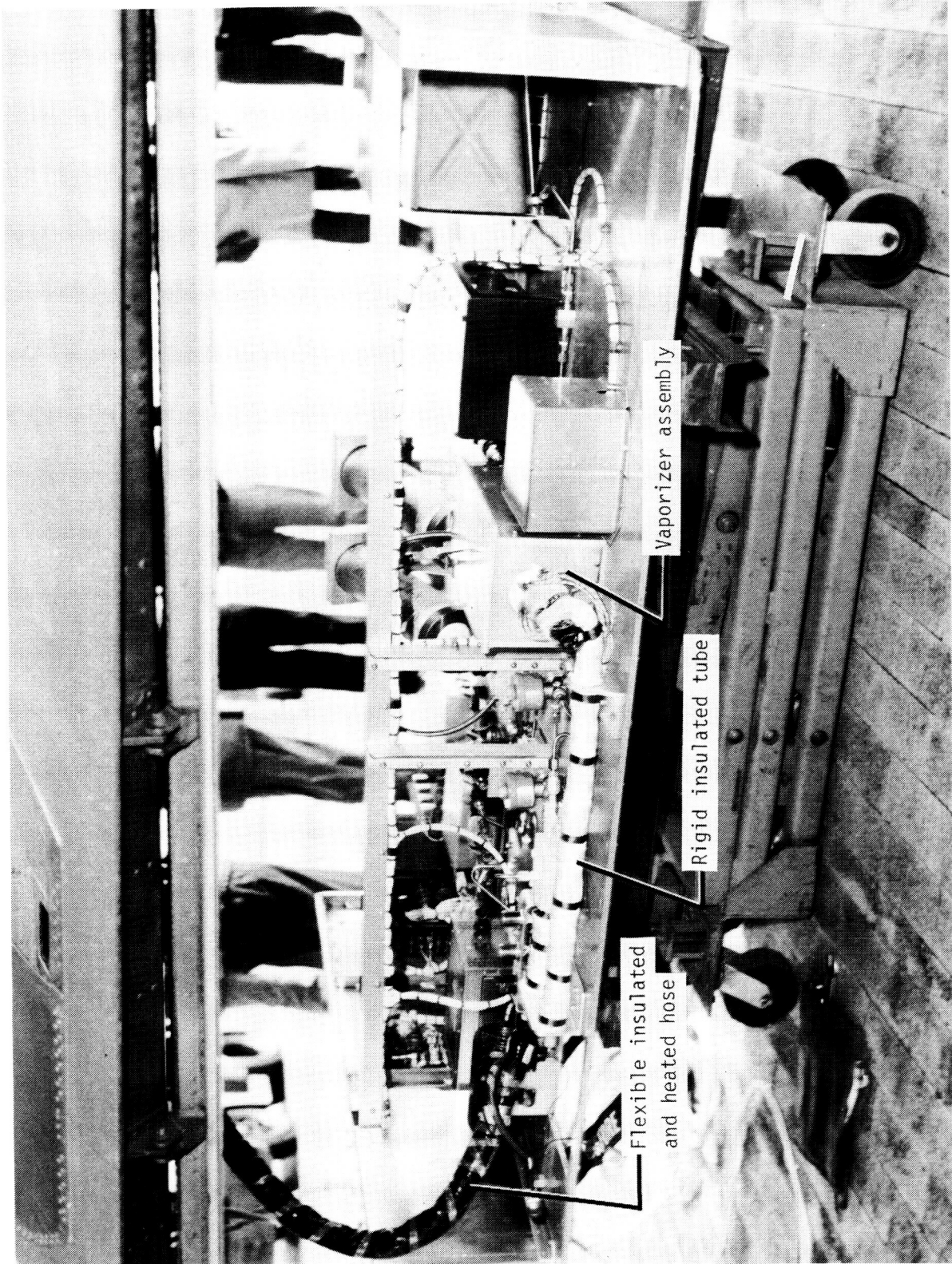


Figure 3. Schematic of the seeding and light-sheet generation systems and routes of seeding tubes. (From Langley drawing LE-317230.)

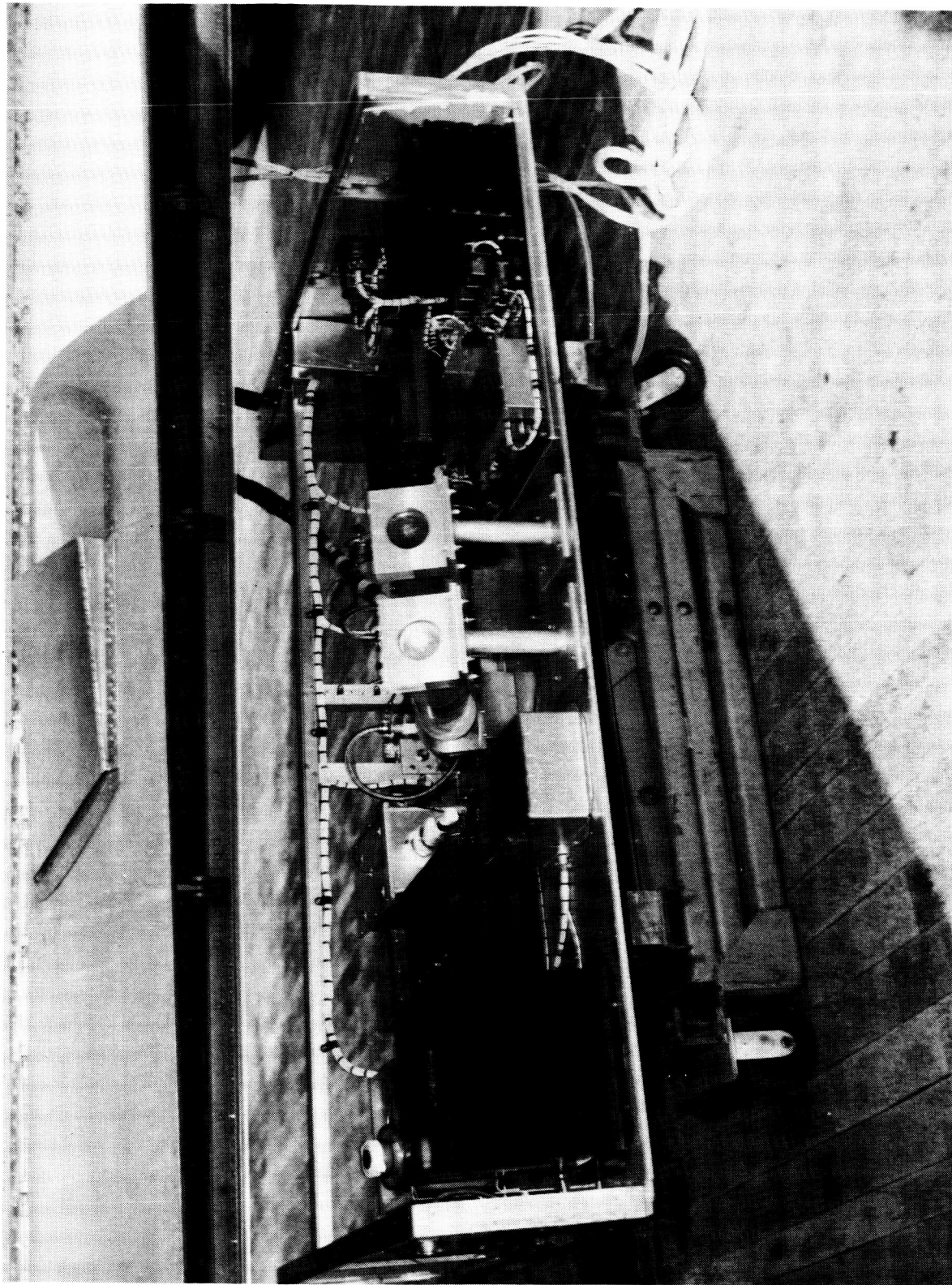


L-85-1236

(a) Left side.

Figure 4. Seeding and light-sheet generation systems on missile bay pallet.

ORIGINAL PAGE IS
OF POOR QUALITY



L-85-1238

(b) Right side.

Figure 4. Concluded.

T₂ - VAPORIZER TEMPERATURE
 V₁ - MANUAL LIQUID SHUT OFF VALVE

- NOTE: WORKING PRESSURE IS 10-25 PSI
- 2) MAXIMUM PRESSURE IS 30 PSI
- 3) HYDROSTATIC PROOF TEST TO 45 PSI
- 4) ALL TUBING IS TO BE 1/4" CLASS 947 CRES (035MM) ALL FITTINGS TO BE EITHER TRIPLE-LOK OR FERULOK-BITE TYPE.

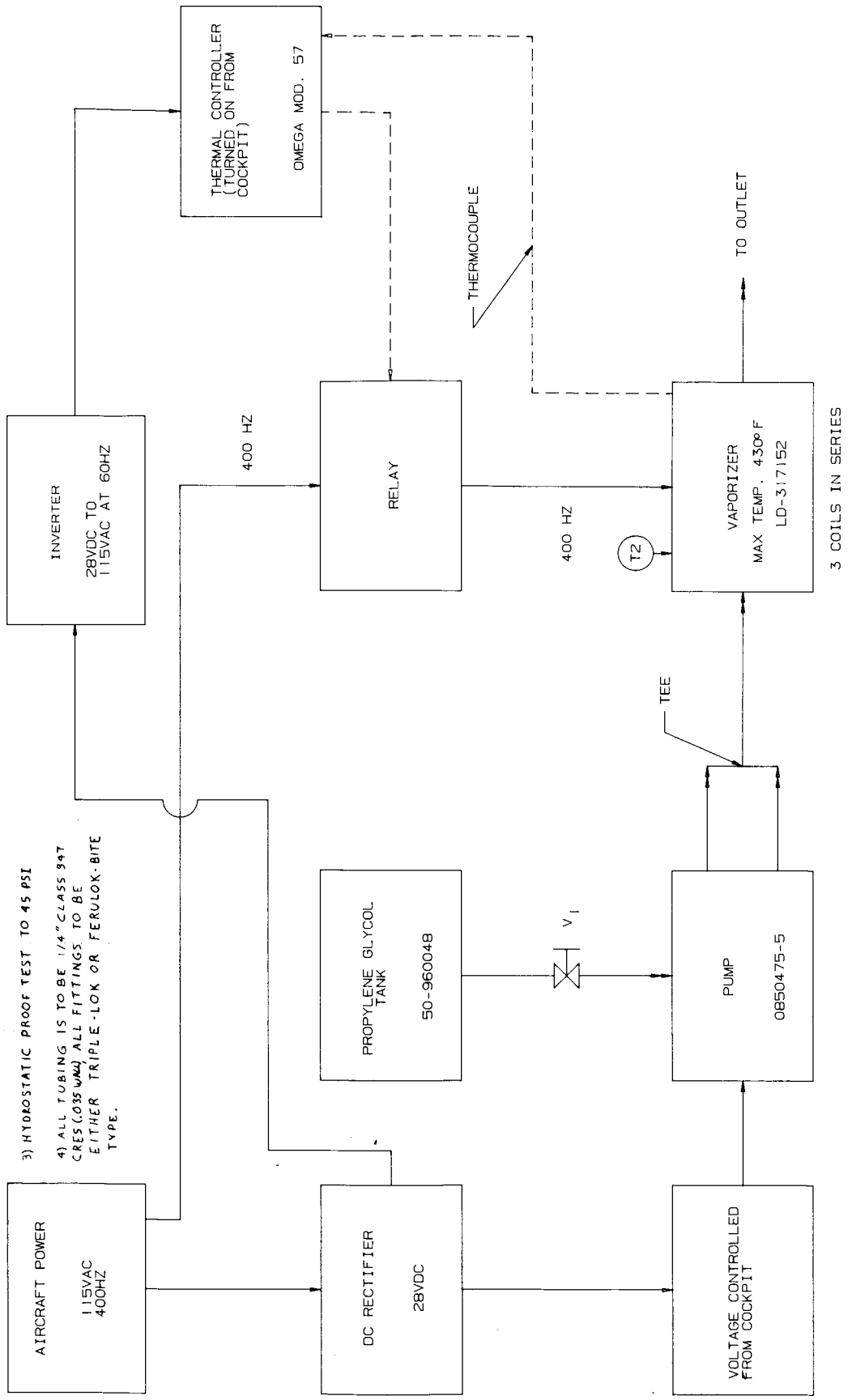


Figure 5. Schematic of the propylene glycol seeding system. (Langley drawing LC-317160.)

ORIGINAL PAGE IS
OF POOR QUALITY

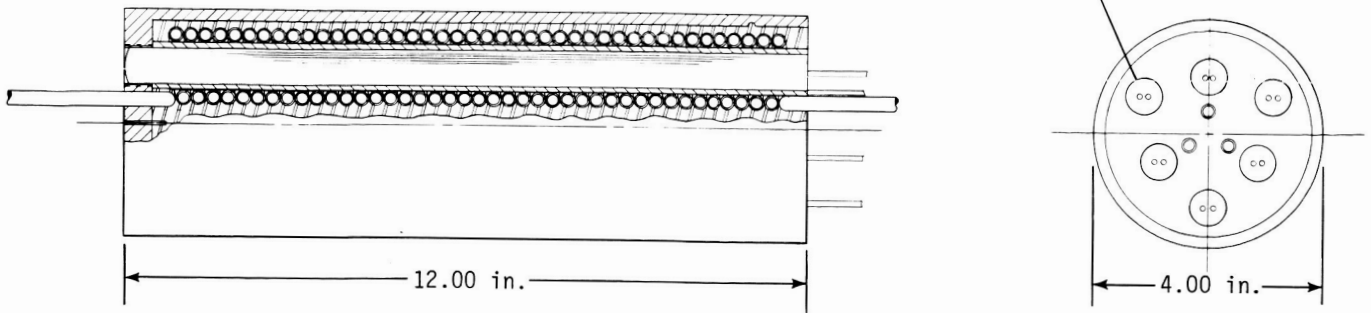


Figure 6. Assembly drawing of the vaporizer. (From Langley drawing LD-317152B.)



L-87-586

Figure 7. Composite photograph showing the fore and aft external housings.

No.	d, in.	r, in.	s, in.
1	52-5/8	8-1/2	13/16
2	52-5/16	6-3/8	1-1/16
3	54-1/2	3/8	3/8
4*	56-1/2	7-1/2	1-3/8
5	28	2-1/4	1-1/16
6	34-15/16	6-9/16	5/16

s = distance from center of probe to wing surface.

* Probe was angled up 17°

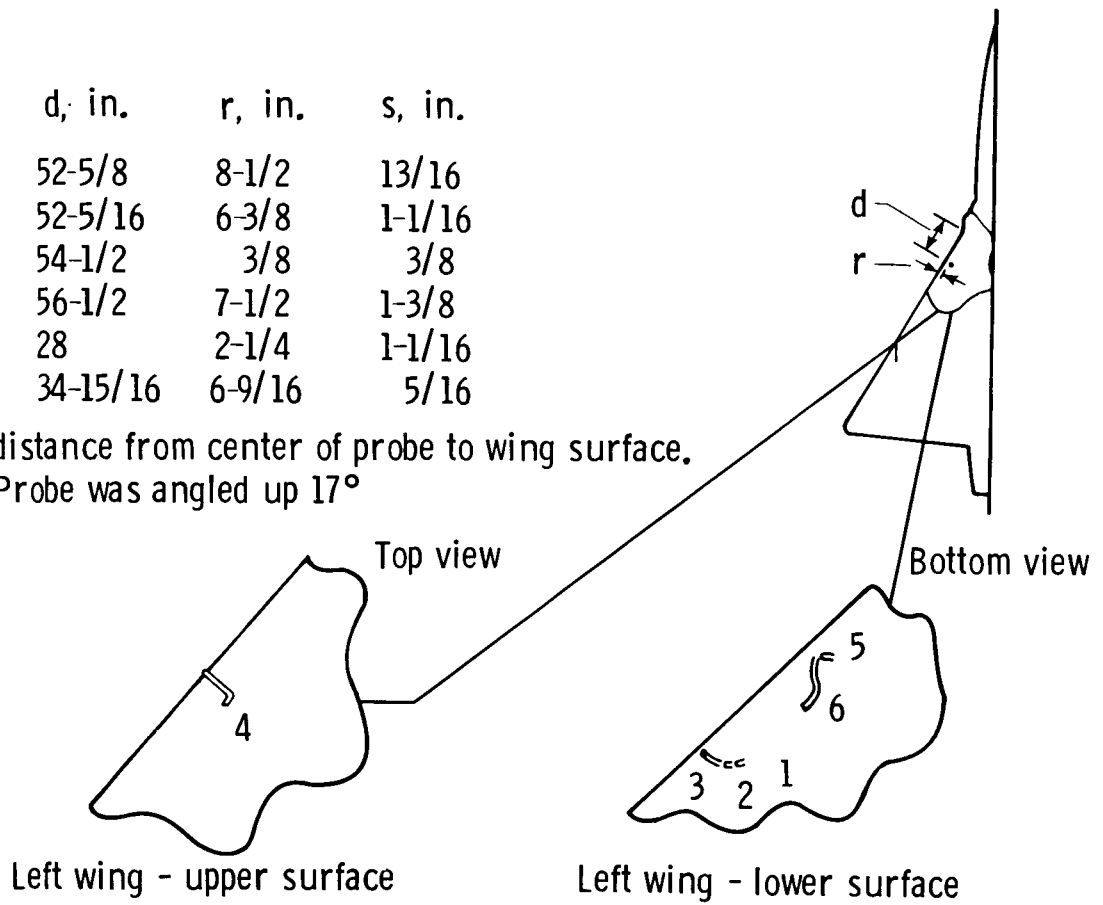
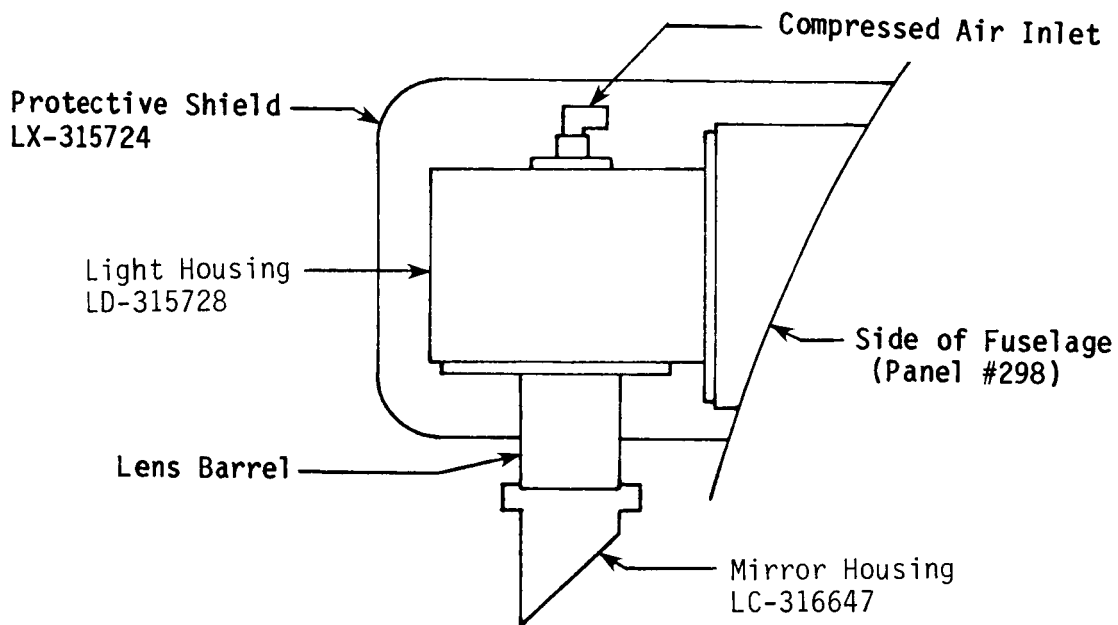
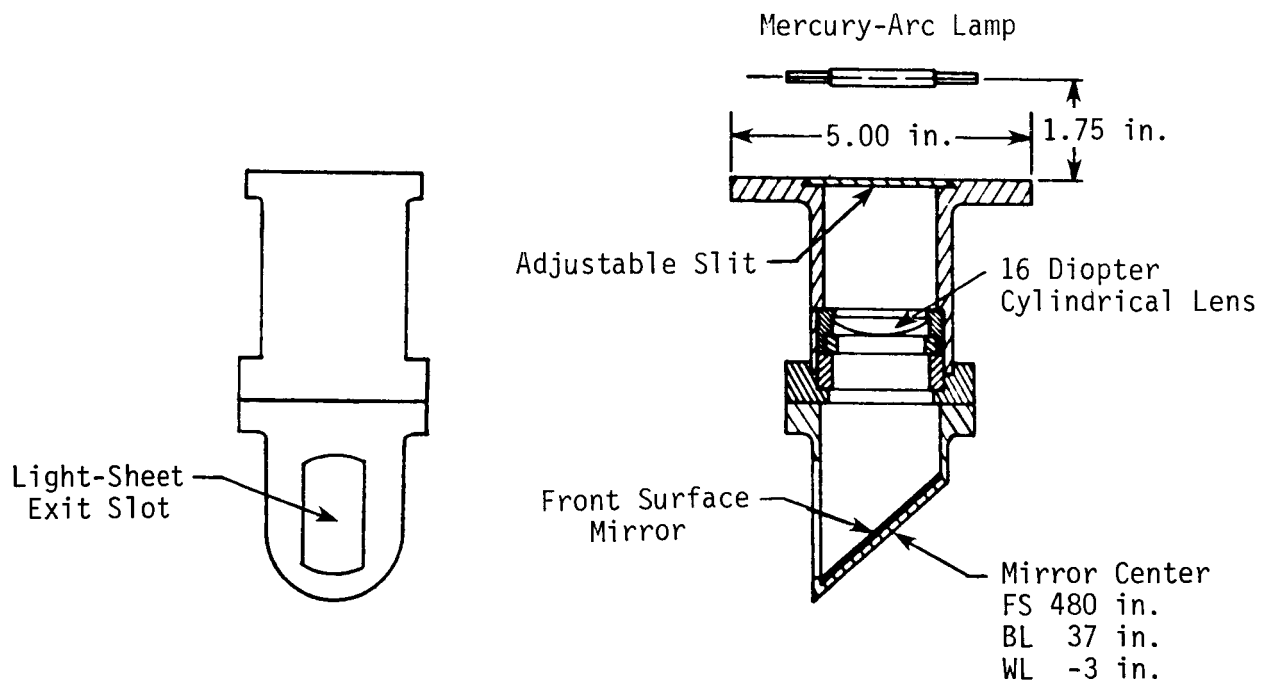


Figure 8. Seeding system probe-tip positions.

**Light Assembly
LX-317168**

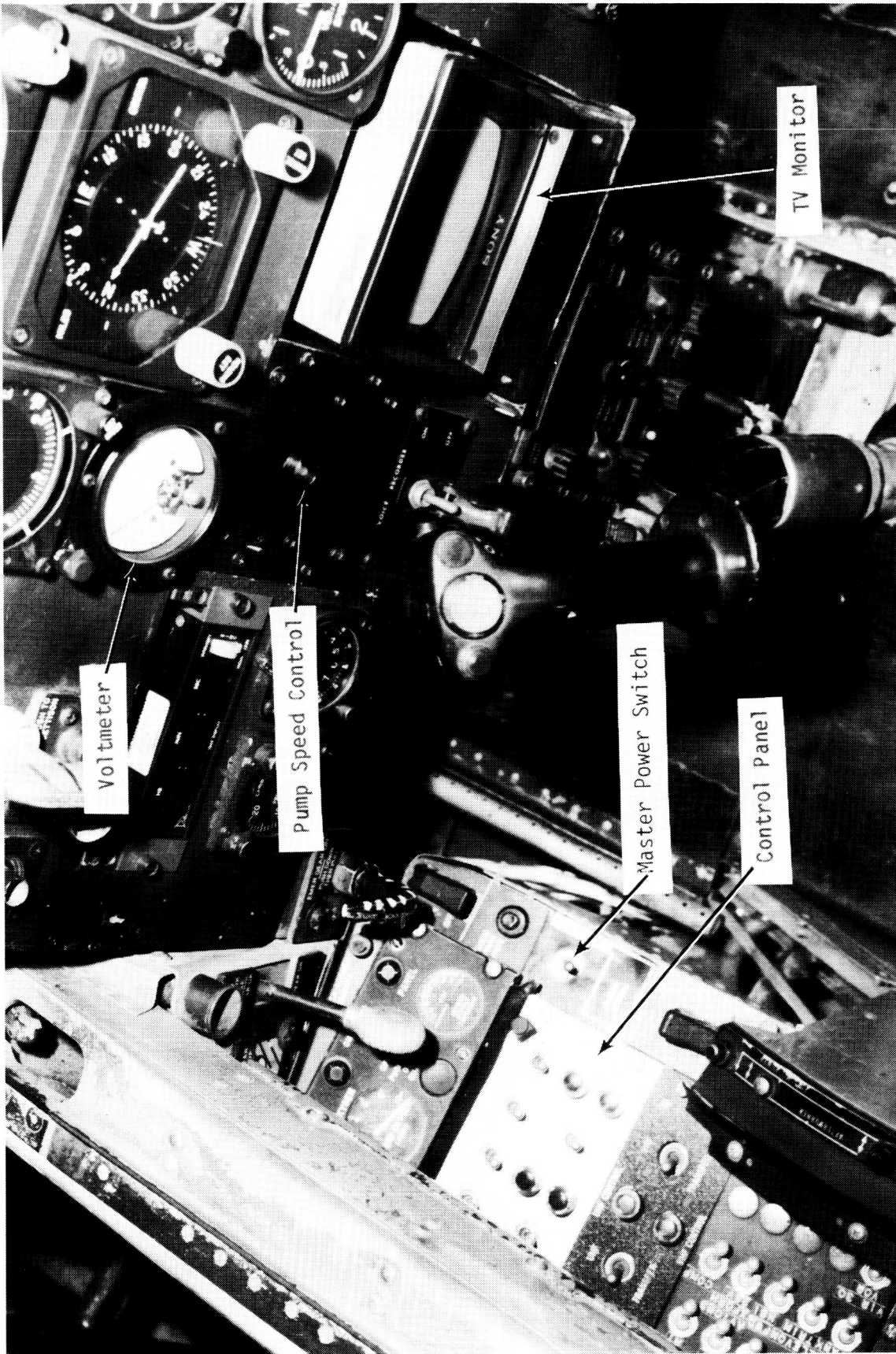


(a) Forward looking view.



(b) Slit-lens-mirror assembly.

Figure 10. Sketches of mercury-arc lamp assembly.



L-85-1333

Figure 11. F-106B rear cockpit layout of components of the flow-visualization control and monitoring equipment.



L-85-1335

Figure 12. Components of precision angle-of-attack system mounted in front cockpit.

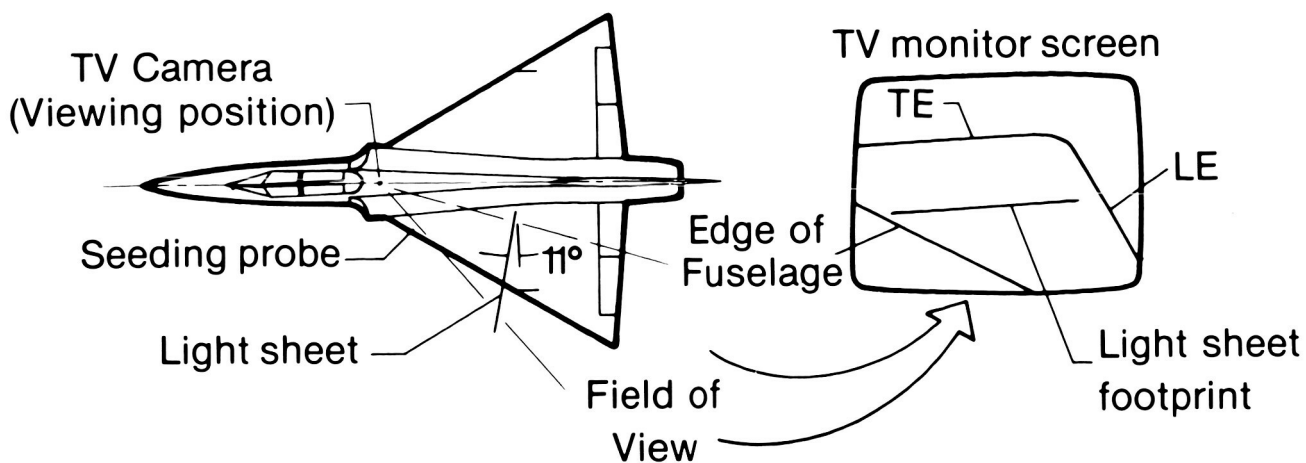


Figure 13. Layout of the flow-visualization system and the camera perspective.

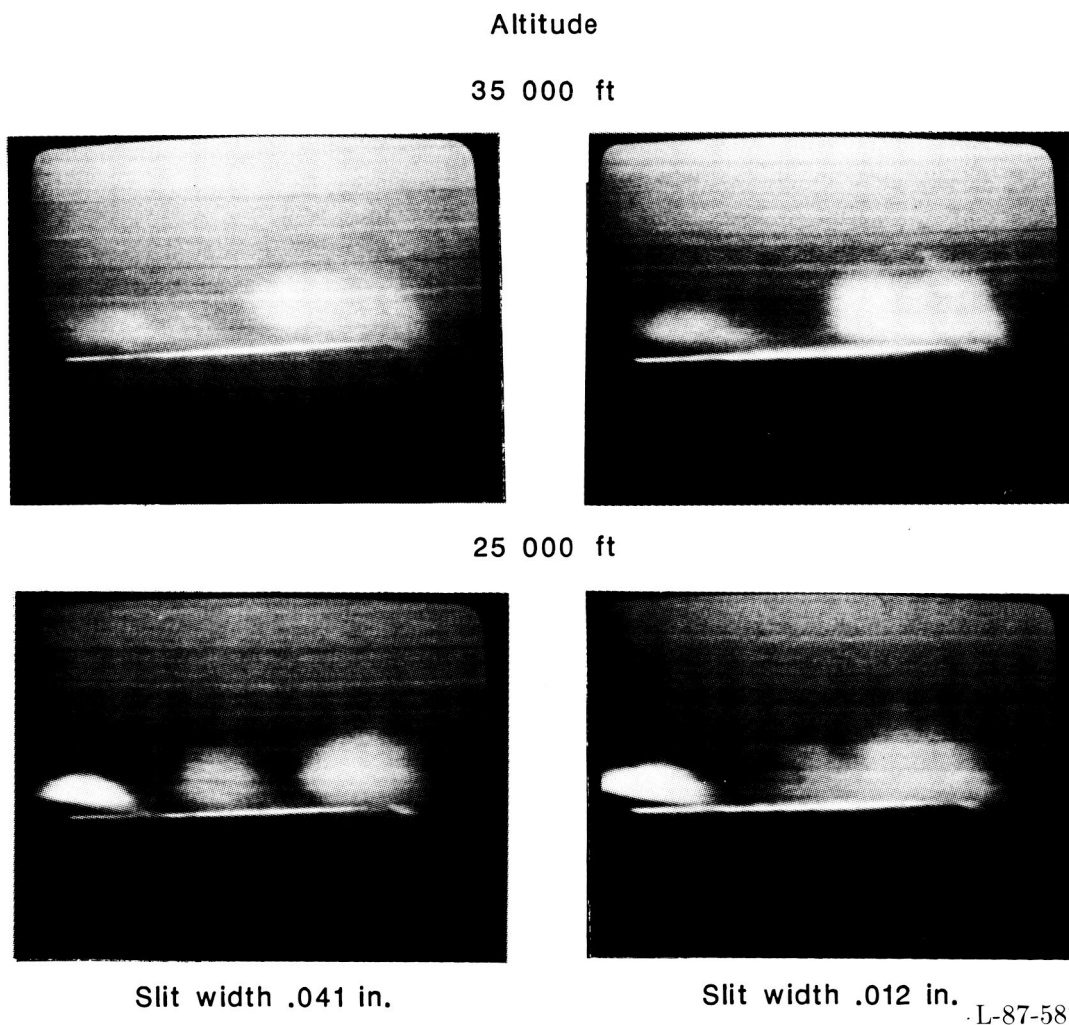


Figure 14. Vortex system details at two slit widths. 1g maneuver; $M \approx 0.4$; probe tip 6; $\alpha \approx 18^\circ$.

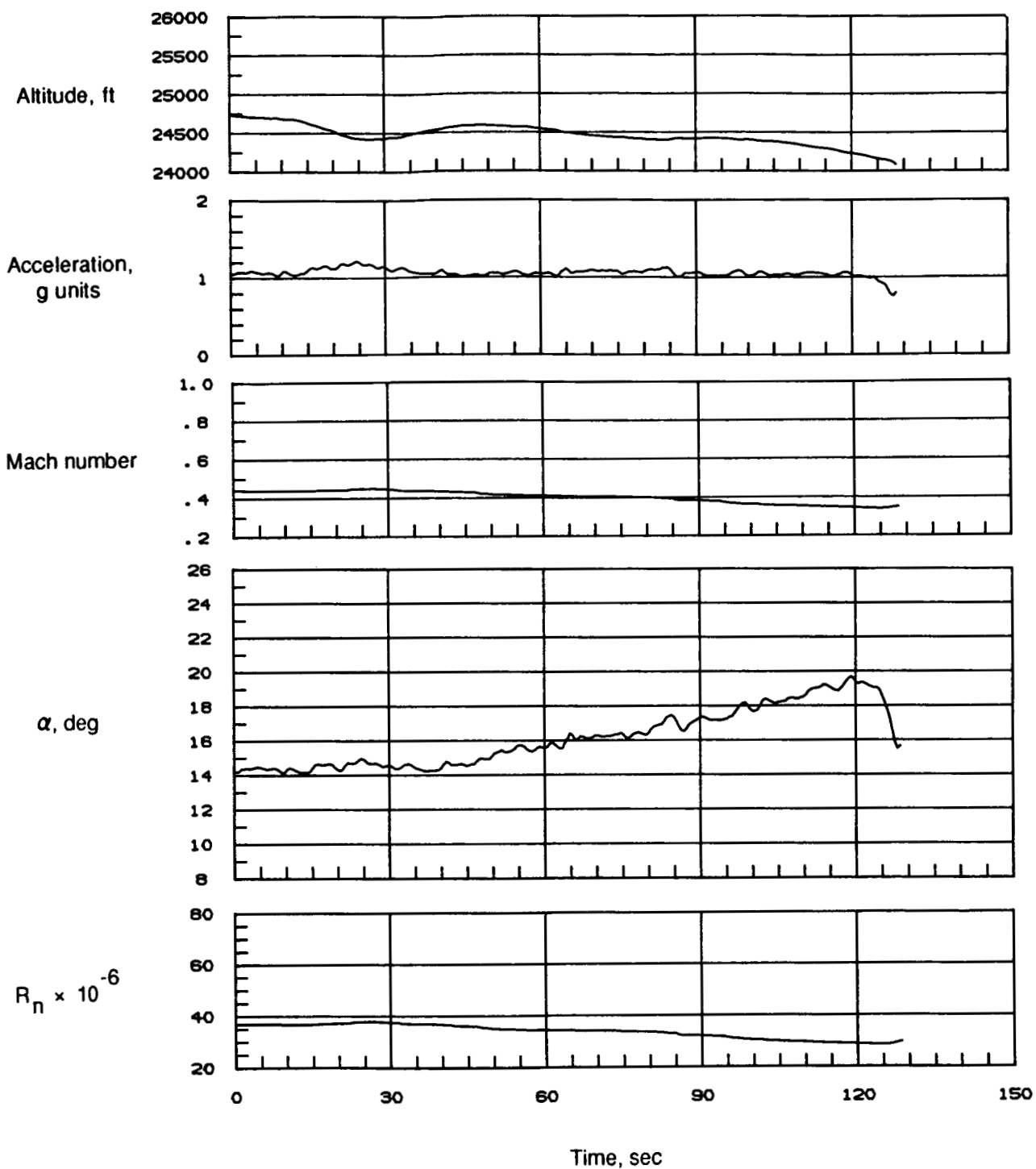


Figure 15. Time history of selected flight parameters for 1g deceleration at 25 000 ft (85-007/06).

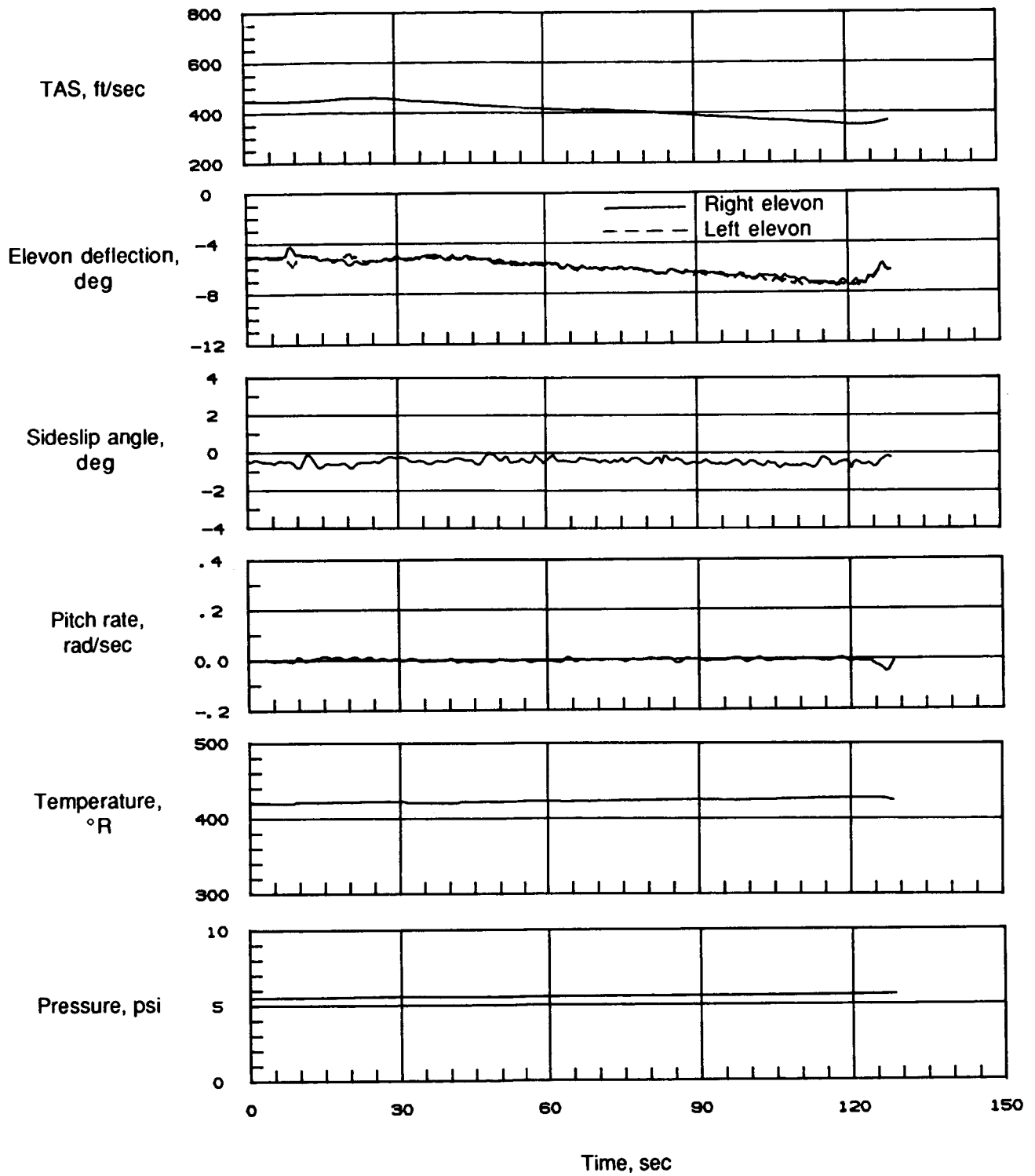


Figure 15. Concluded.

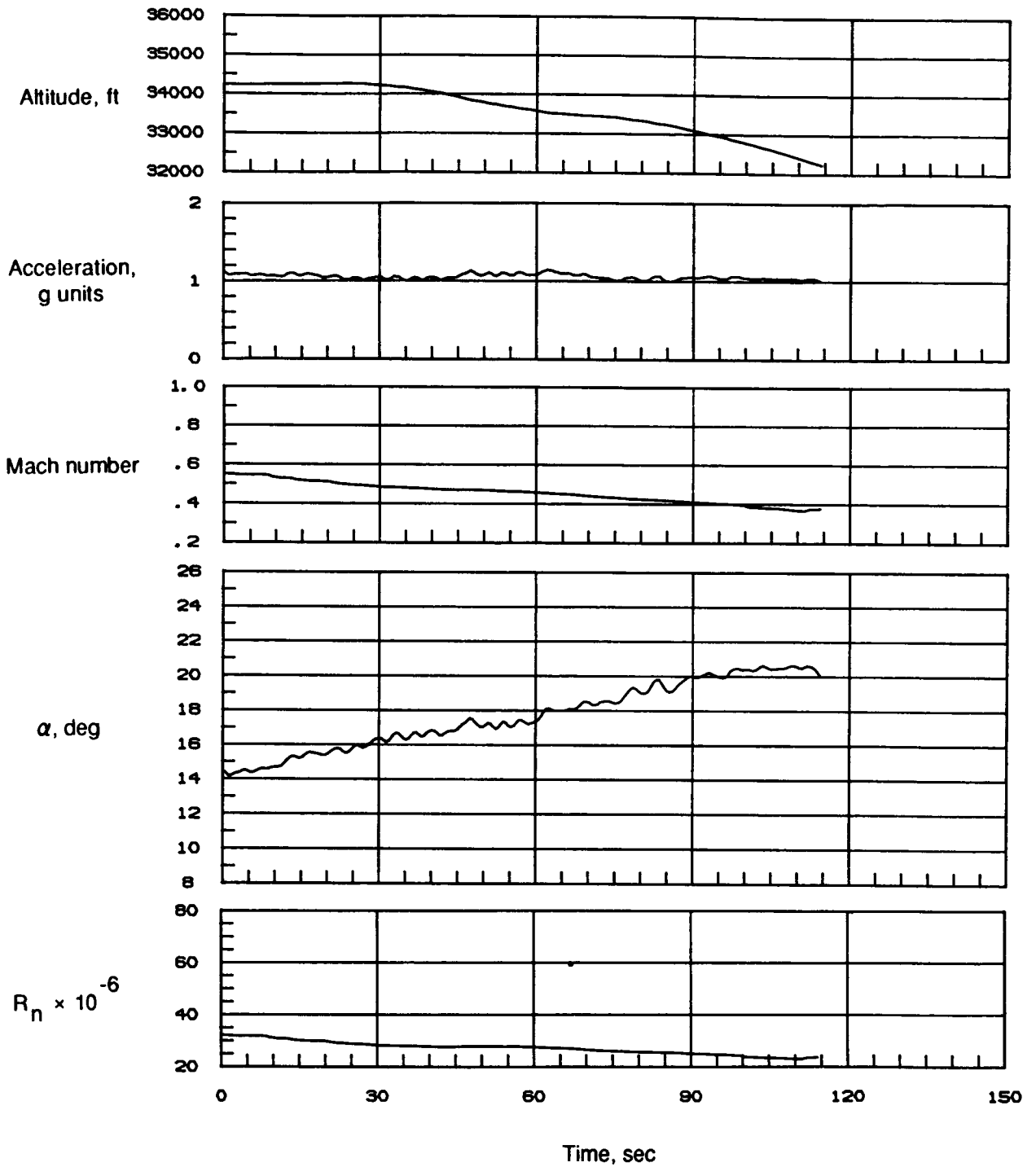


Figure 16. Time history of selected flight parameters for 1g deceleration at 35 000 ft (85-007/07).

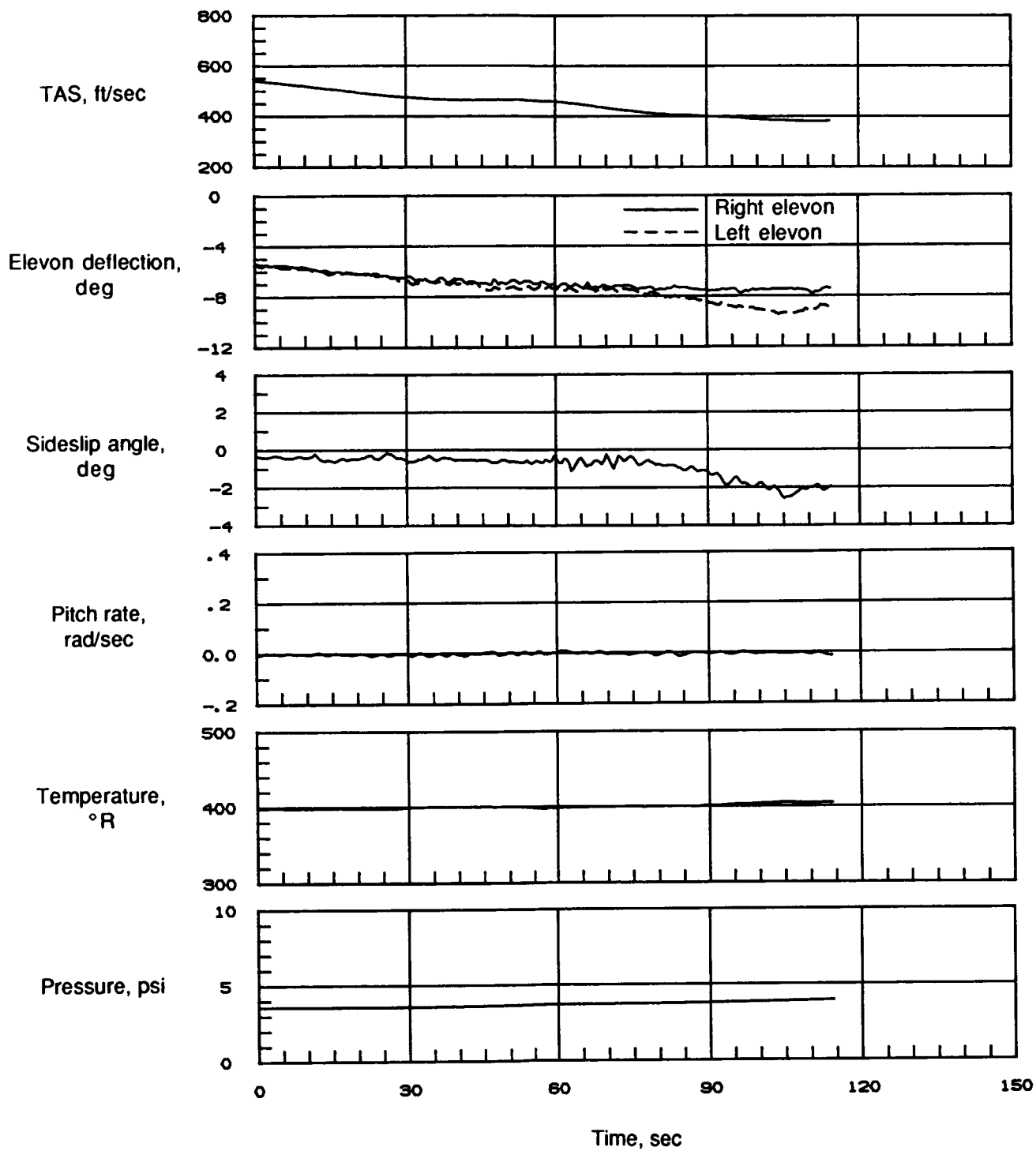


Figure 16. Concluded.

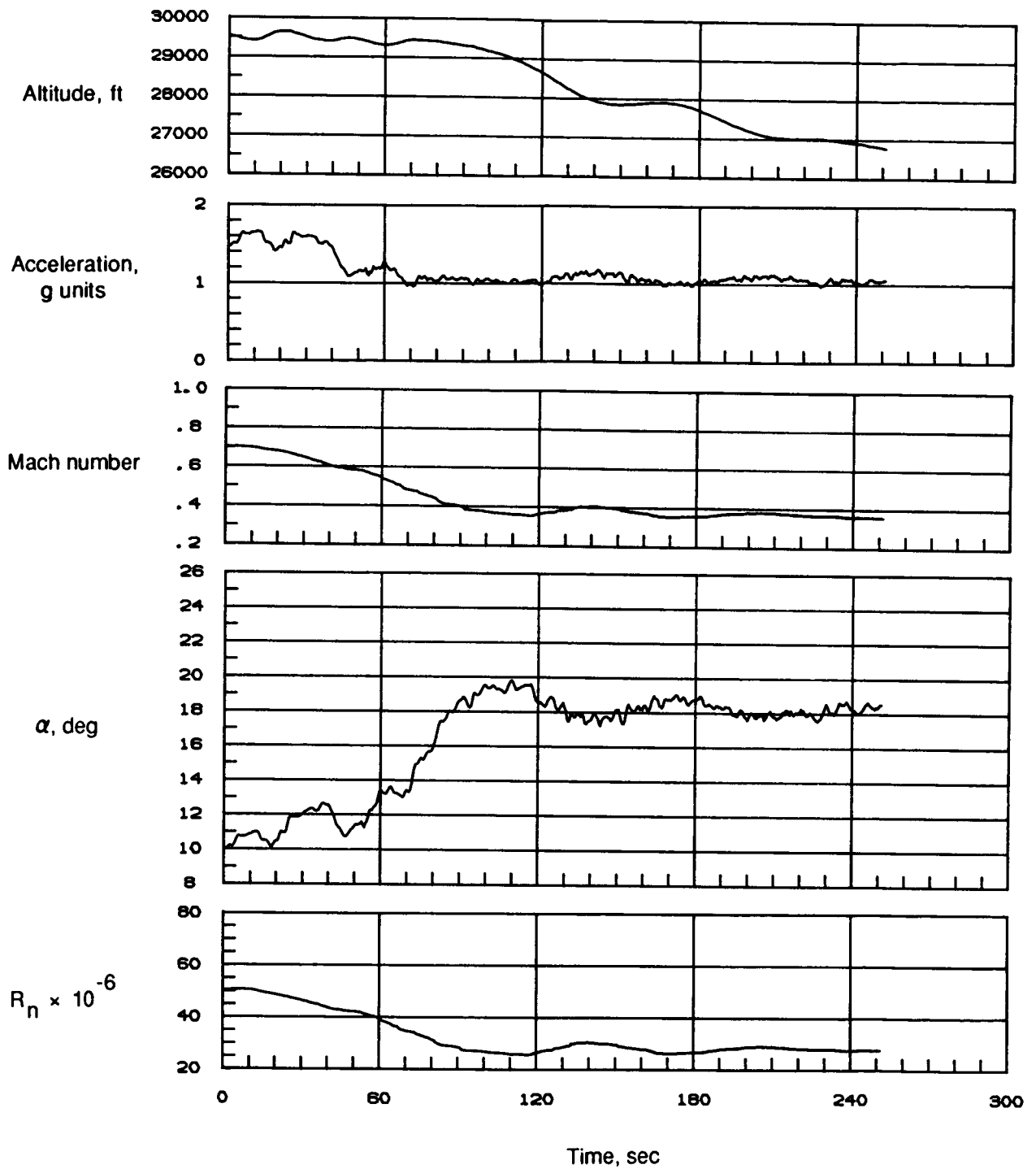


Figure 17. Time history of selected flight parameters for 1g deceleration at 30 000 ft (85-007/08).

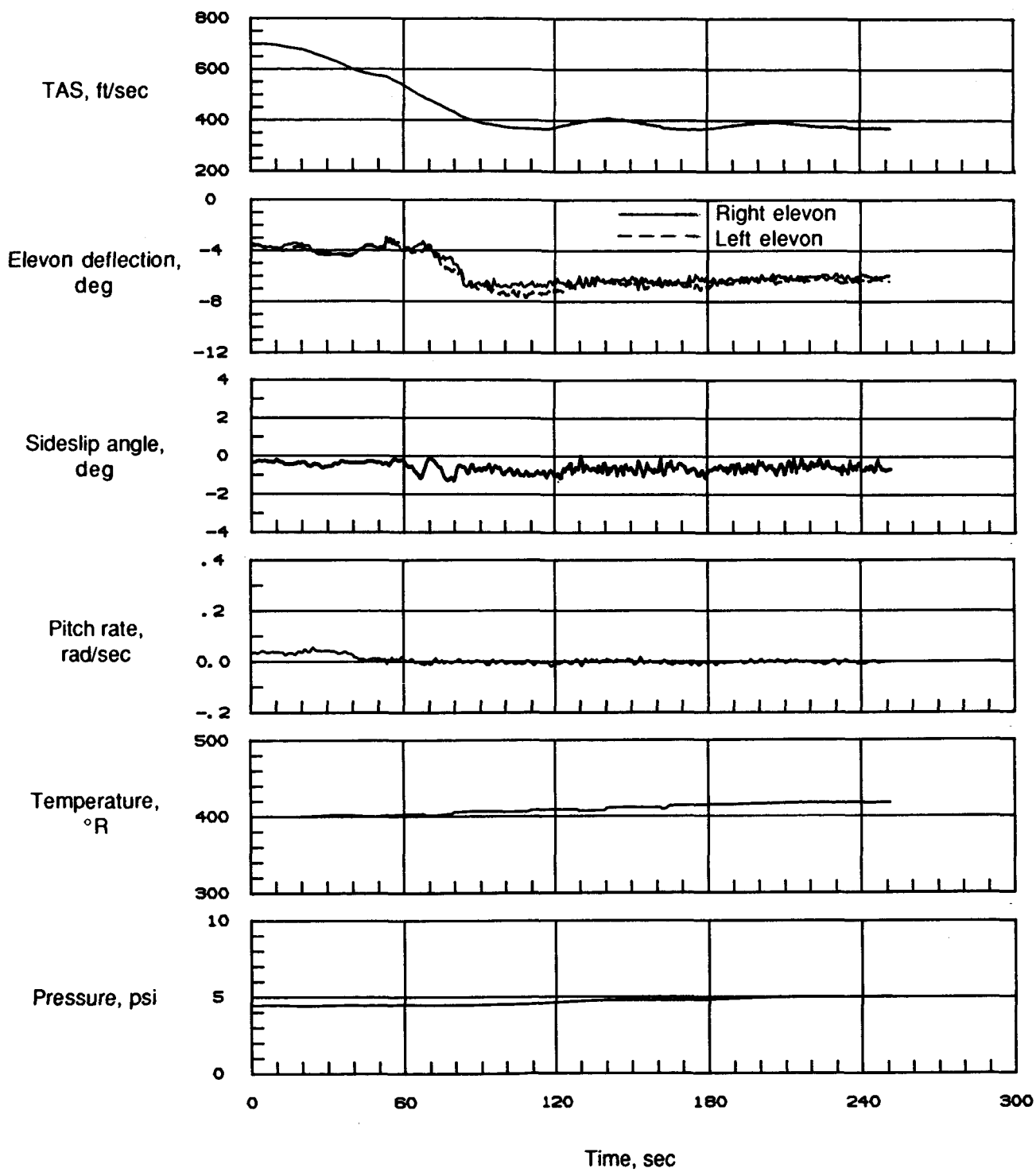


Figure 17. Concluded.

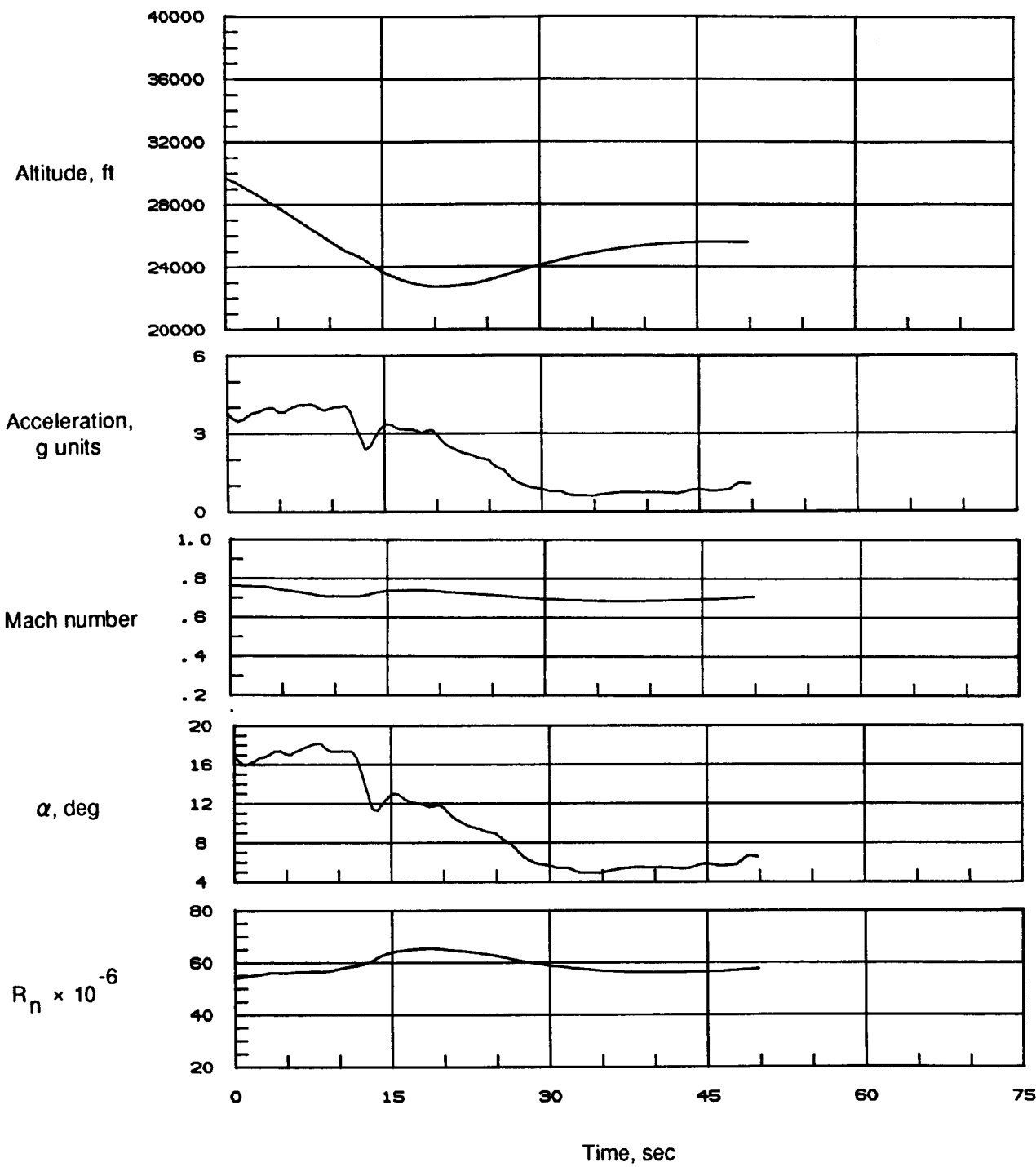


Figure 18. Time history of selected flight parameters at high-g during left spiral descent (85-007/10).

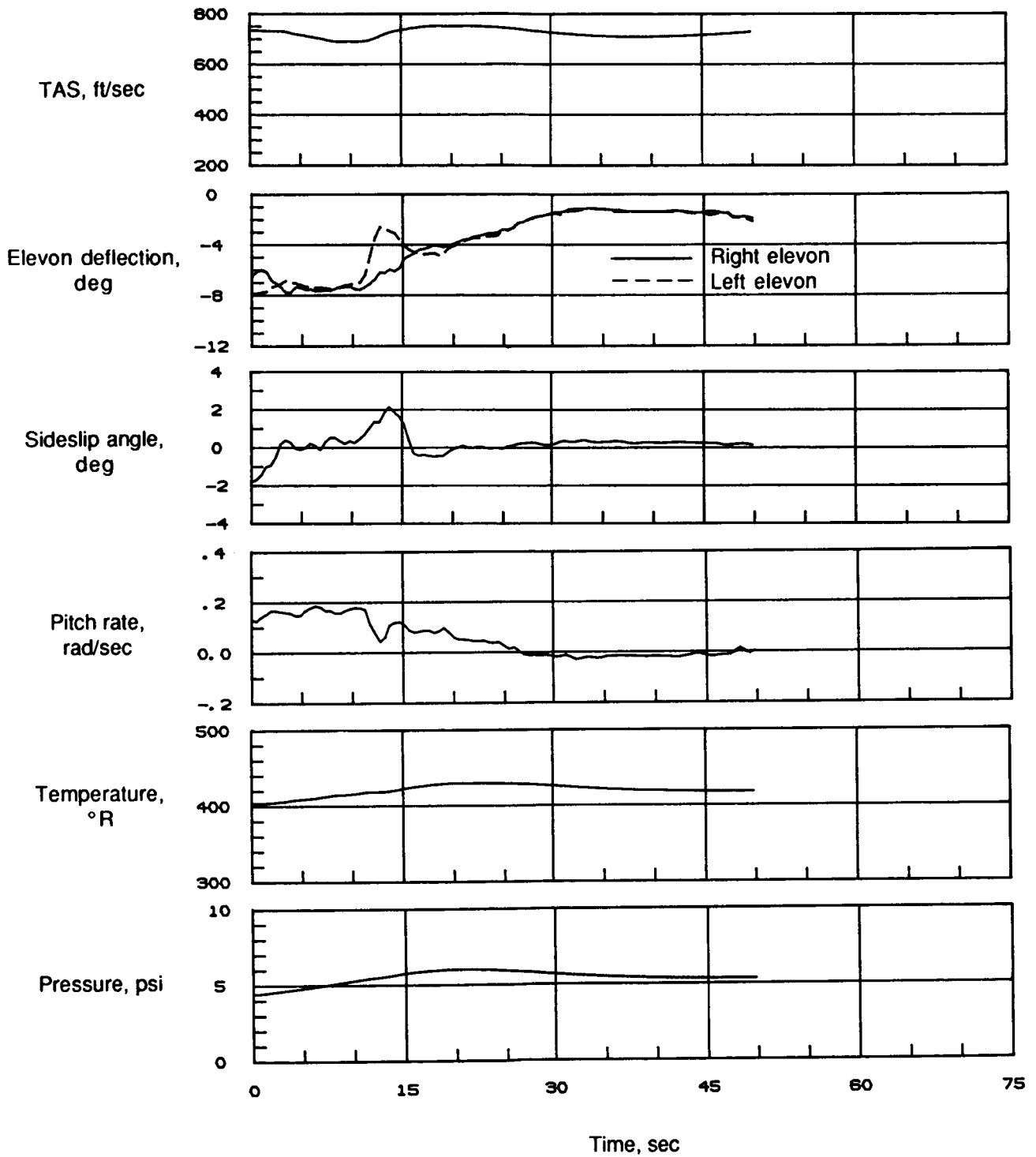


Figure 18. Concluded.

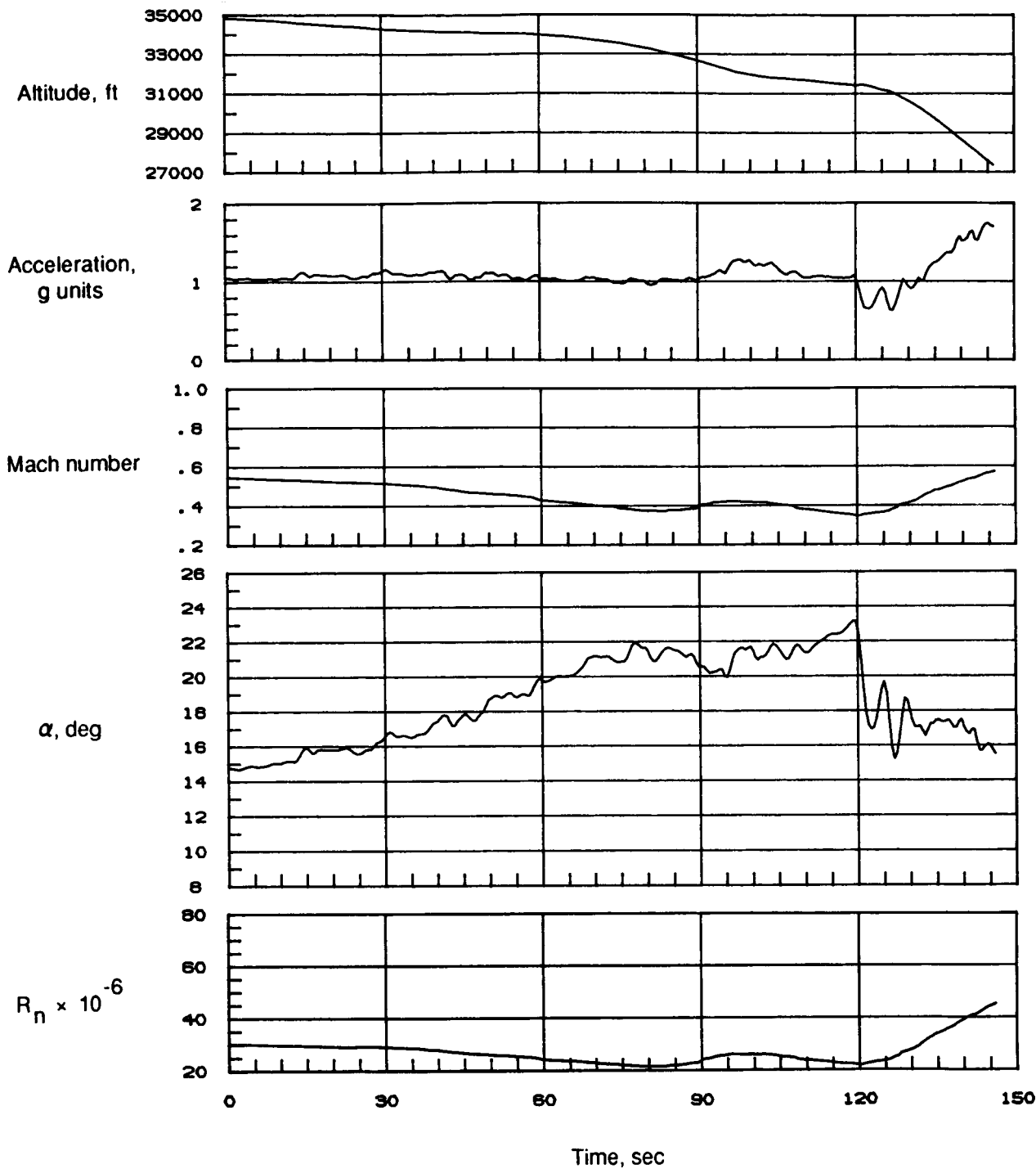


Figure 19. Time history of selected flight parameters for 1g deceleration at 35 000 ft (85-009/04).

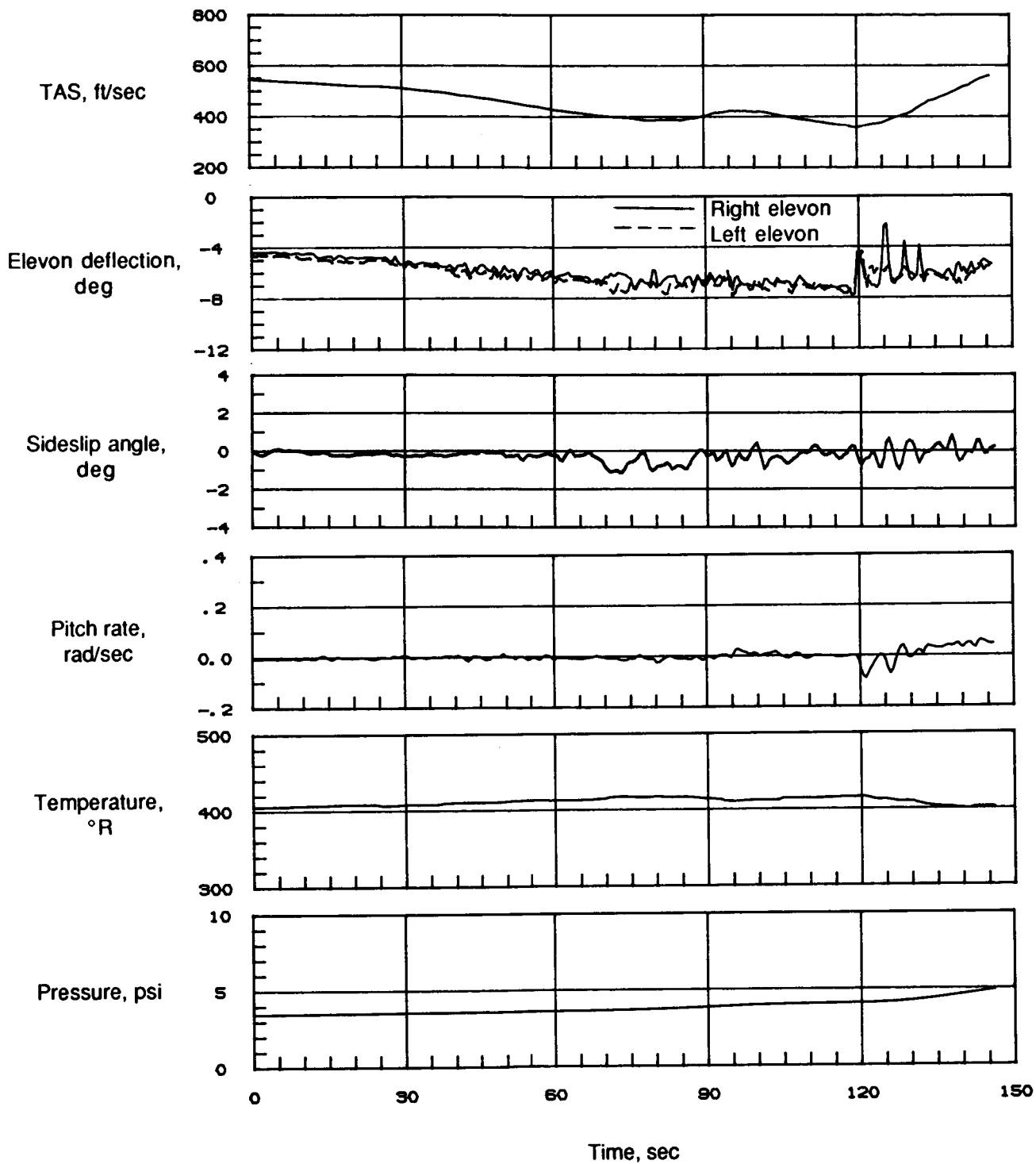


Figure 19. Concluded.

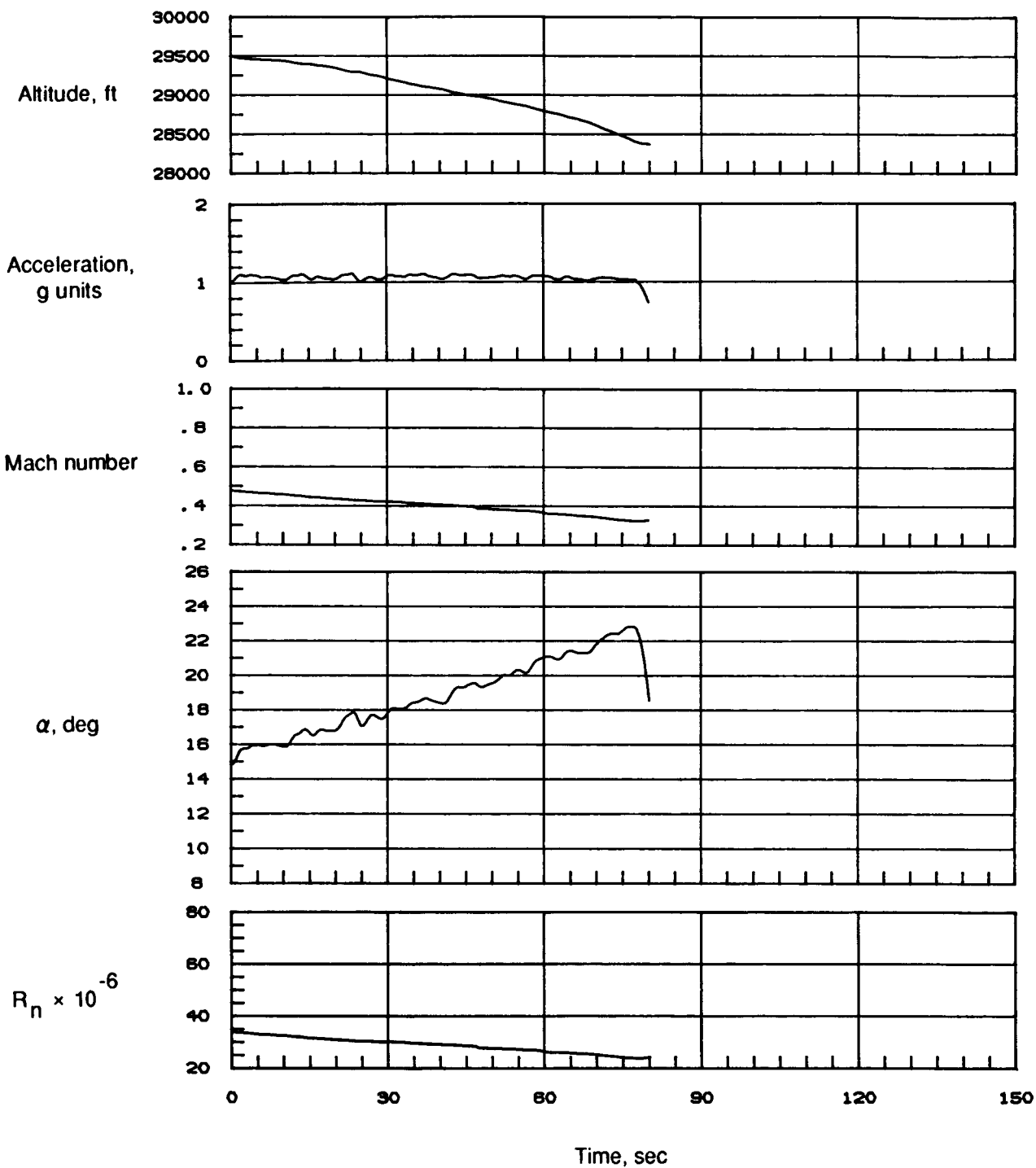


Figure 20. Time history of selected flight parameters for 1g deceleration at 30 000 ft (85-009/05).

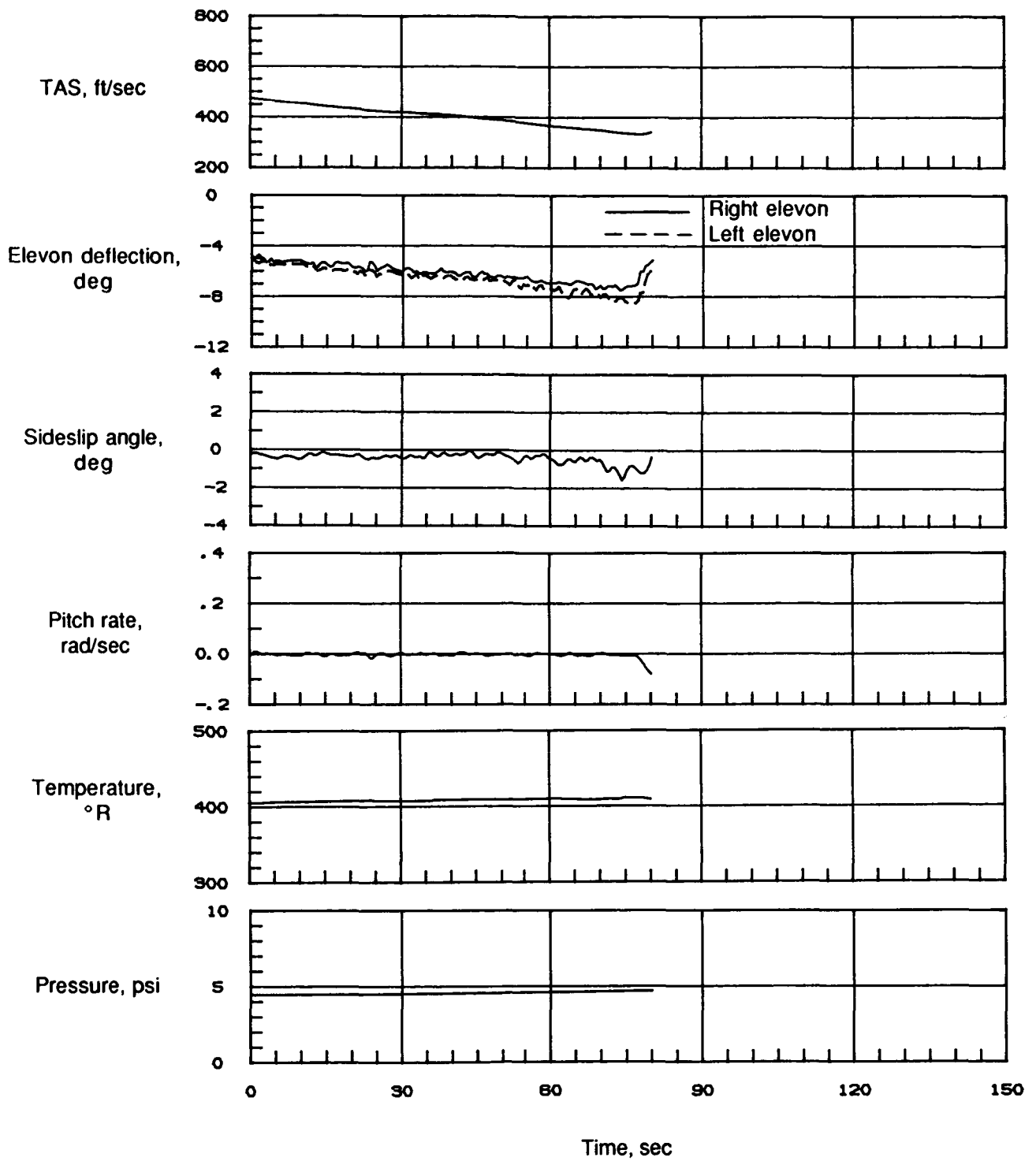


Figure 20. Concluded.

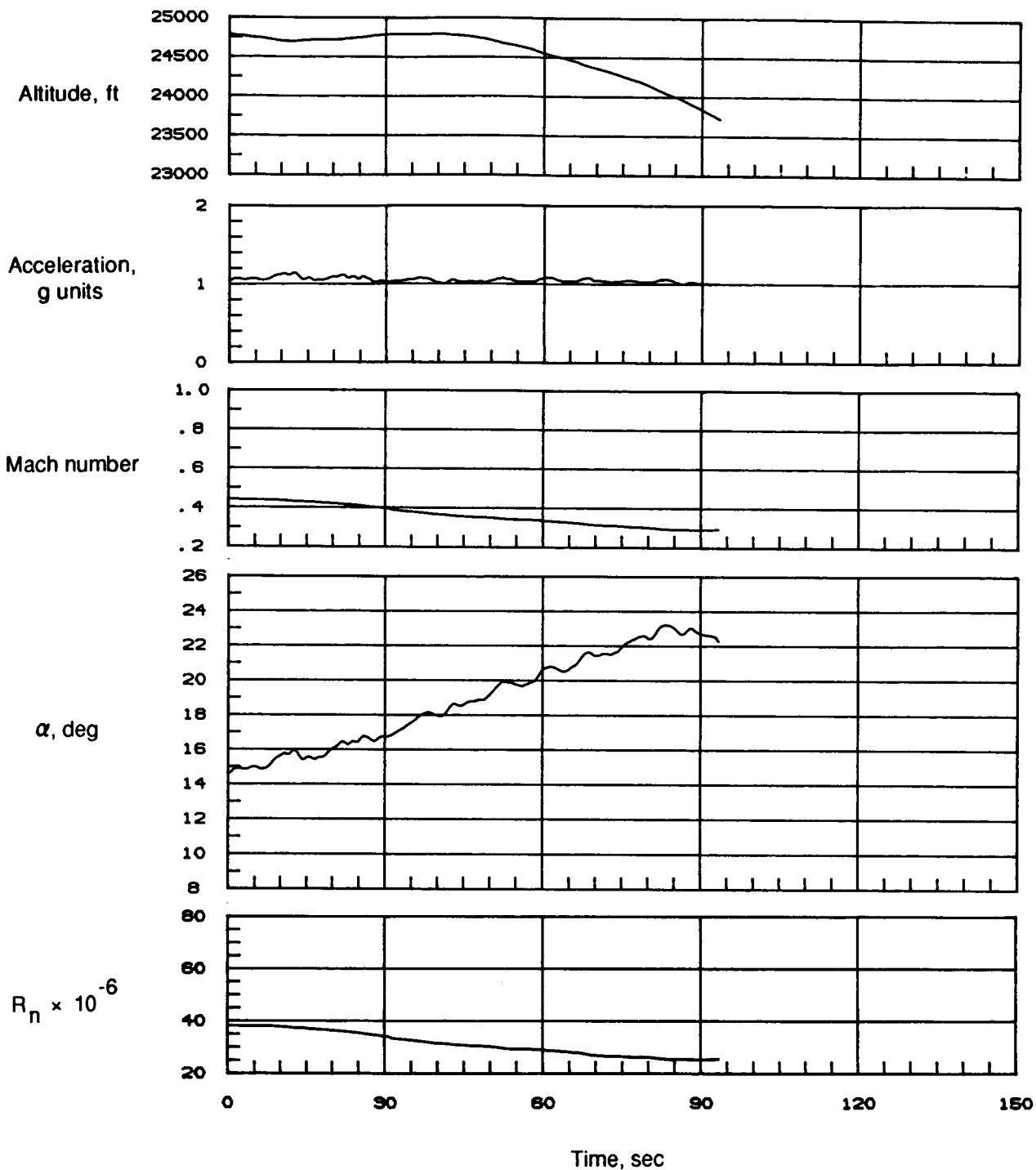


Figure 21. Time history of selected flight parameters for 1g deceleration at 25 000 ft (85-009/06a).

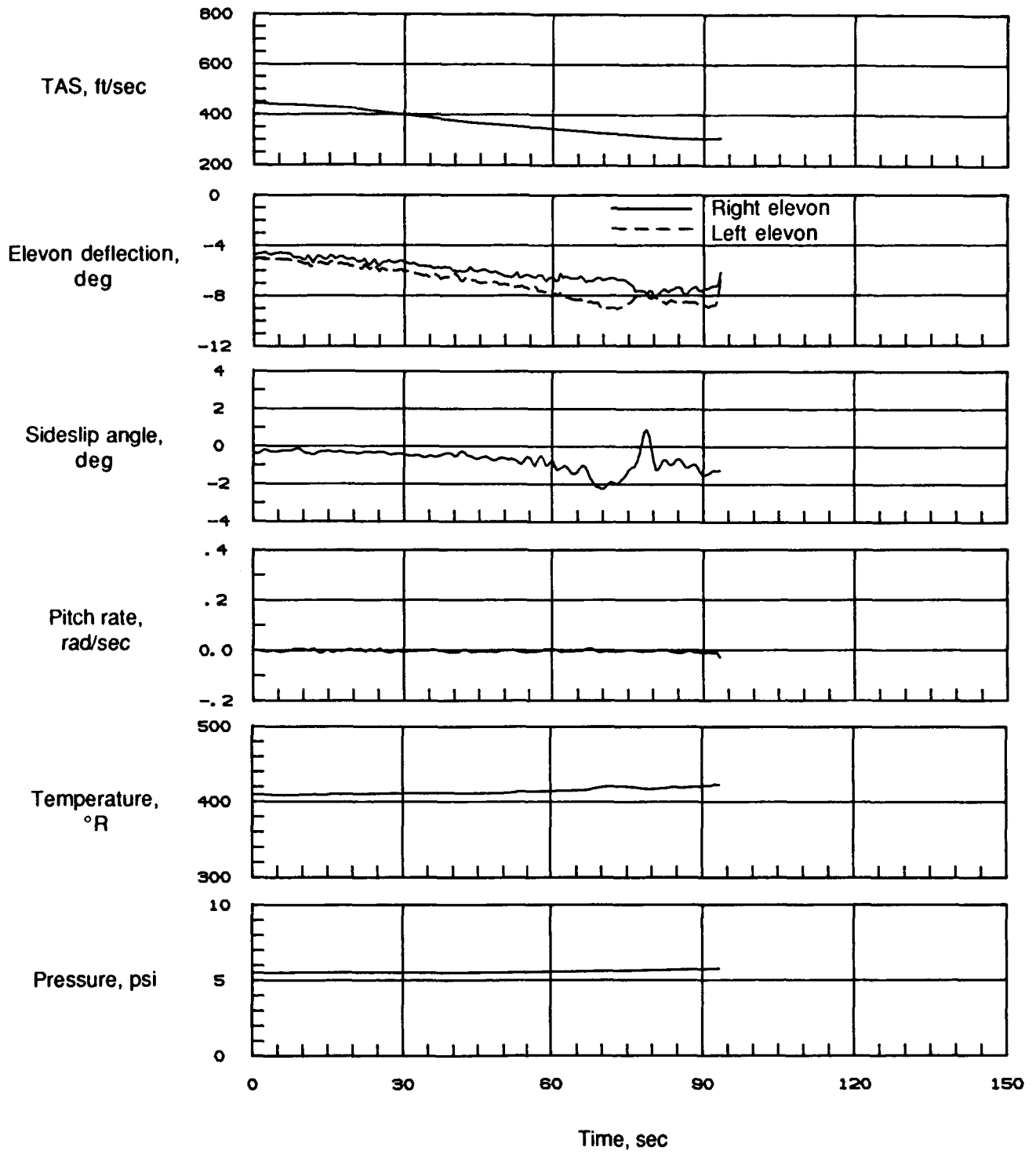


Figure 21. Concluded.

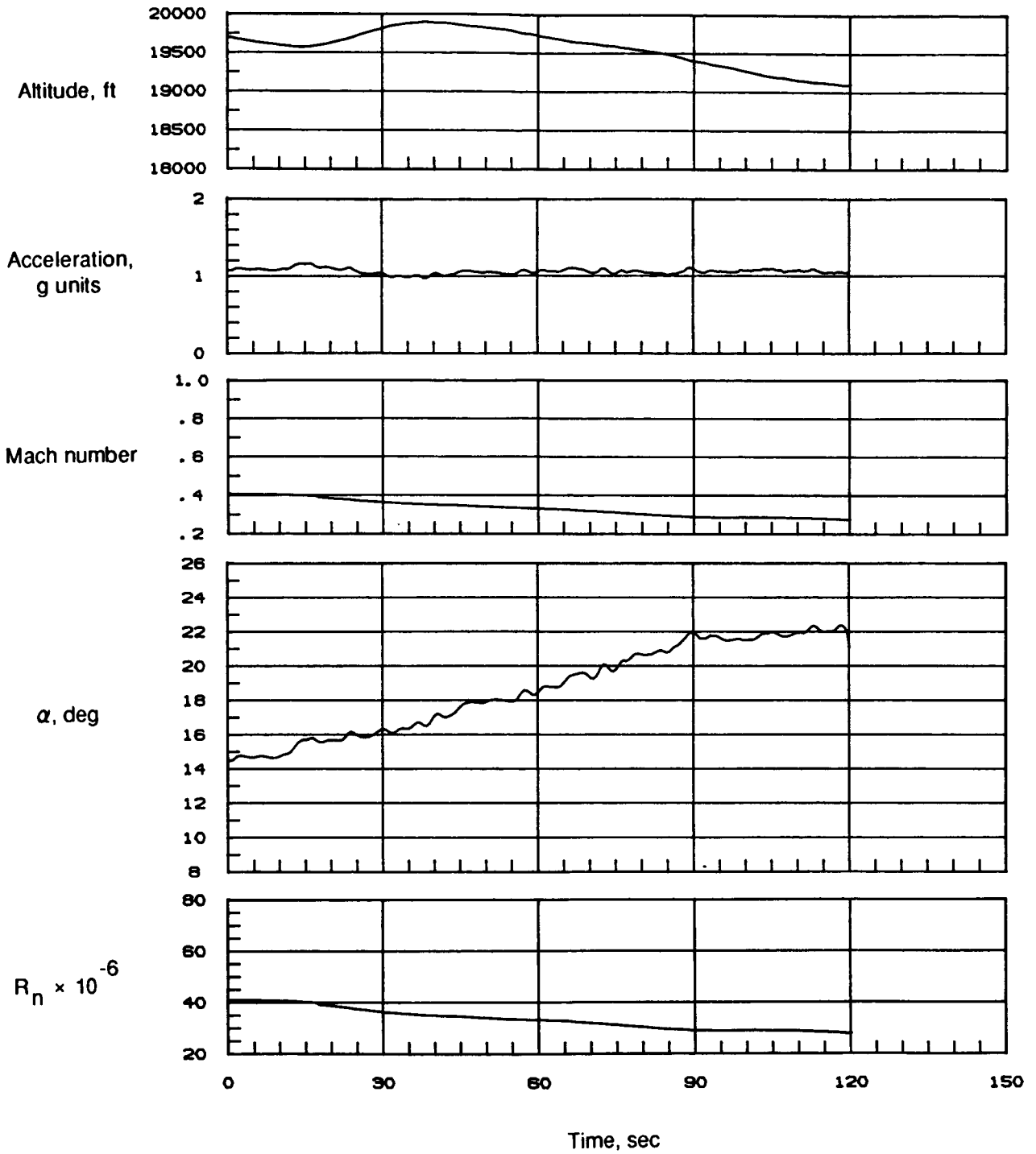


Figure 22. Time history of selected flight parameters for 1g deceleration at 20 000 ft (85-009/06b).

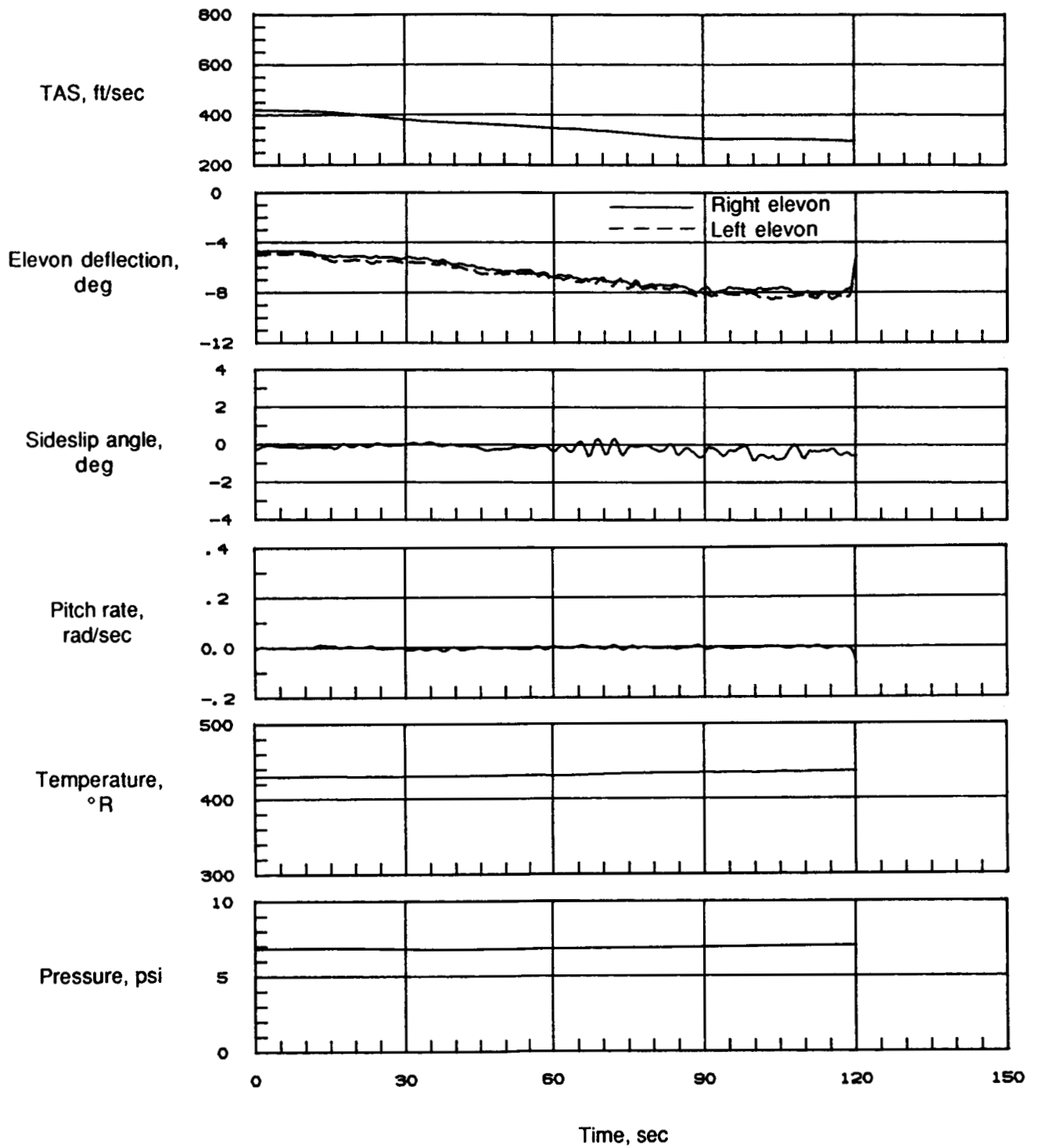


Figure 22. Concluded.

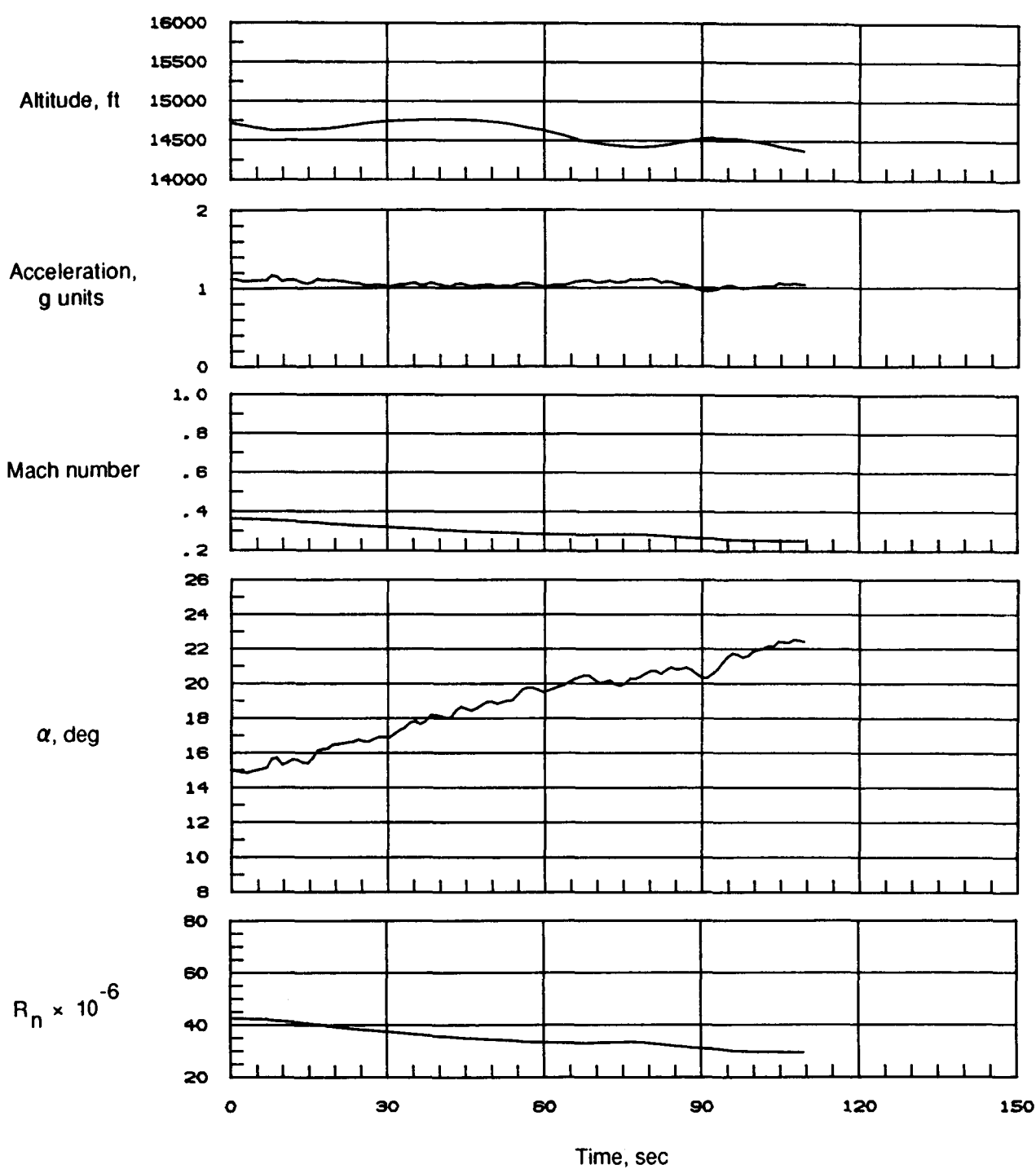


Figure 23. Time history of selected flight parameters for 1g deceleration at 15 000 ft (85-009/07).

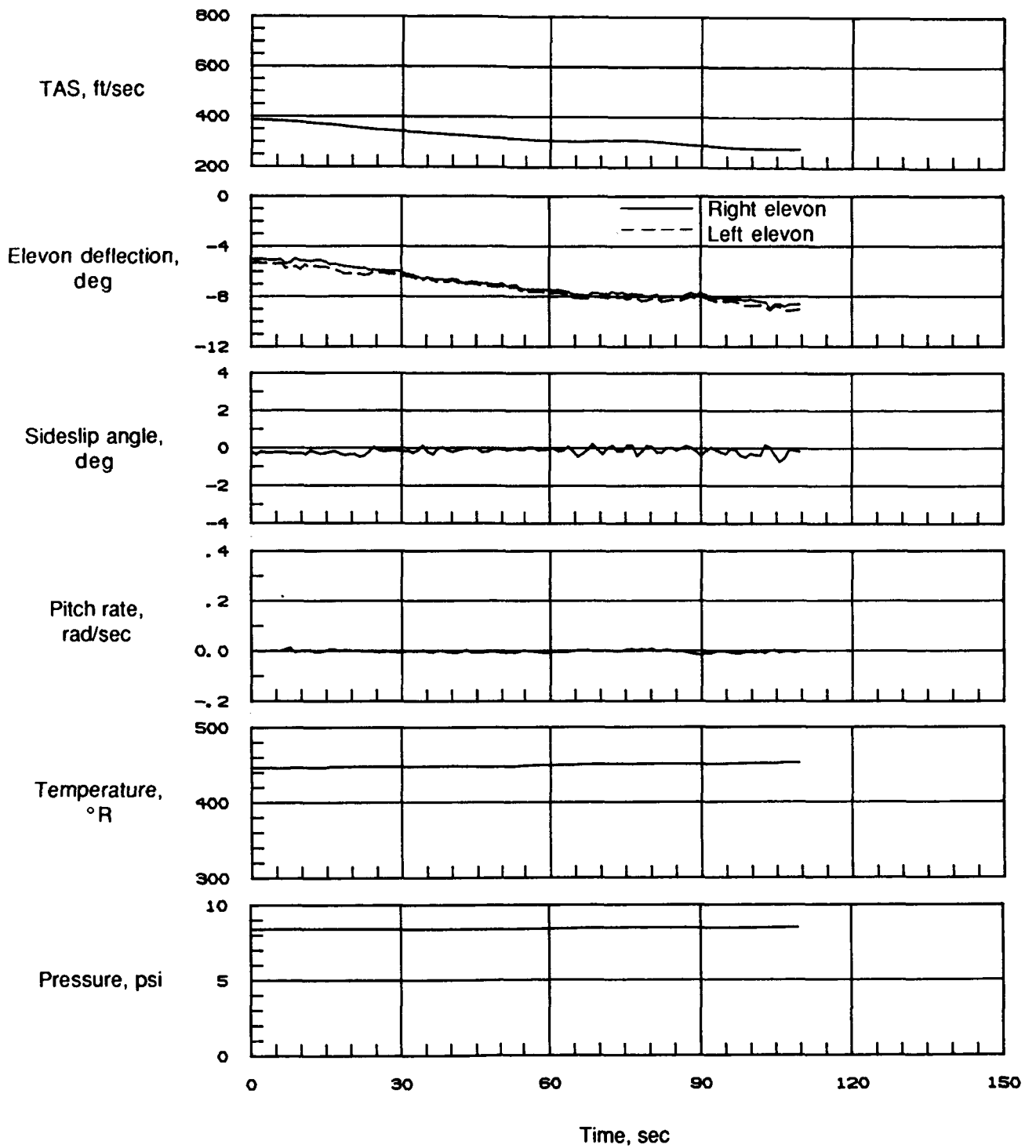


Figure 23. Concluded.

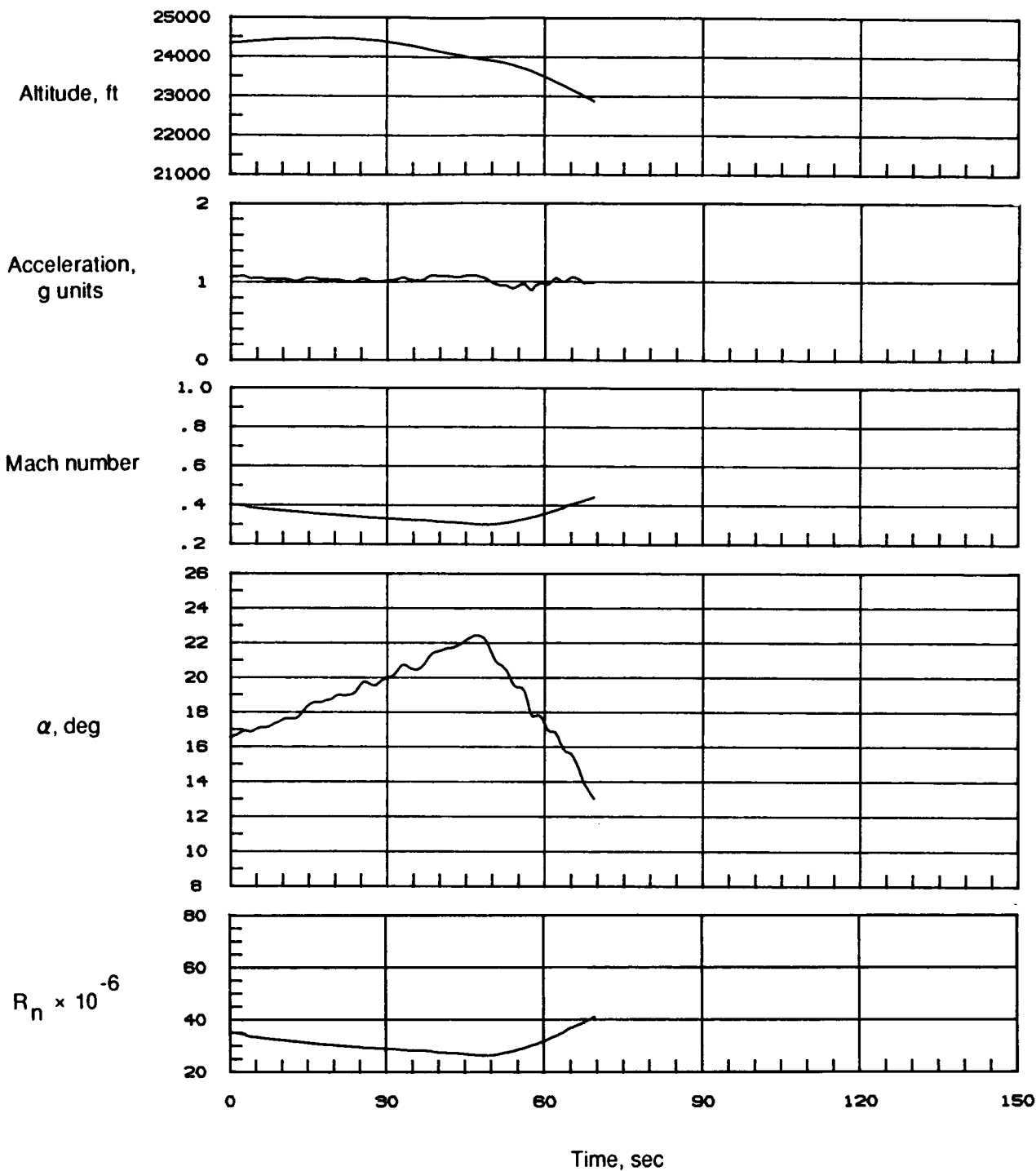


Figure 24. Time history of selected flight parameters for 1g deceleration at 25 000 ft (85-009/09).

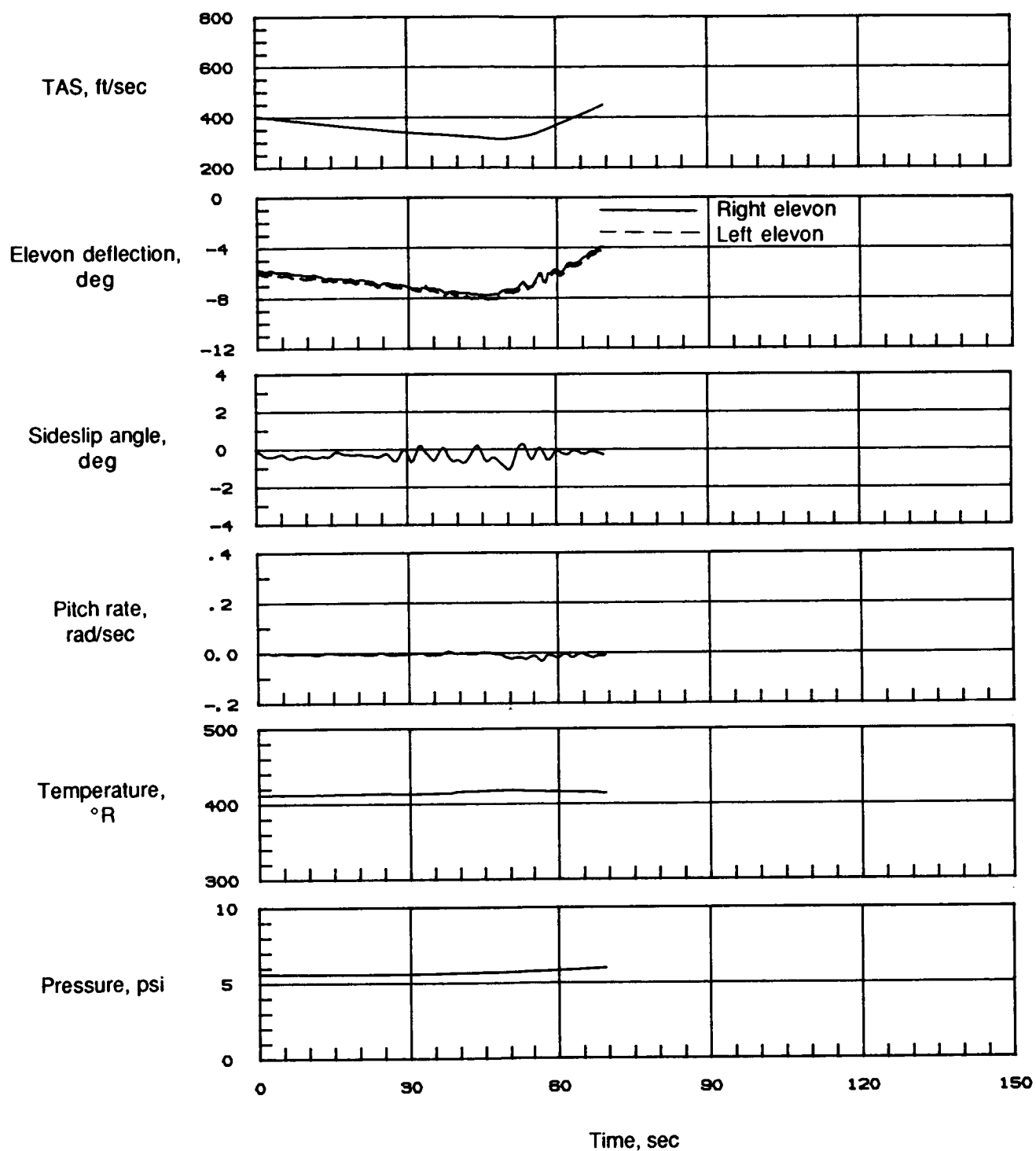


Figure 24. Concluded.

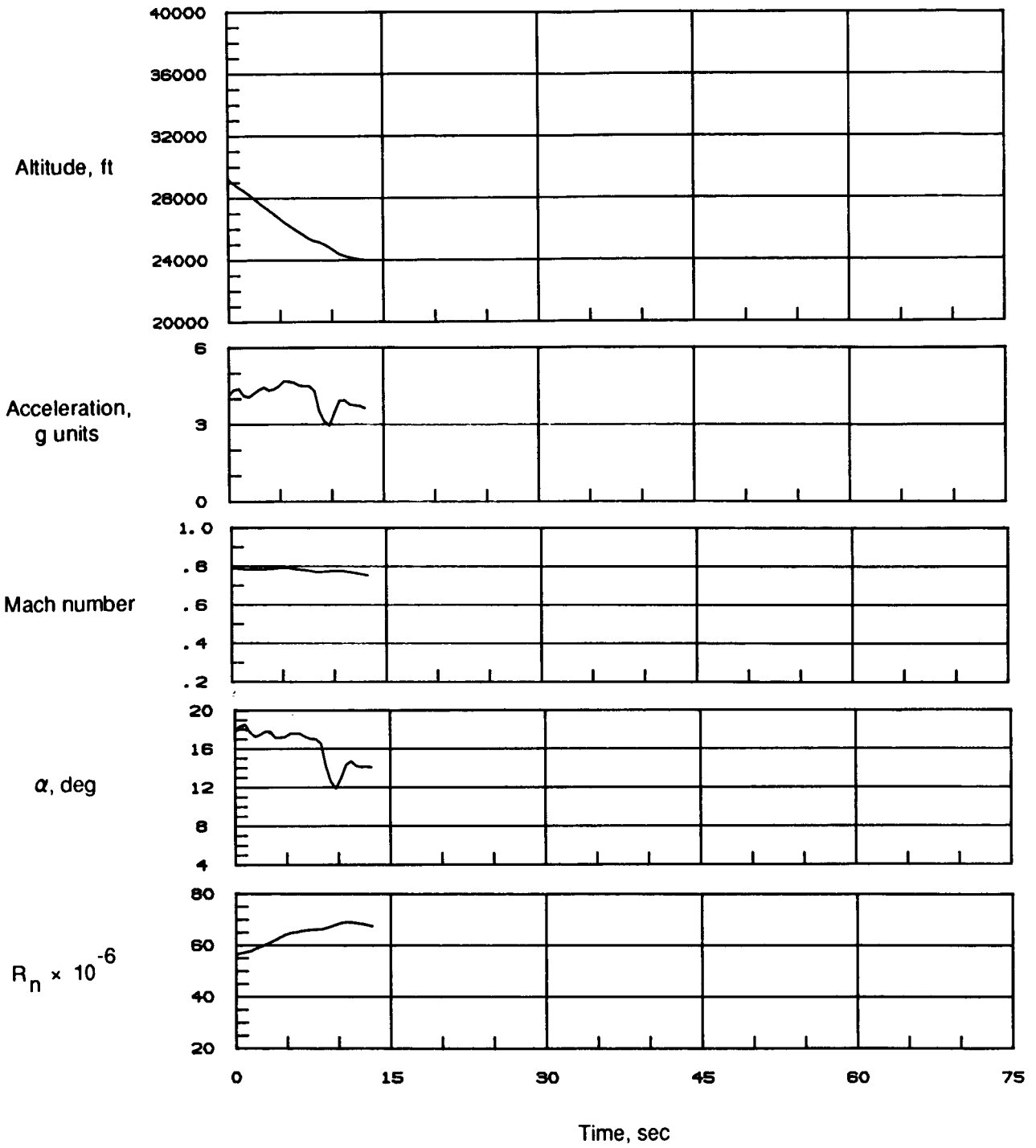


Figure 25. Time history of selected flight parameters at high-g during left spiral descent (85-009/10).

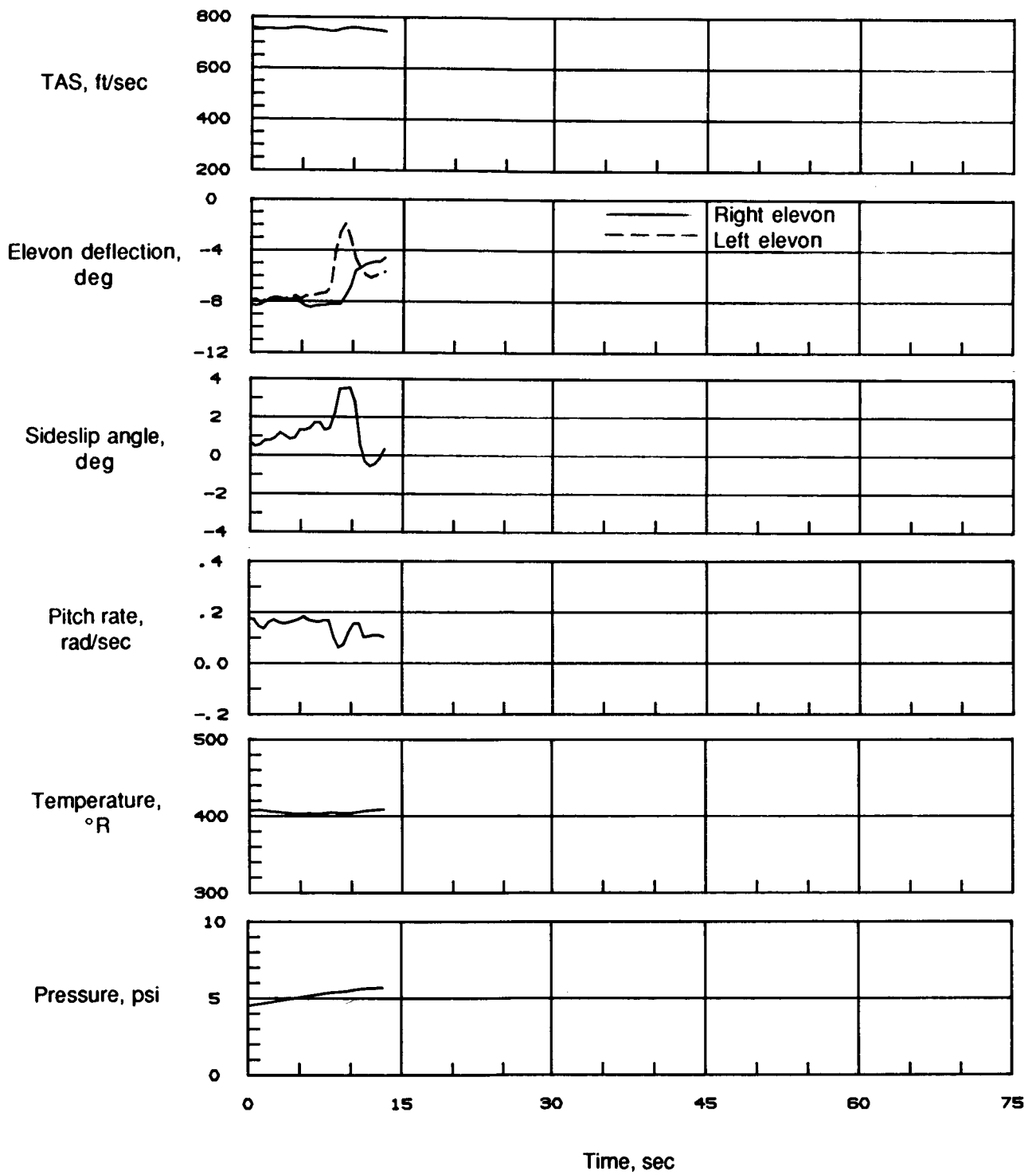


Figure 25. Concluded.

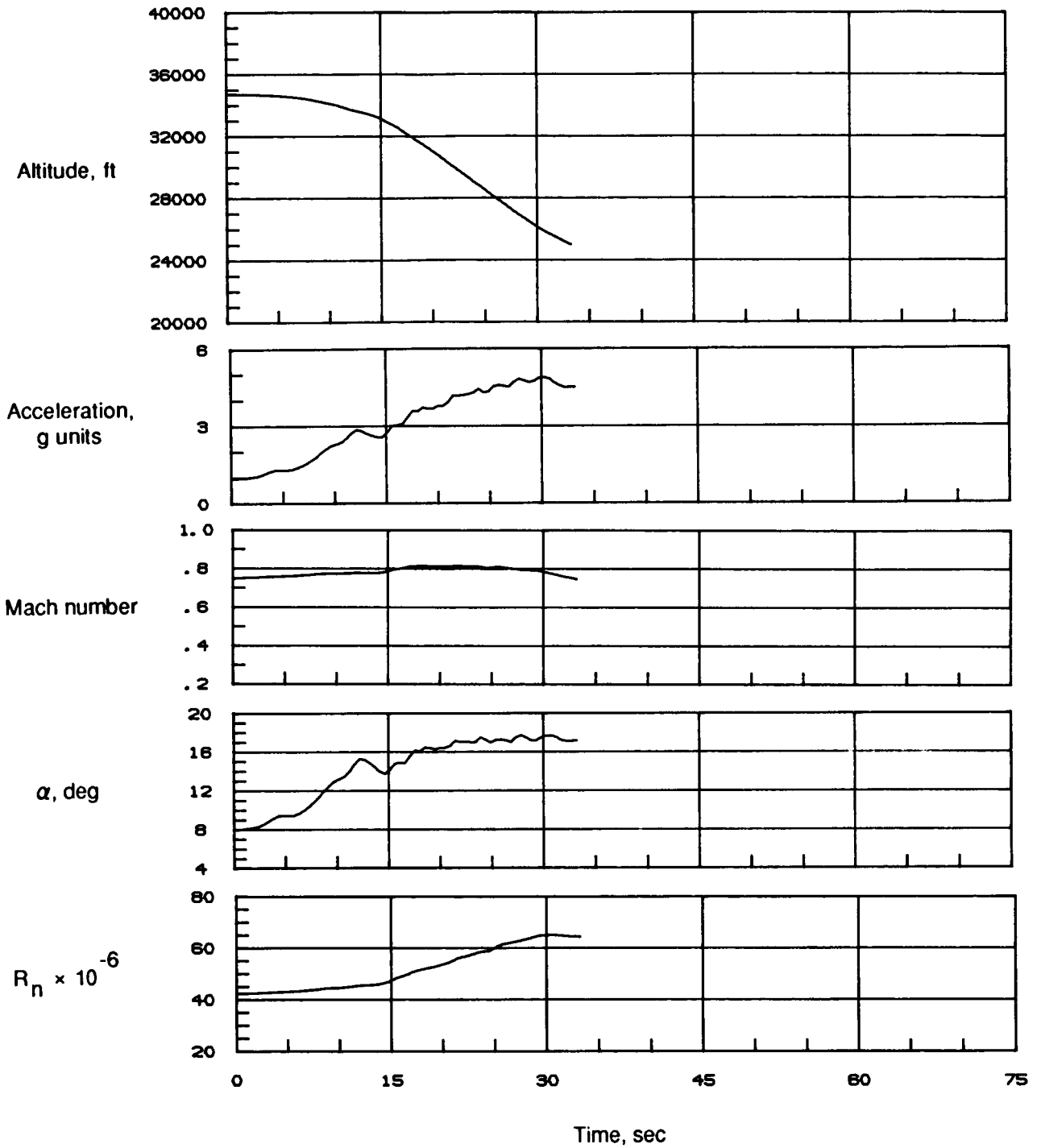


Figure 26. Time history of selected flight parameters at high-g during right spiral descent (85-009/11).

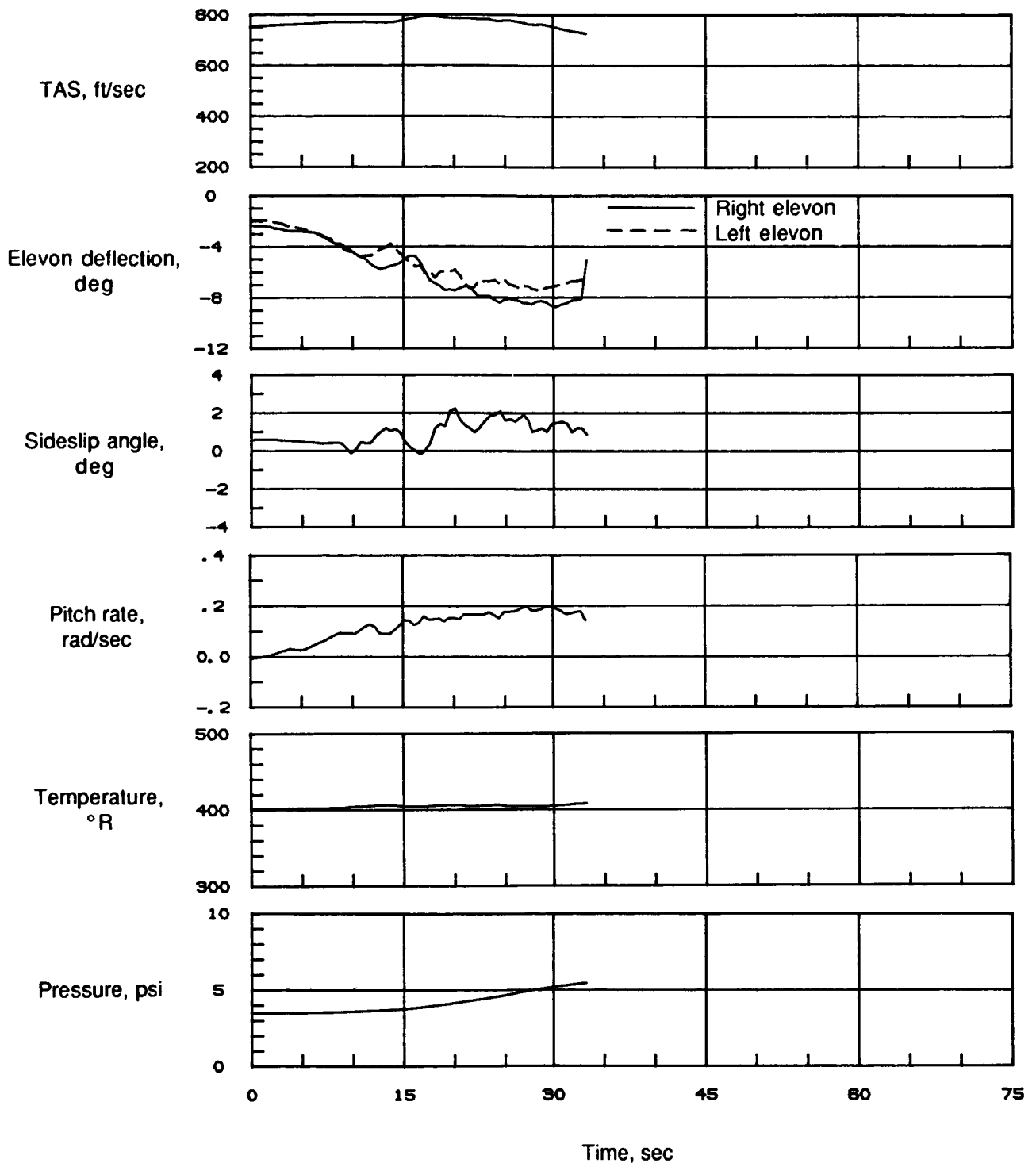


Figure 26. Concluded.

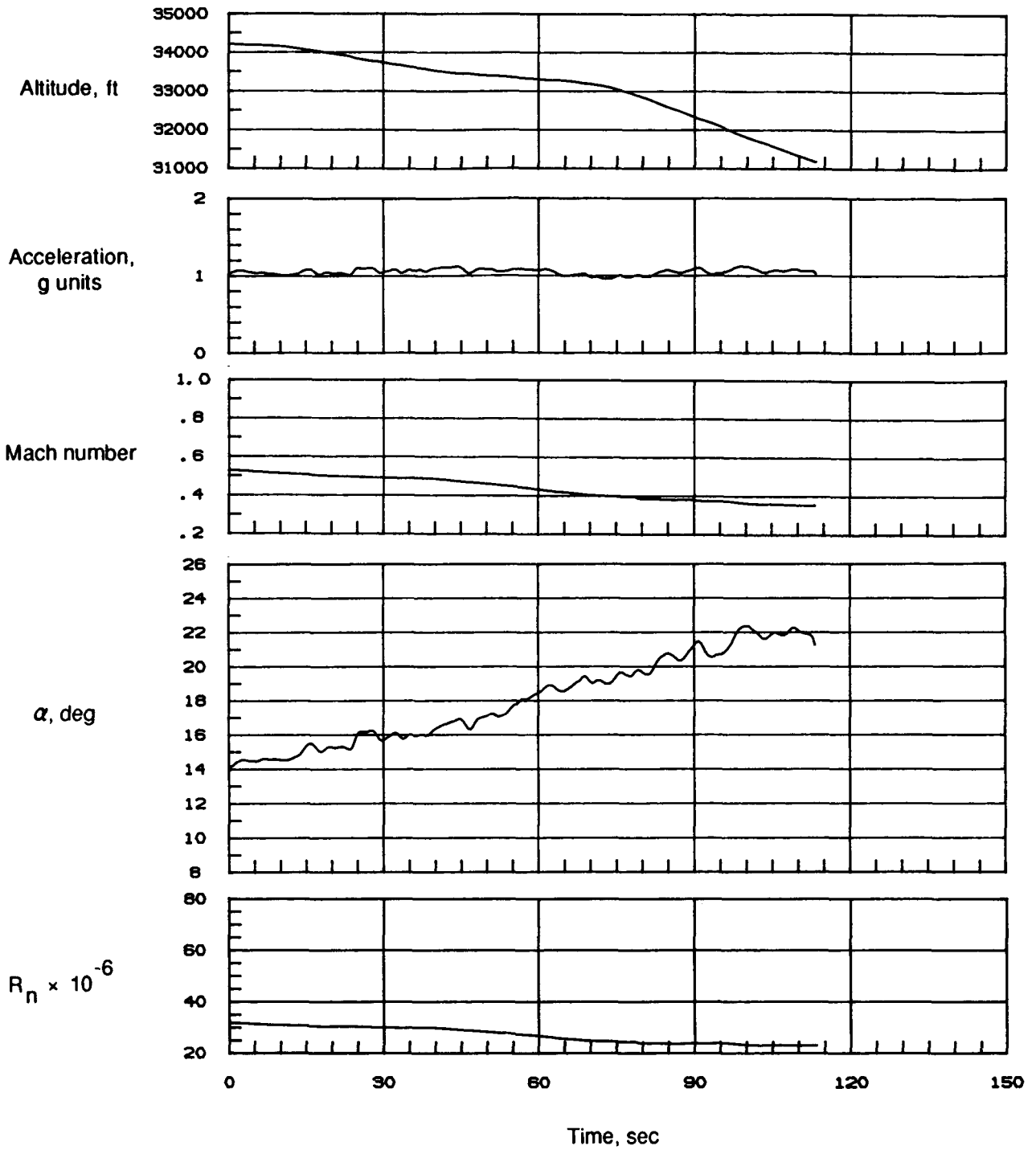


Figure 27. Time history of selected flight parameters for 1g deceleration at 35 000 ft (85-010/04).

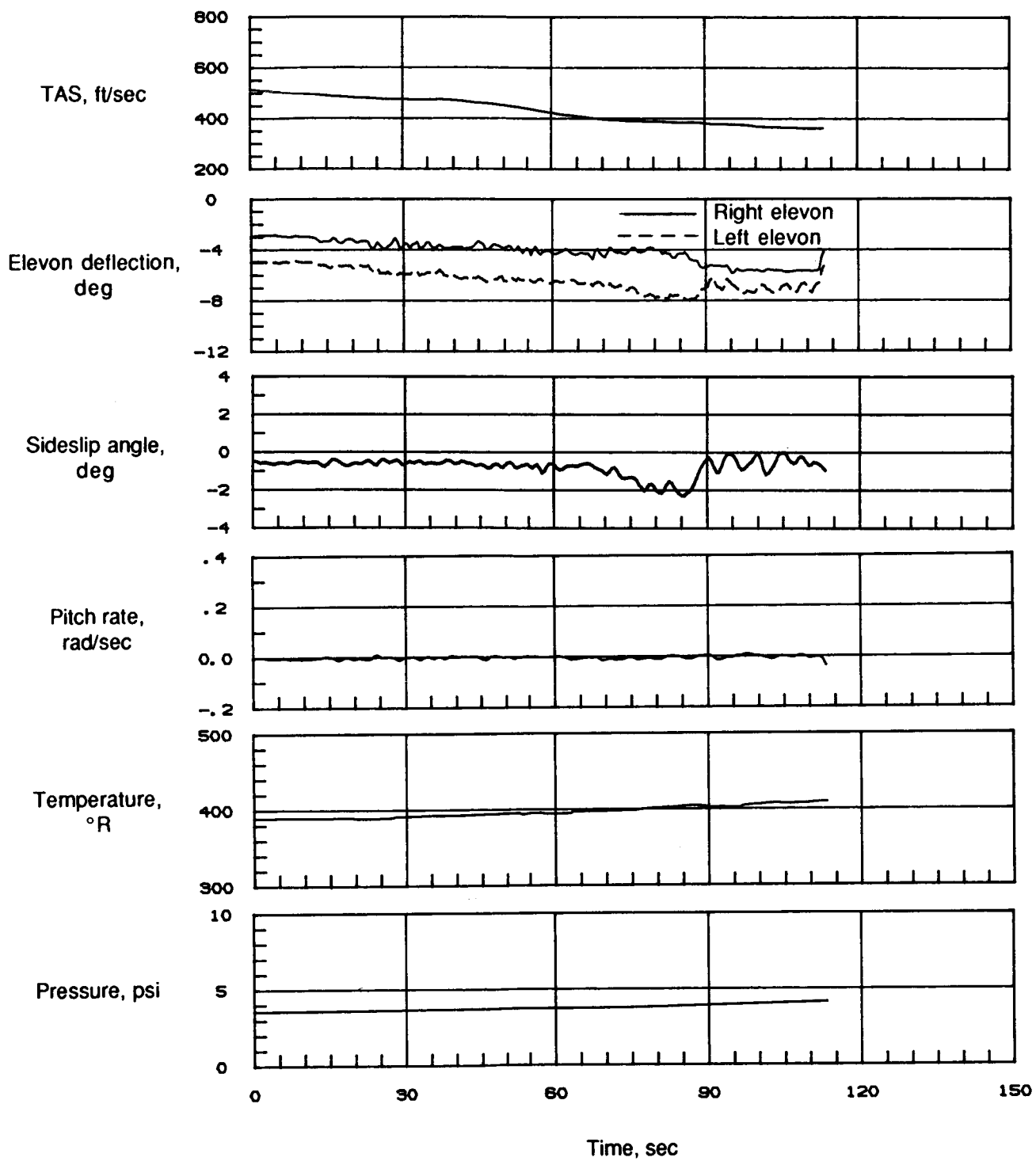


Figure 27. Concluded.

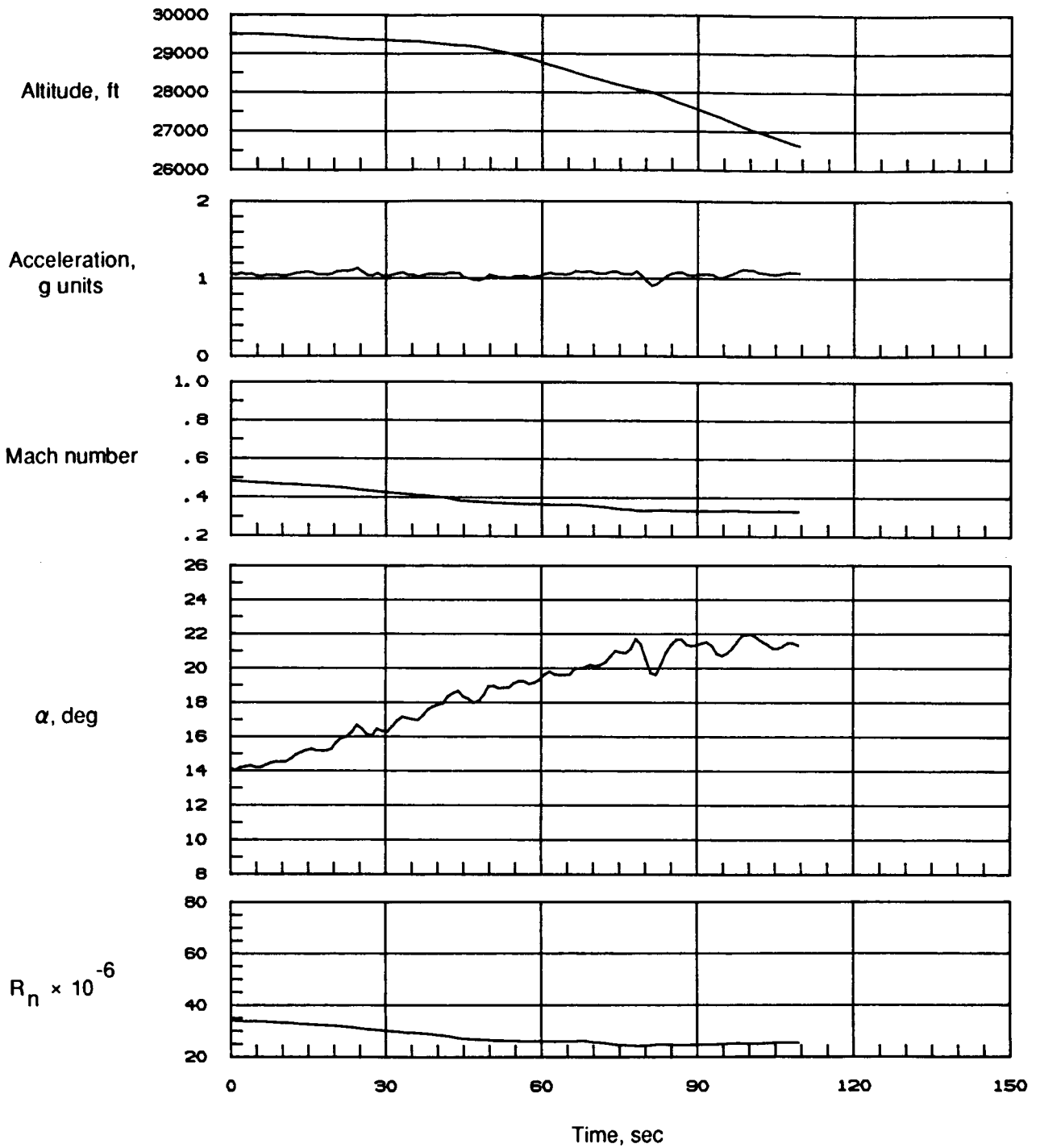


Figure 28. Time history of selected flight parameters for 1g deceleration at 30 000 ft (85-010/05).

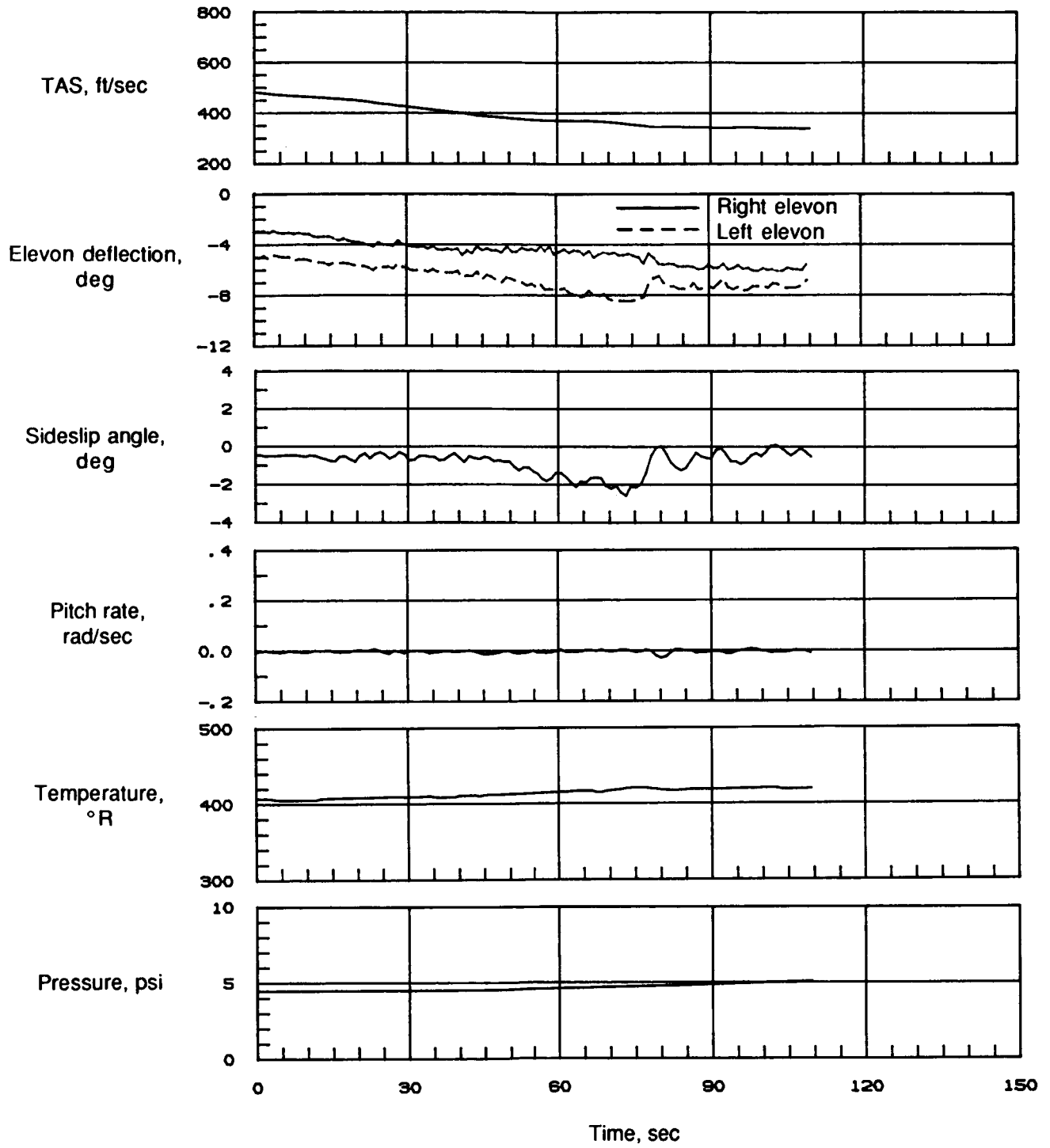


Figure 28. Concluded.

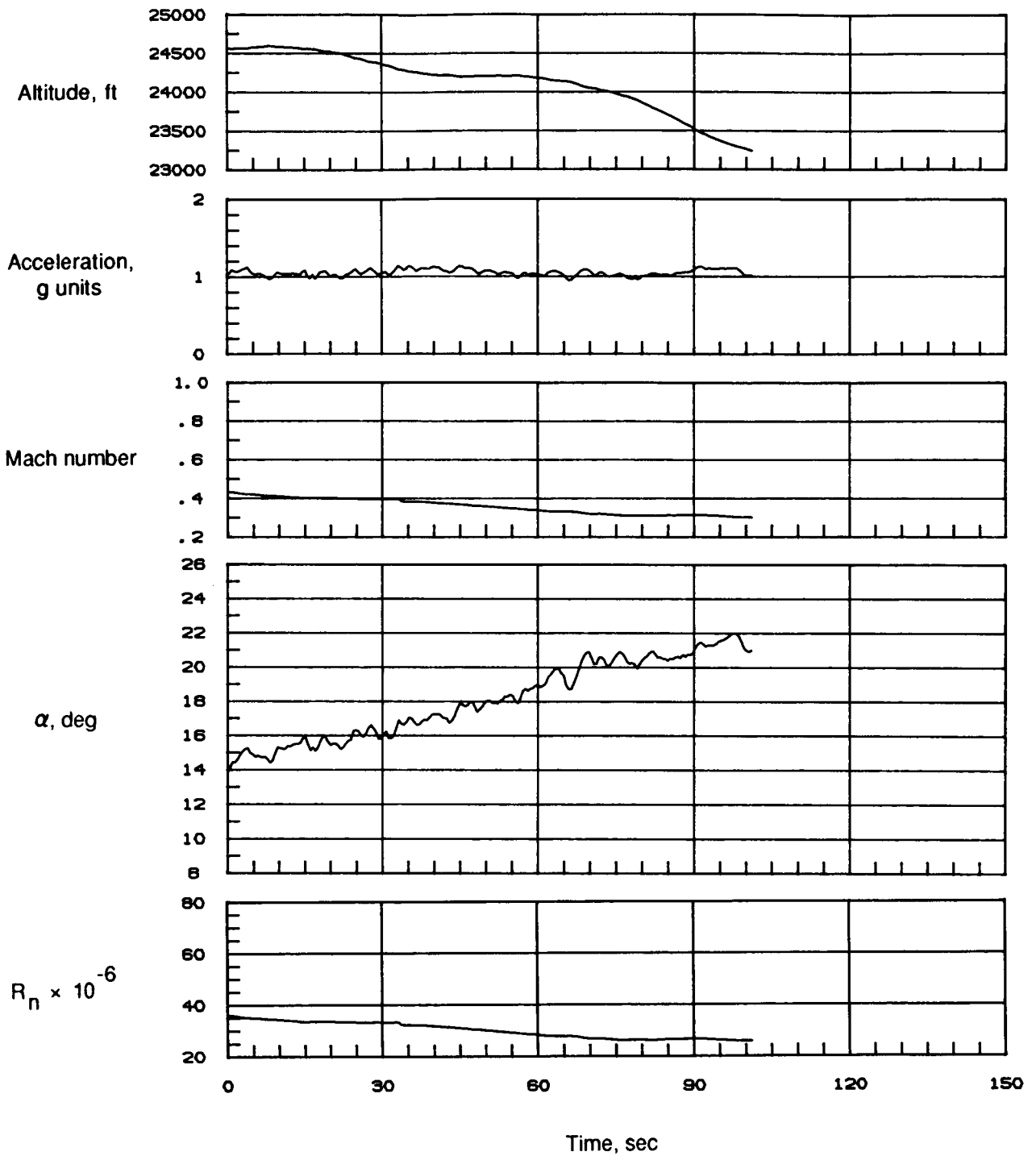


Figure 29. Time history of selected flight parameters for 1g deceleration at 25 000 ft (85-010/06).

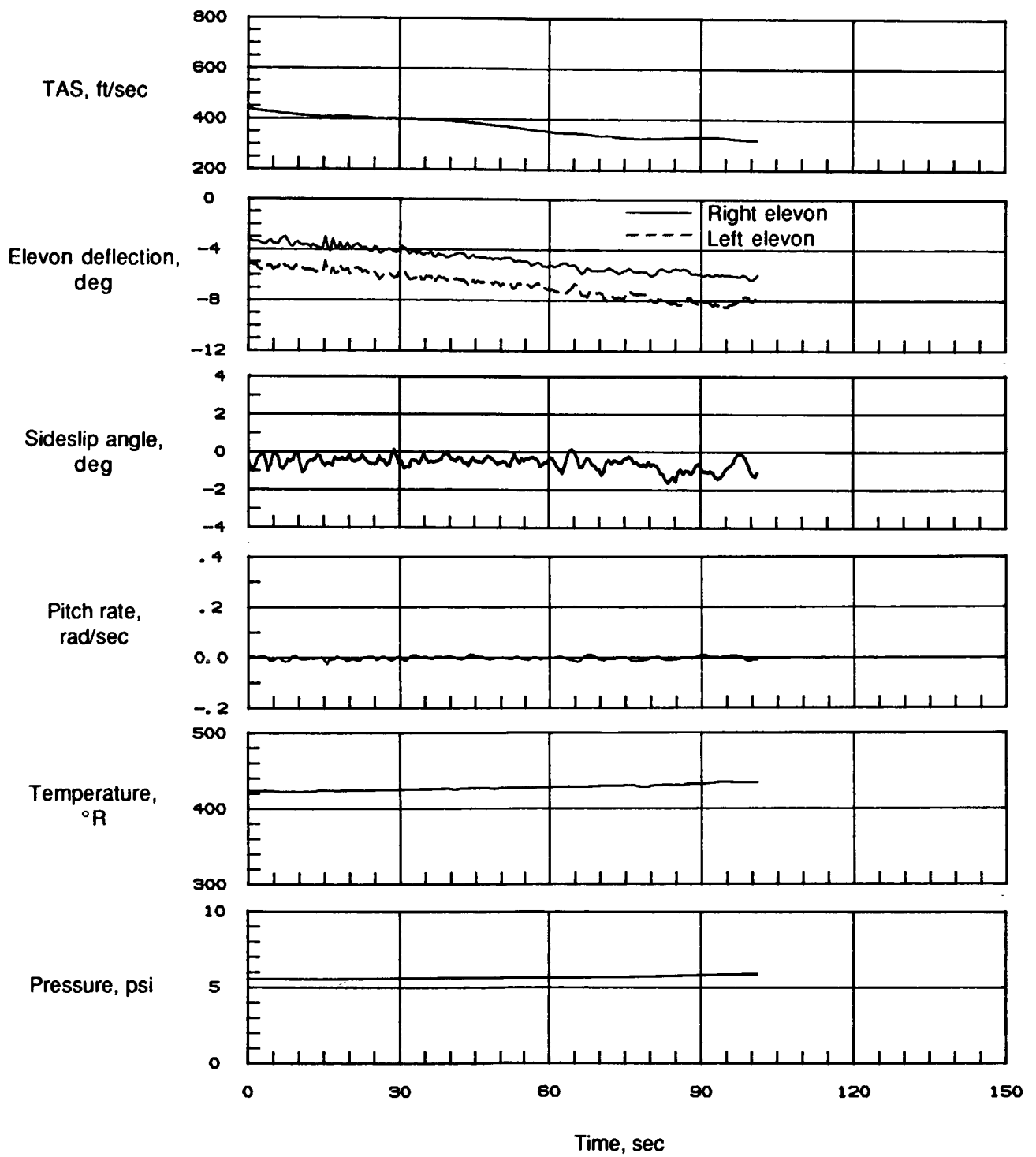


Figure 29. Concluded.

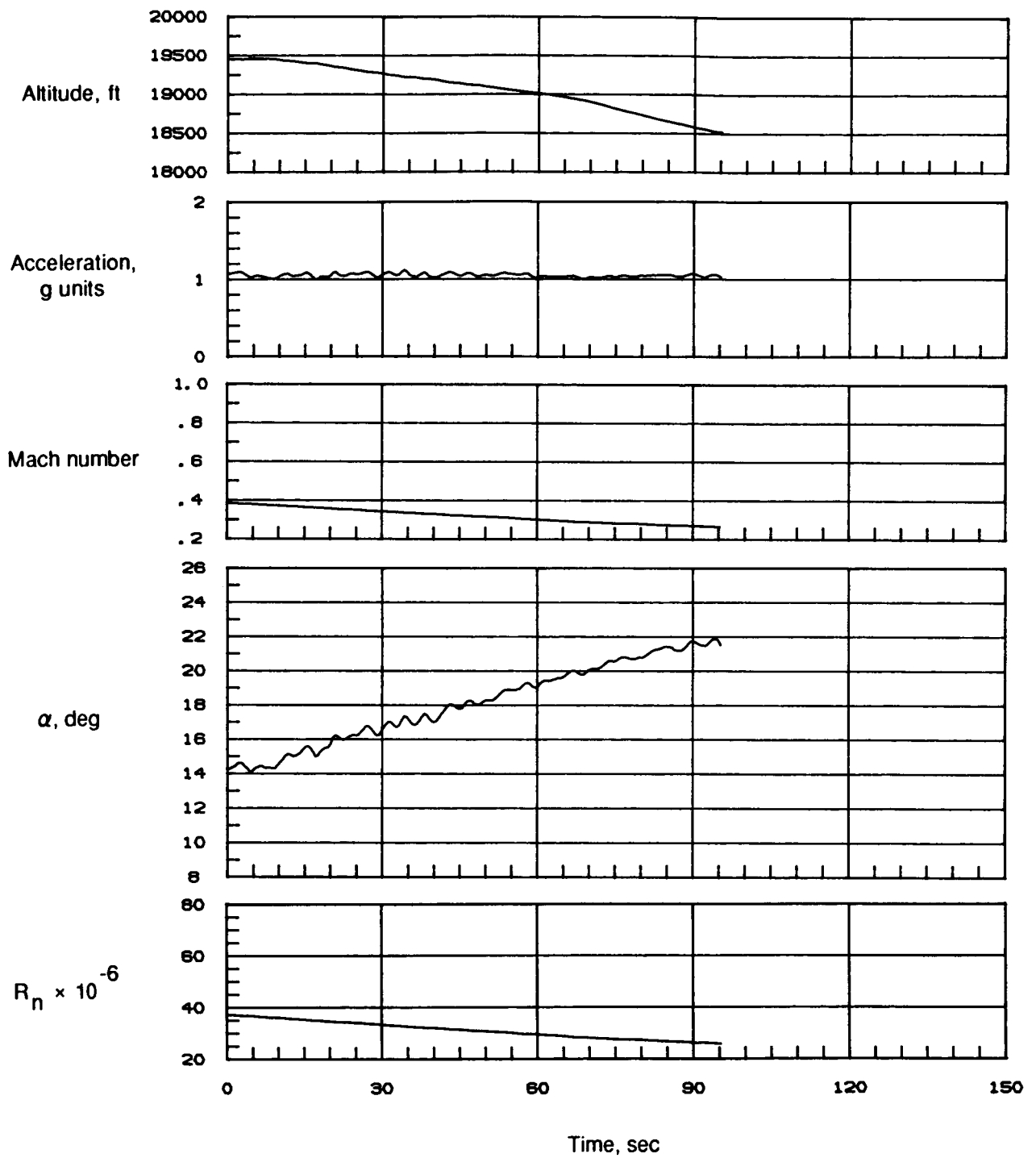


Figure 30. Time history of selected flight parameters for 1g deceleration at 20 000 ft (85-010/07).

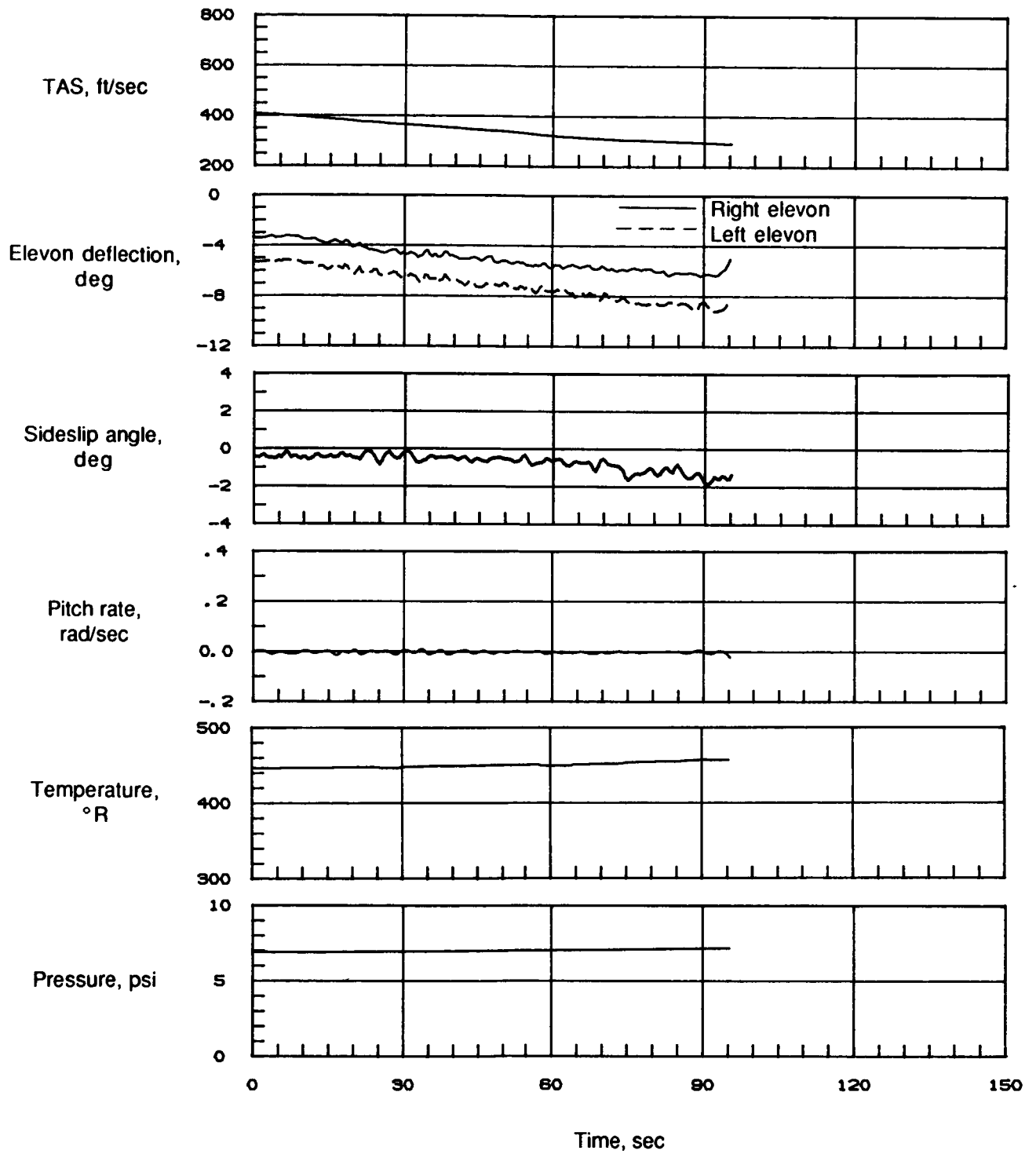


Figure 30. Concluded.

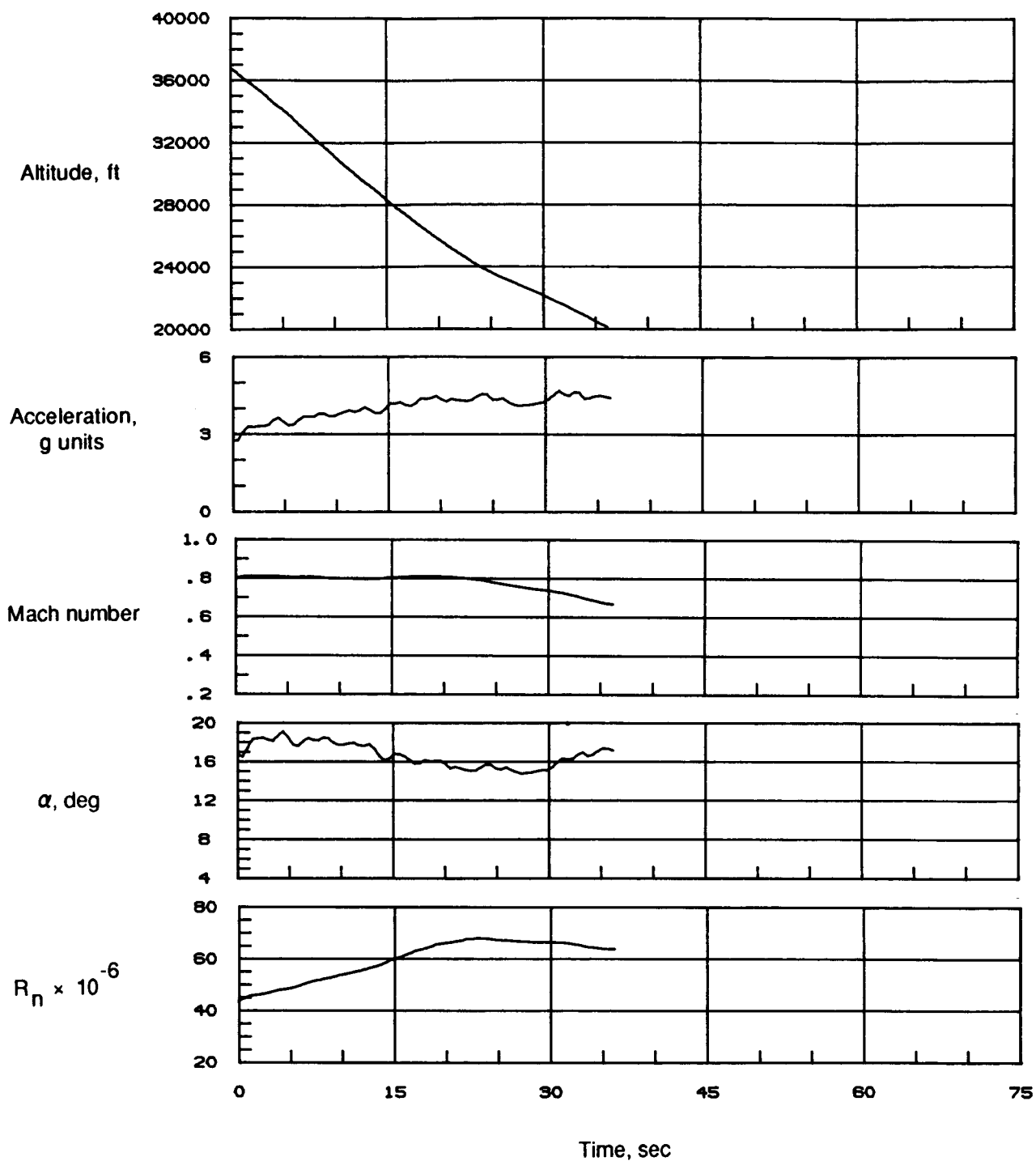


Figure 31. Time history of selected flight parameters at high-g during left spiral descent (85-010/08).

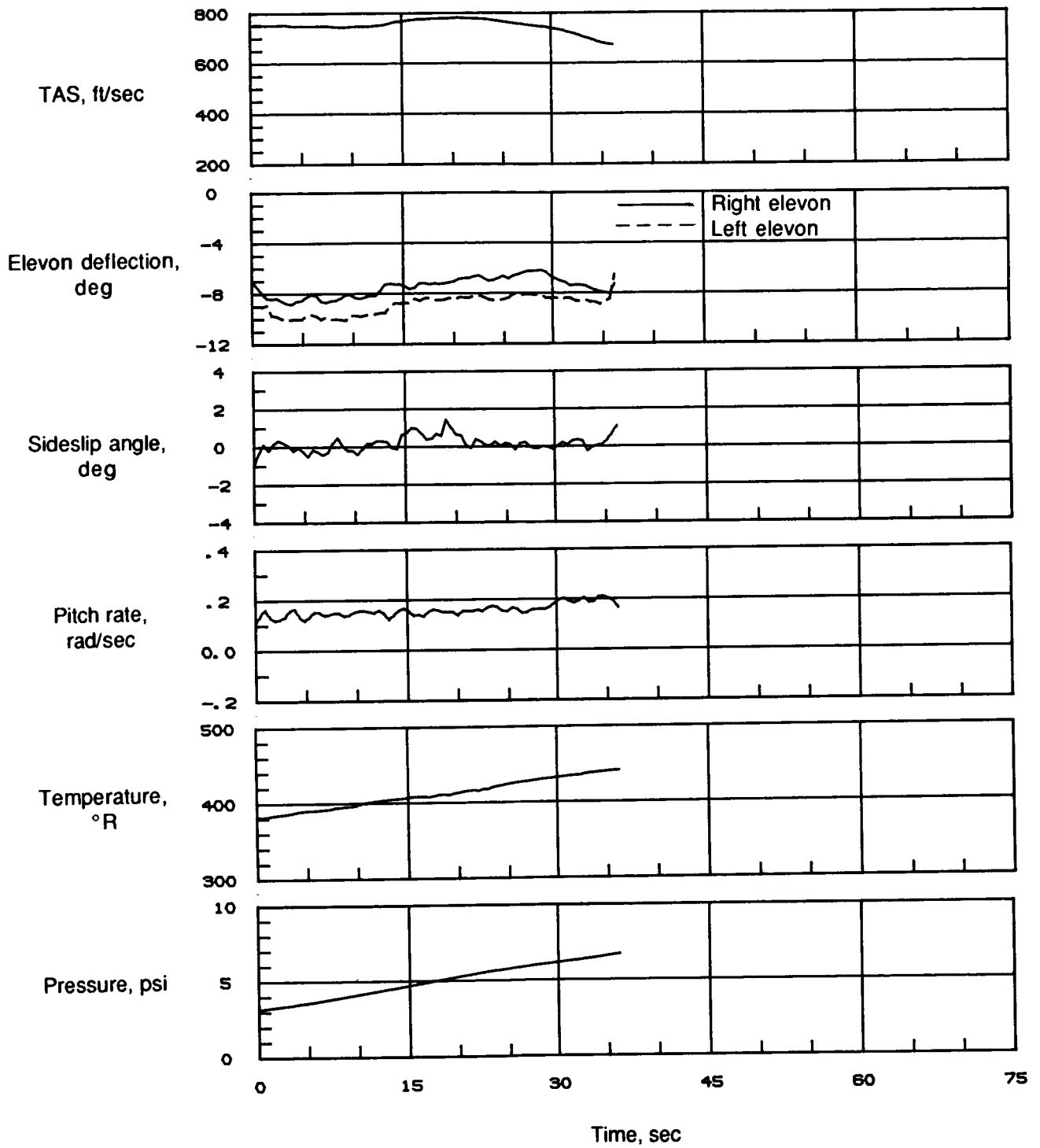


Figure 31. Concluded.

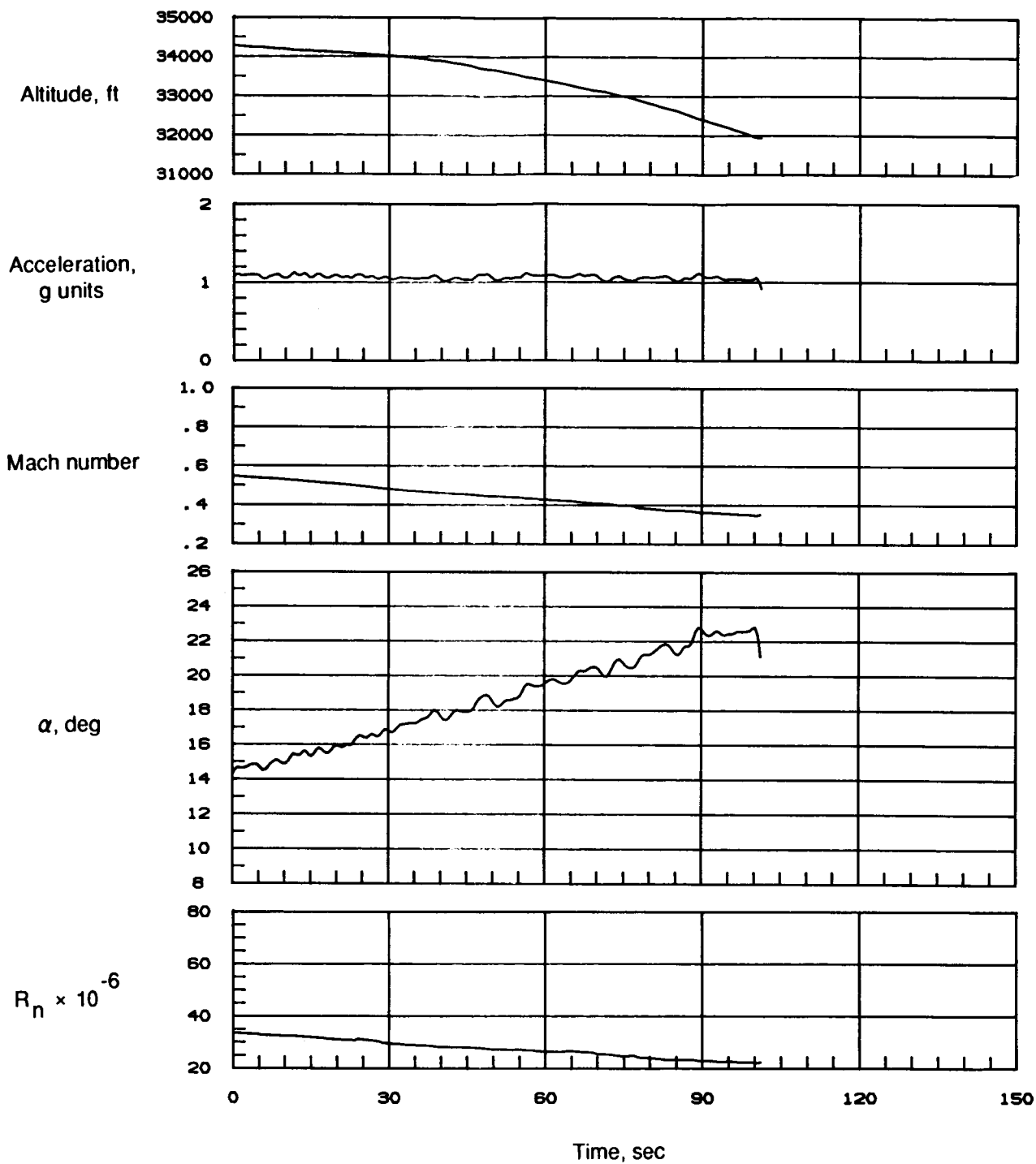


Figure 32. Time history of selected flight parameters for 1g deceleration at 35 000 ft (85-011/03).

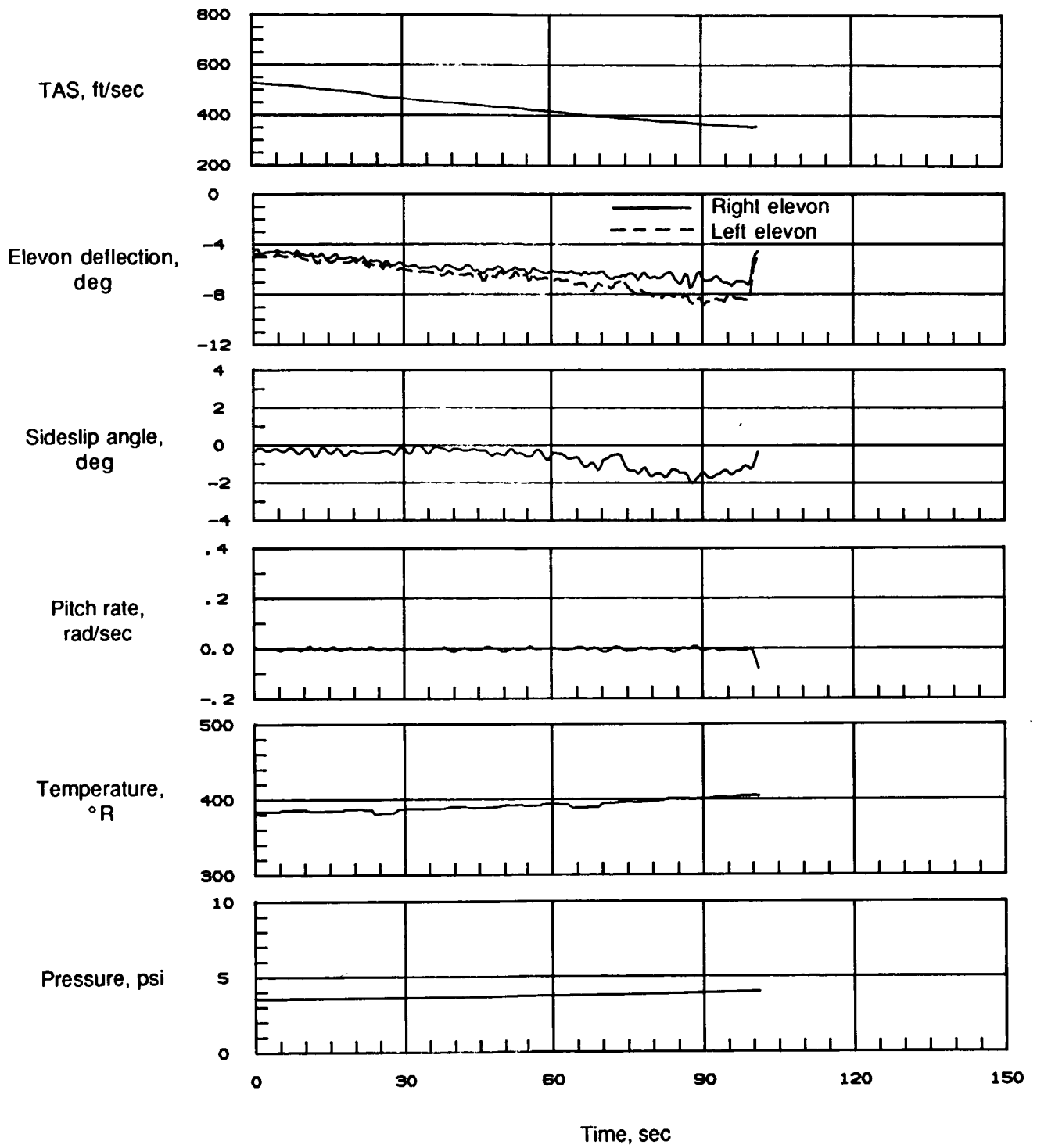


Figure 32. Concluded.

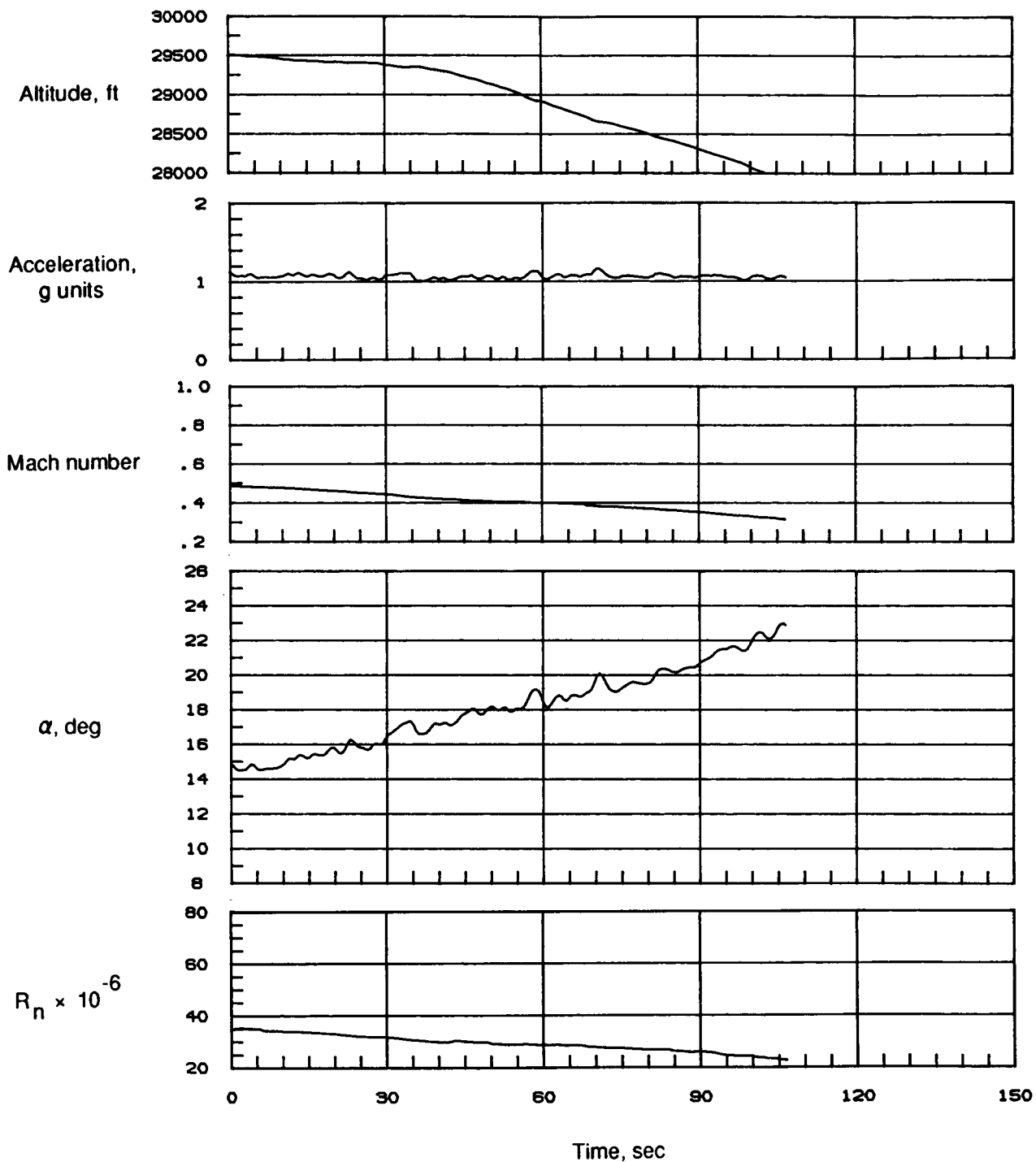


Figure 33. Time history of selected flight parameters for 1g deceleration at 30 000 ft (85-011/04).

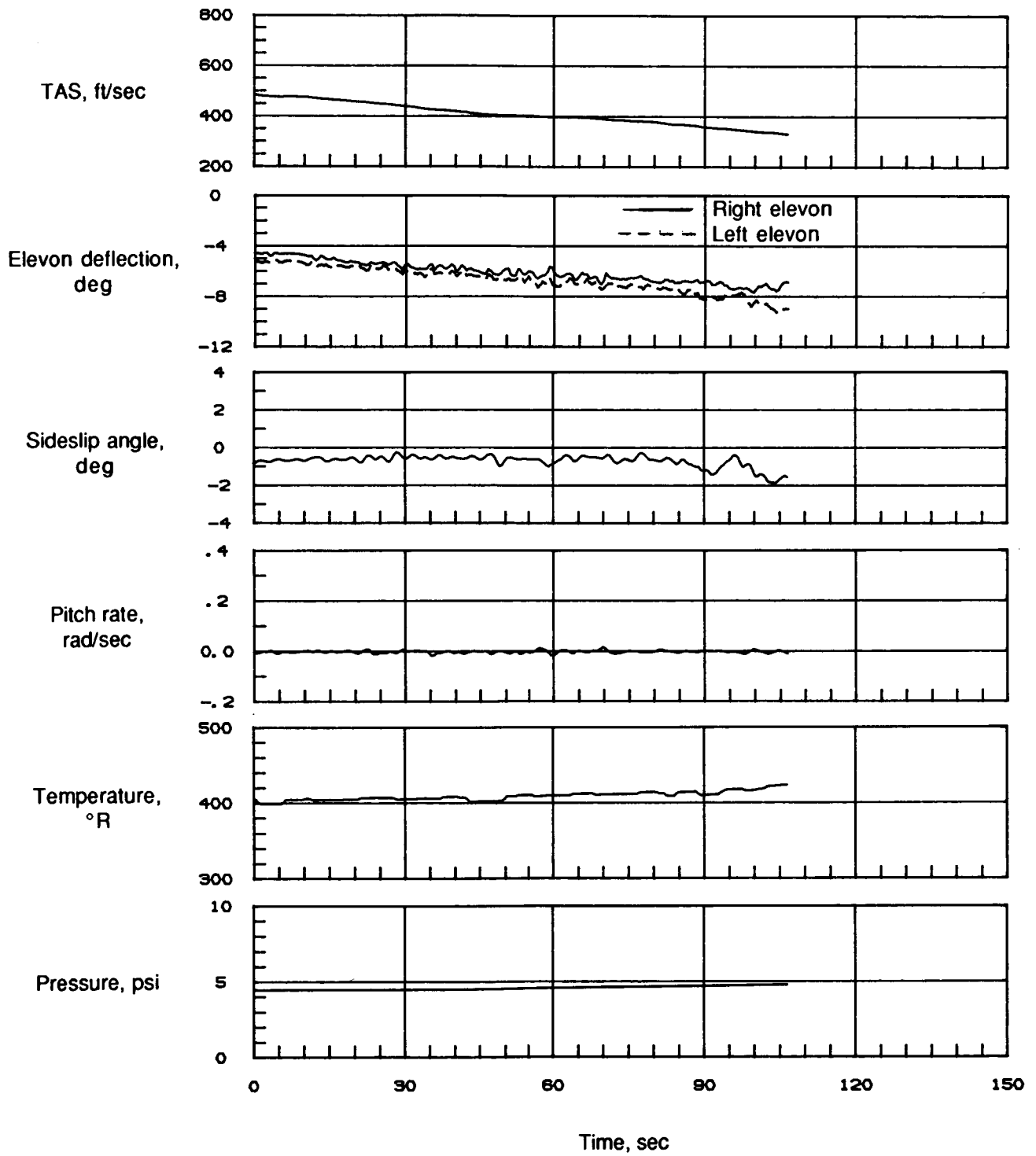


Figure 33. Concluded.

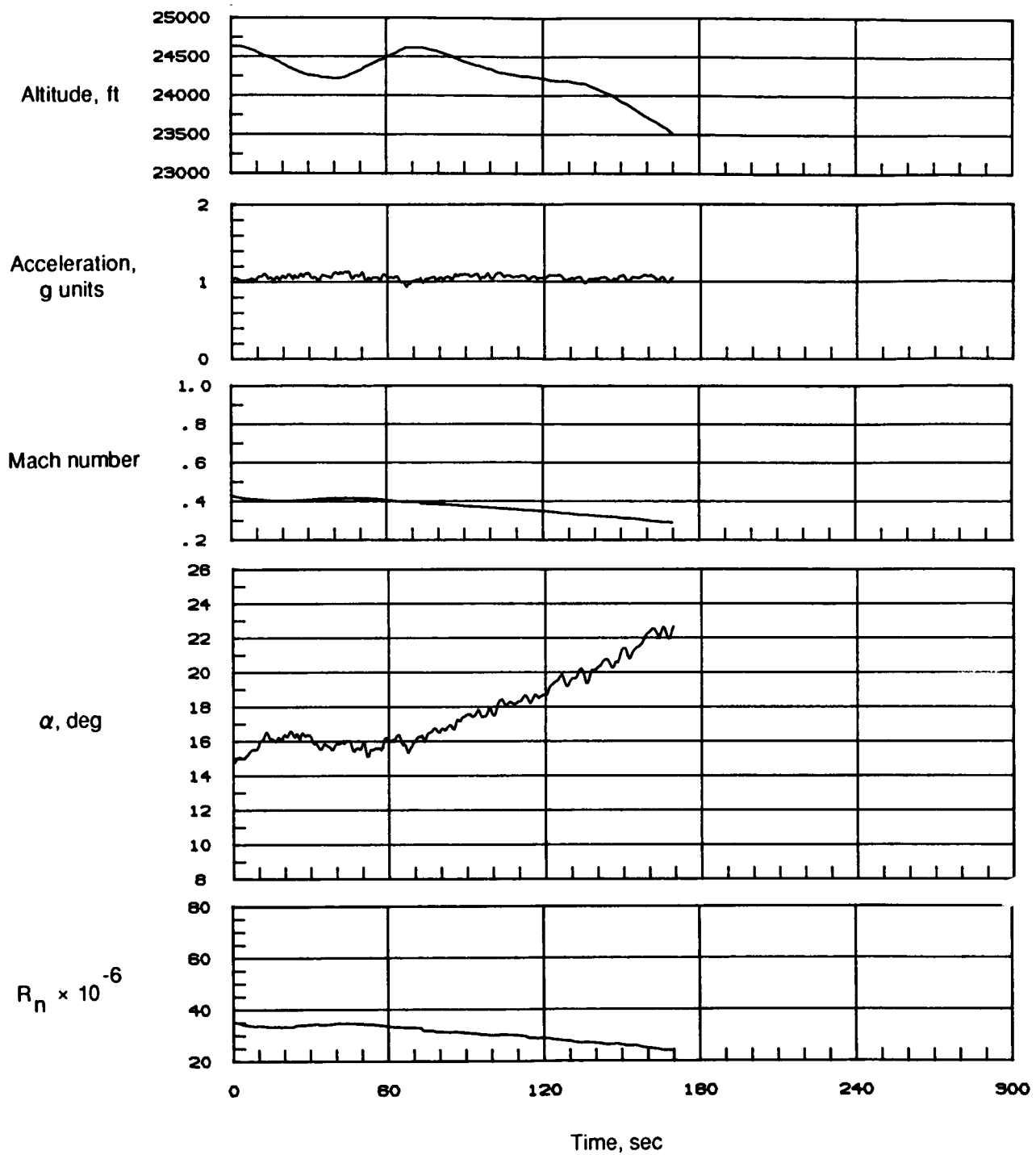


Figure 34. Time history of selected flight parameters for 1g deceleration at 25 000 ft (85-011/05).

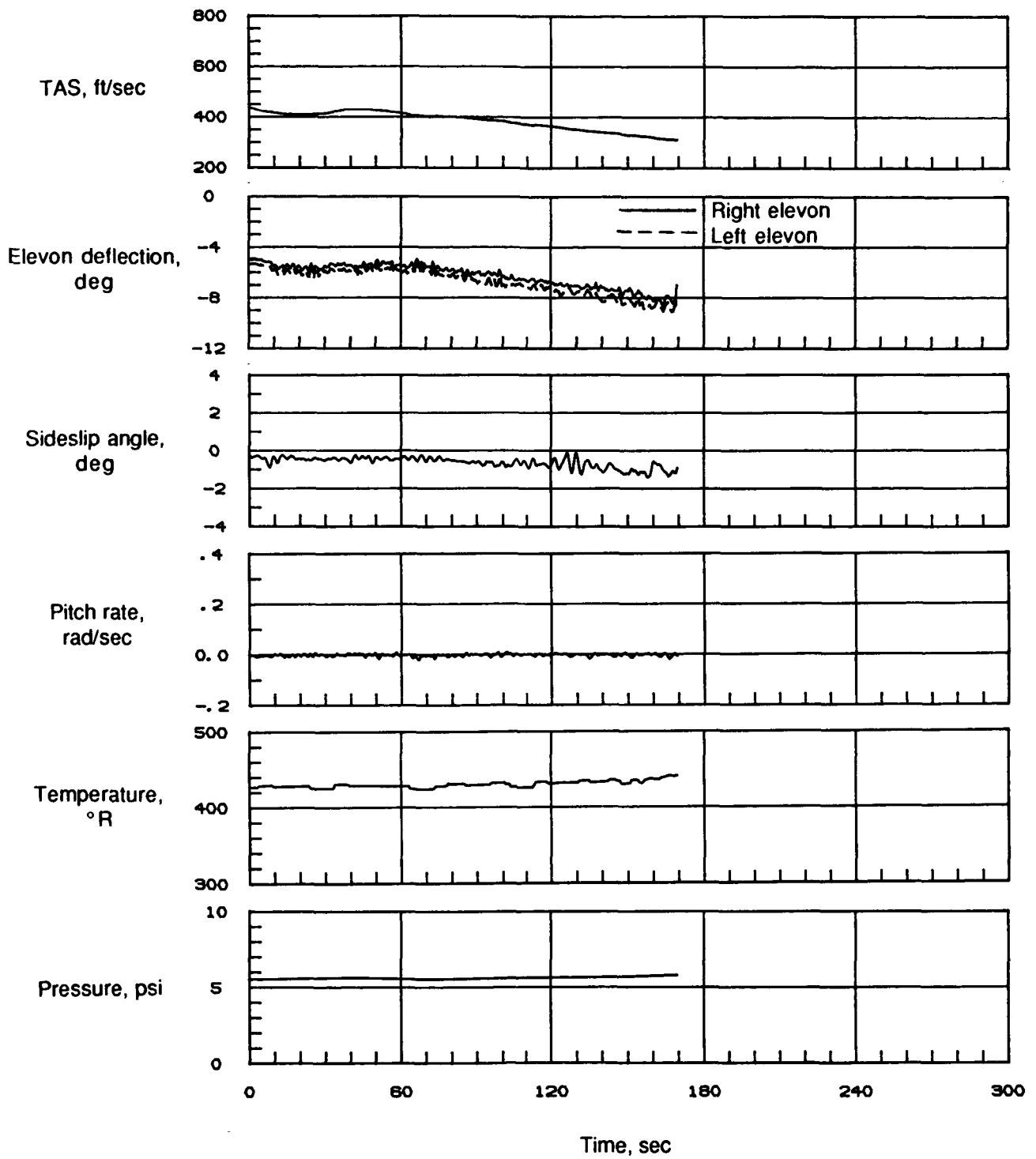


Figure 34. Concluded.

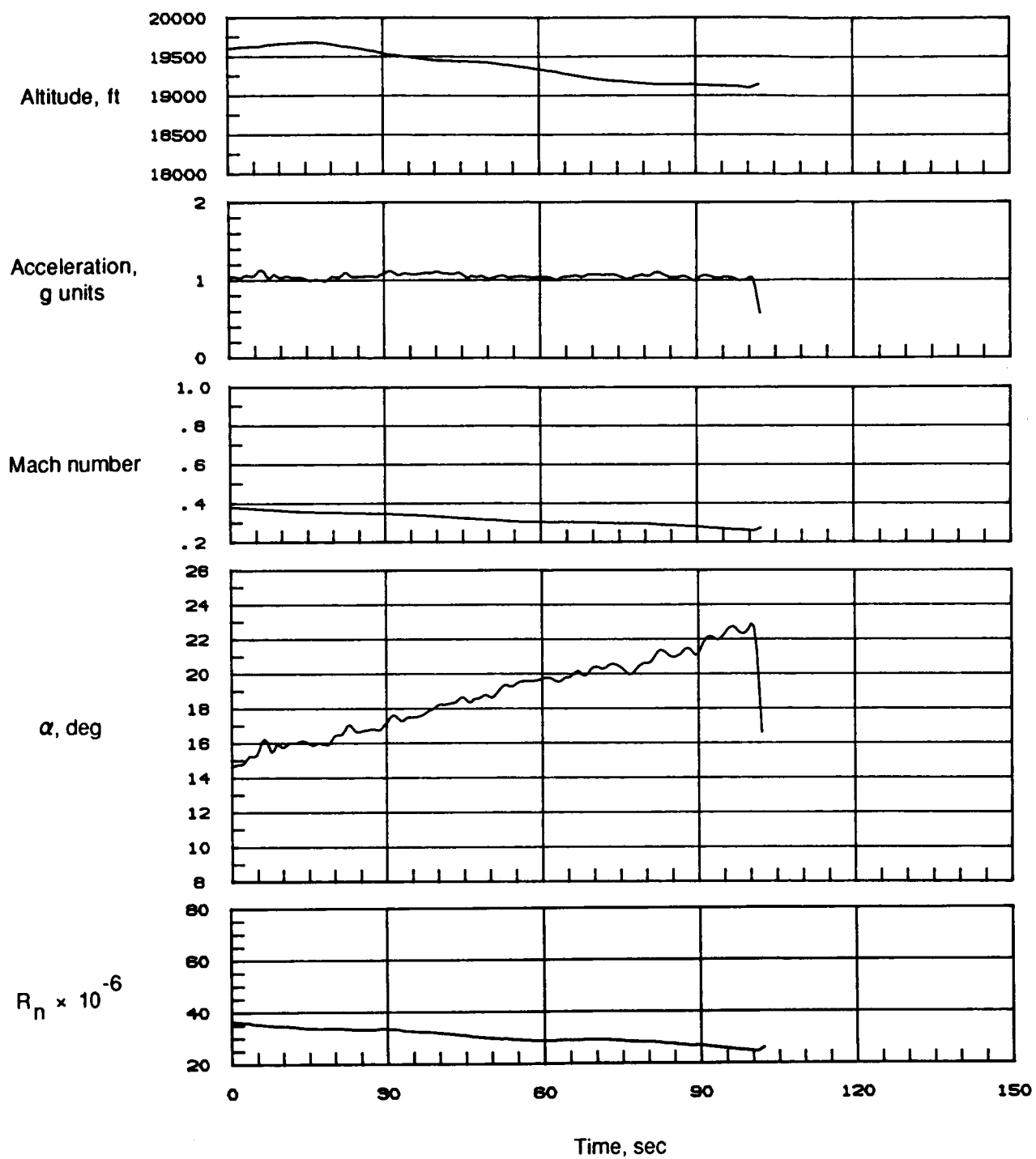


Figure 35. Time history of selected flight parameters for 1g deceleration at 20 000 ft (85-011/06).

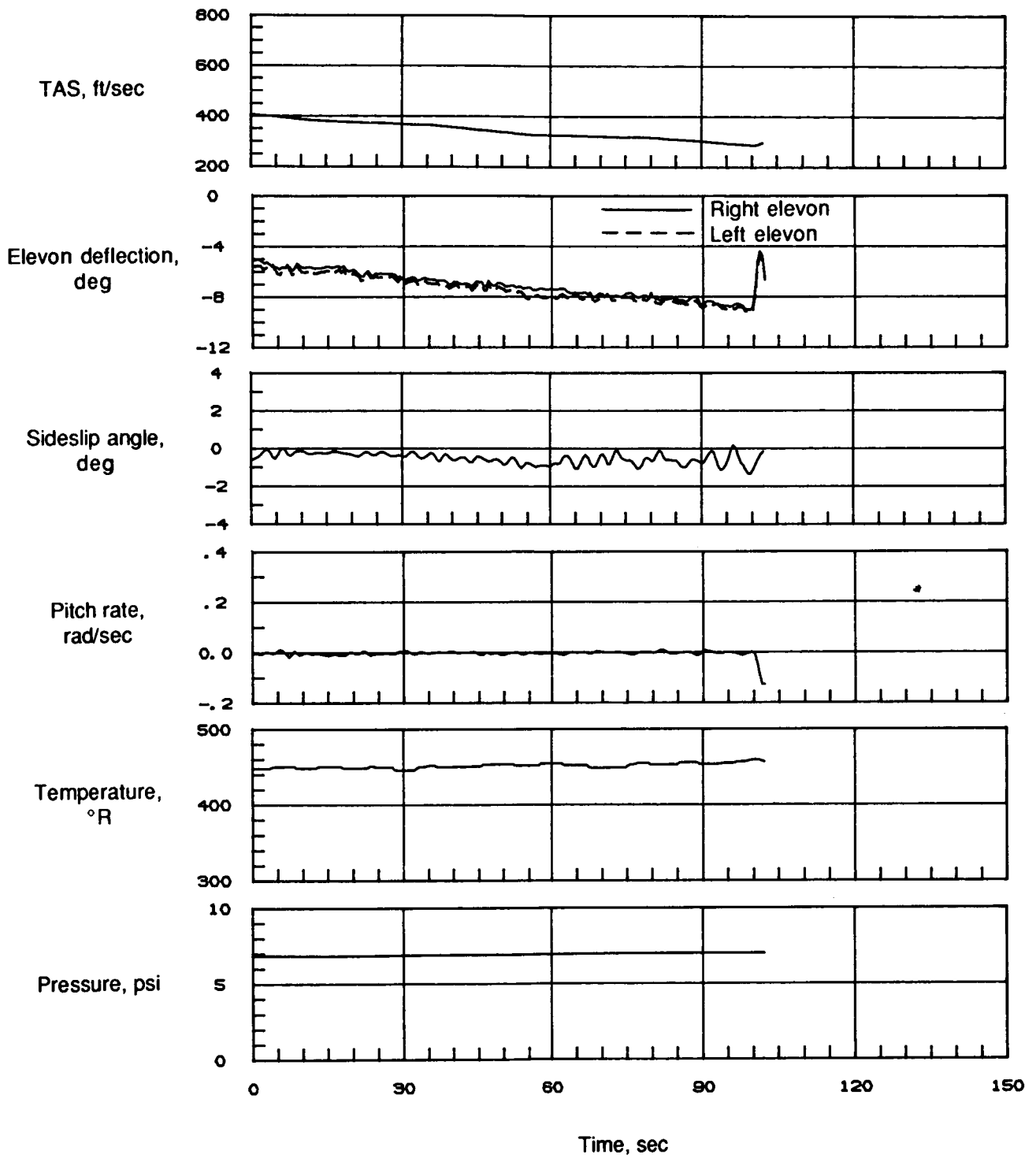


Figure 35. Concluded.

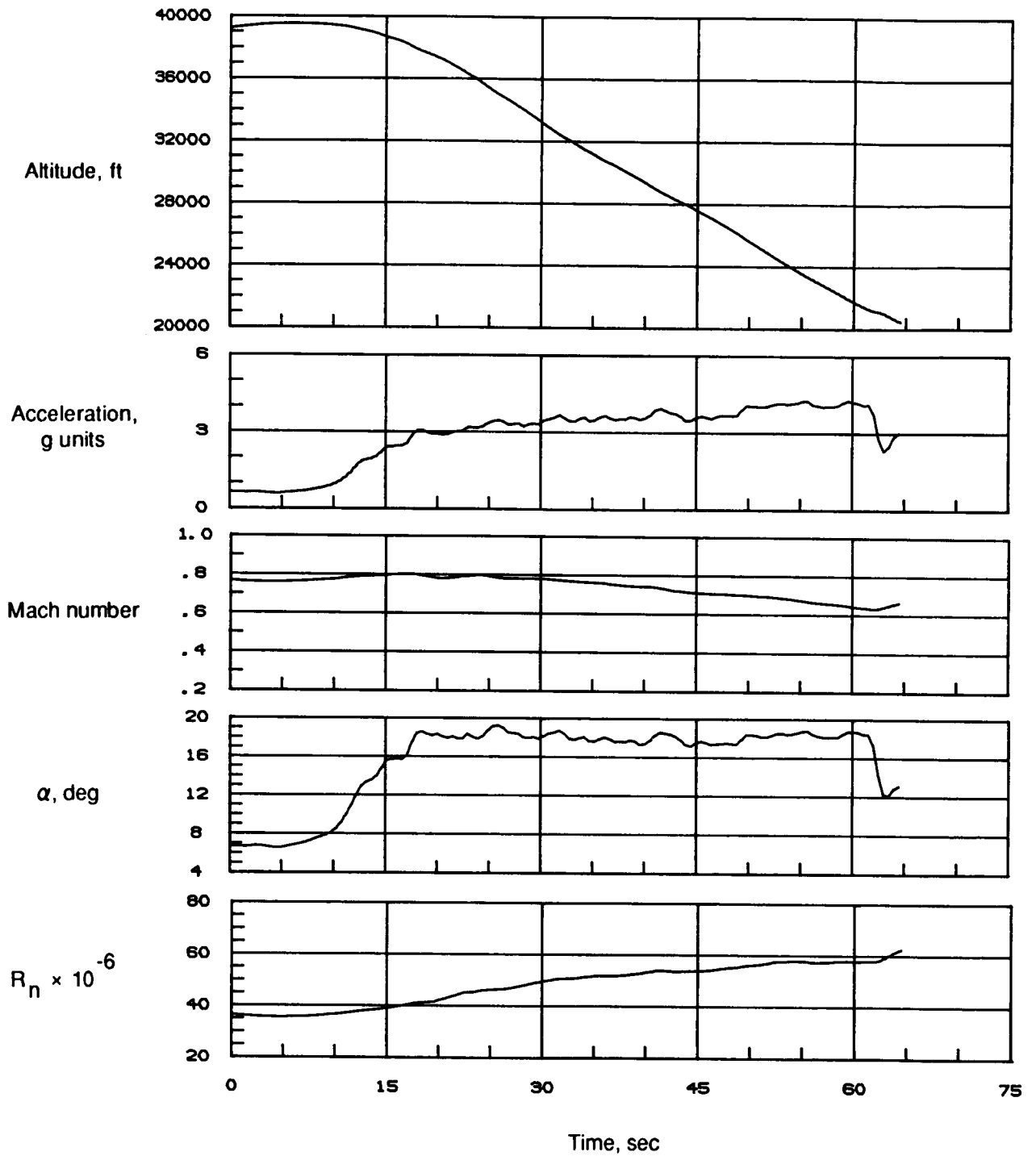


Figure 36. Time history of selected flight parameters at high-g during left spiral descent (85-011/08).

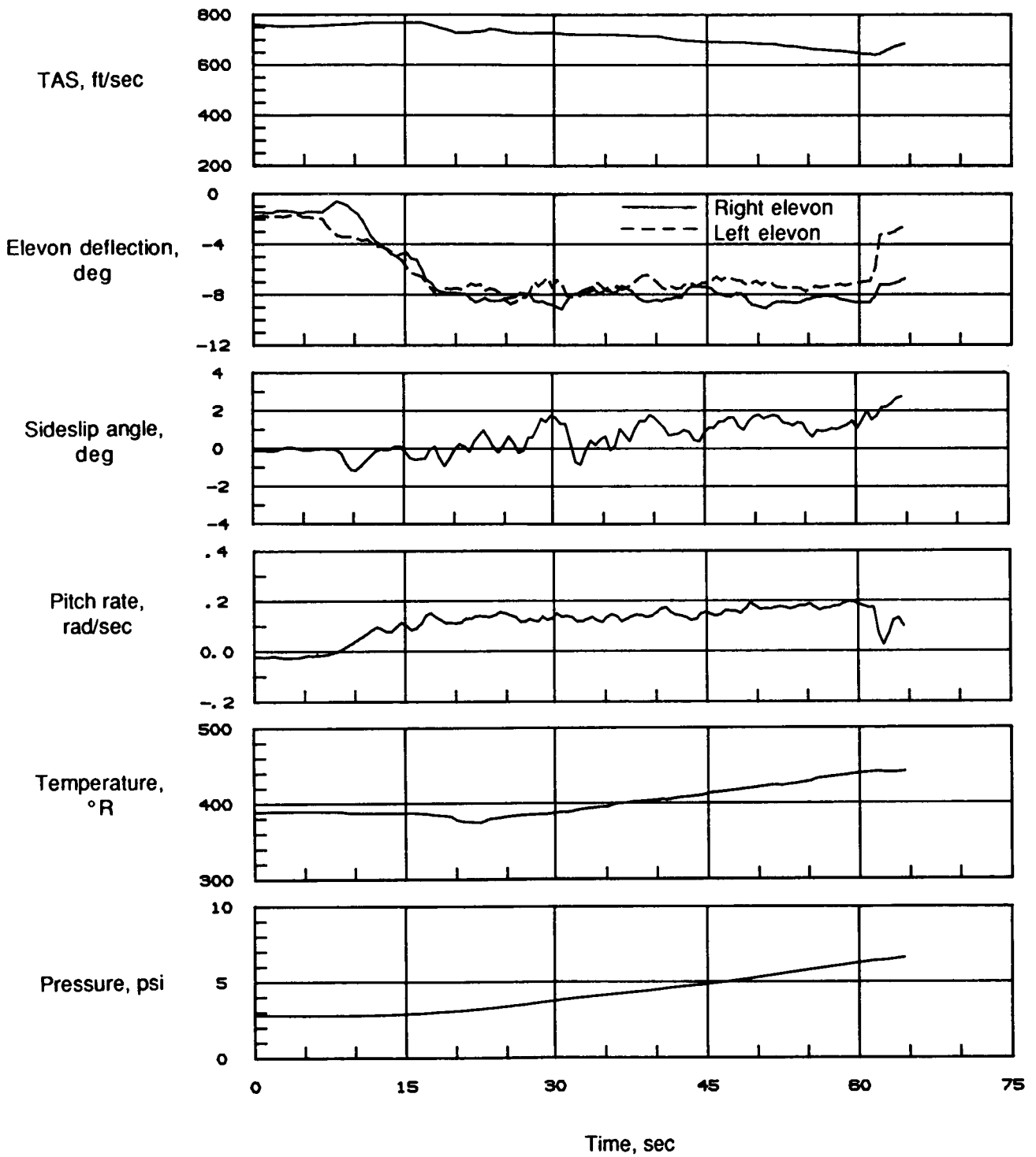


Figure 36. Concluded.

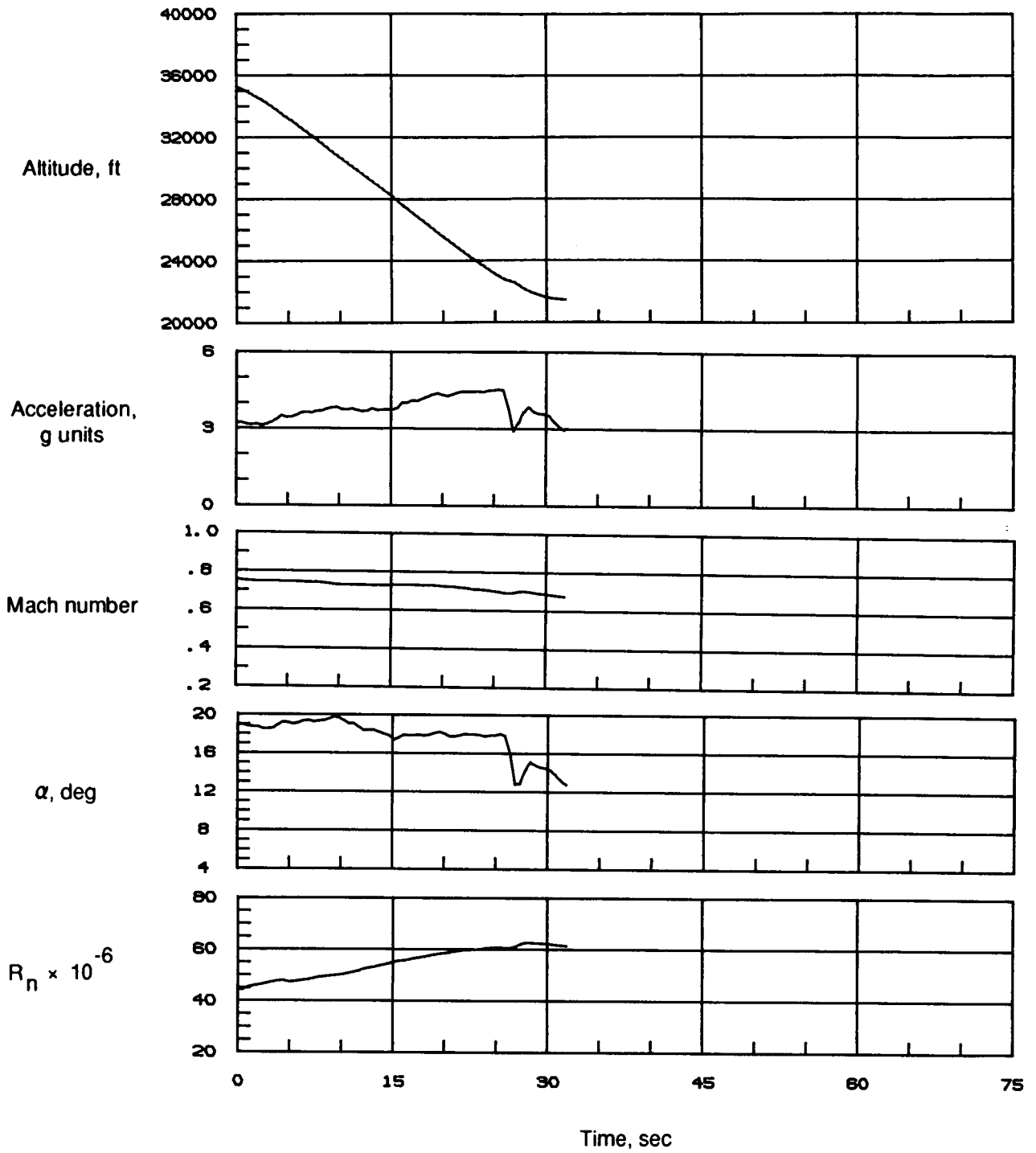


Figure 37. Time history of selected flight parameters at high-g during right spiral descent (85-011/09).

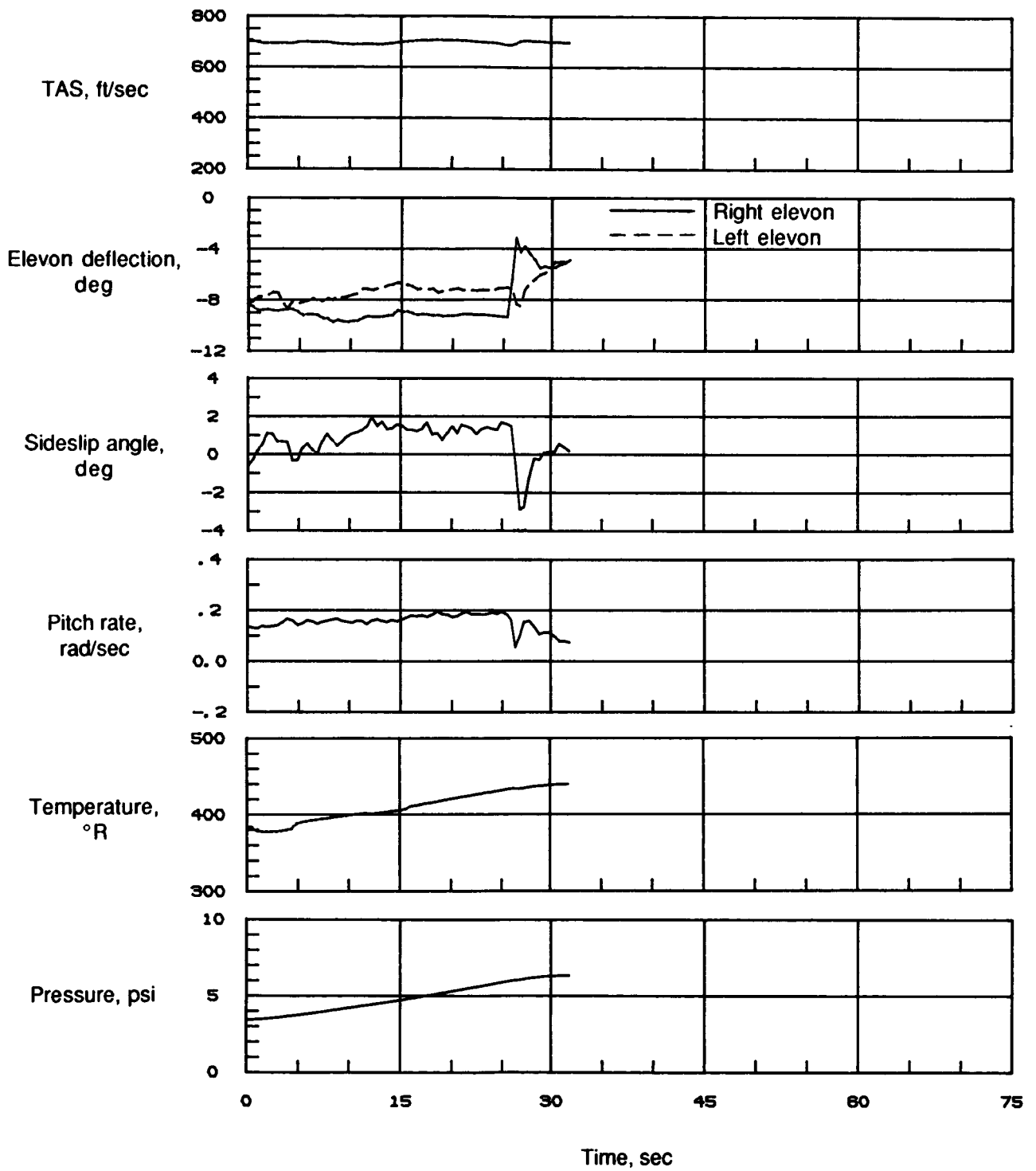


Figure 37. Concluded.

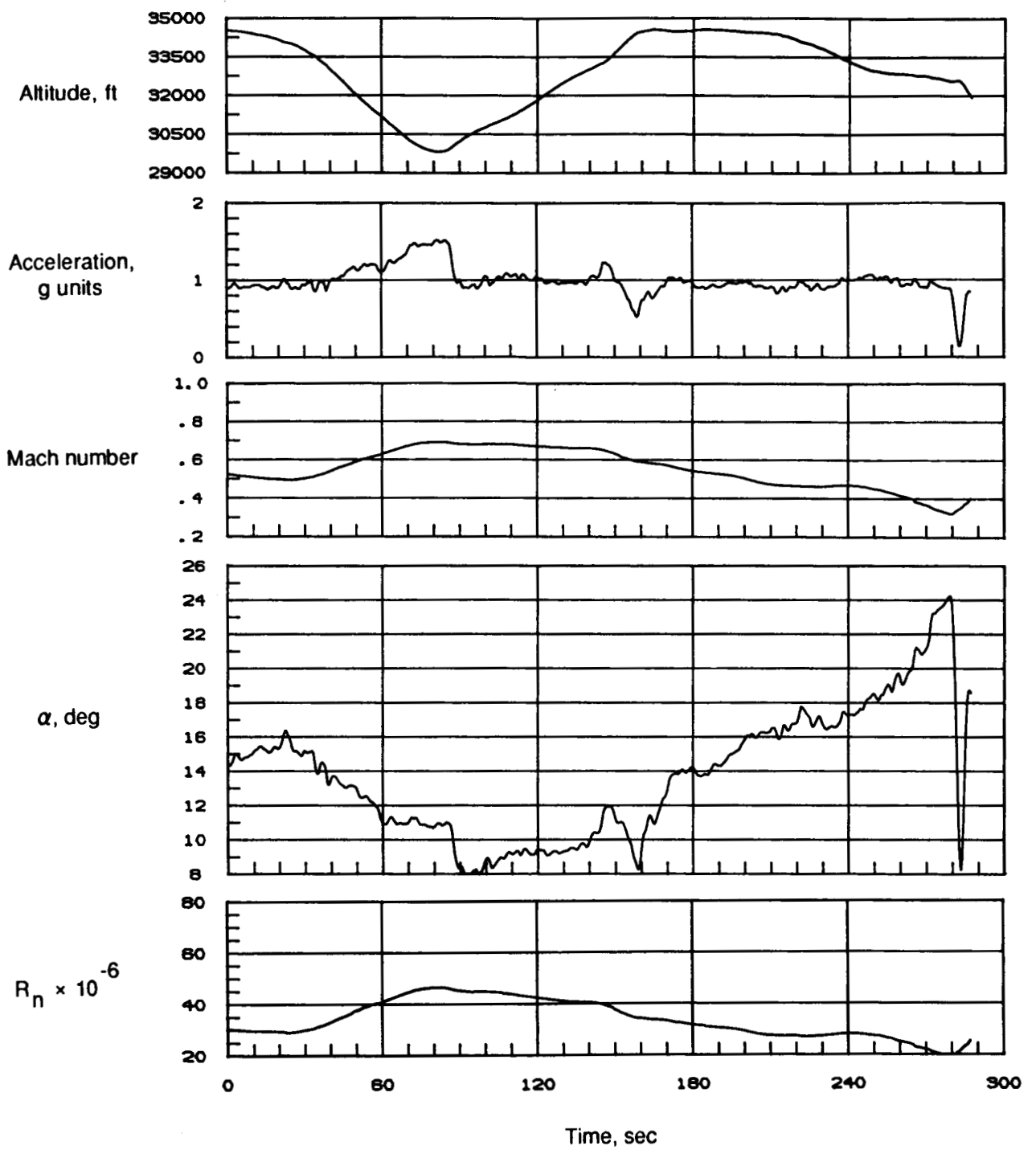


Figure 38. Time history of selected flight parameters for 1g deceleration at 35 000 ft (85-012/04).

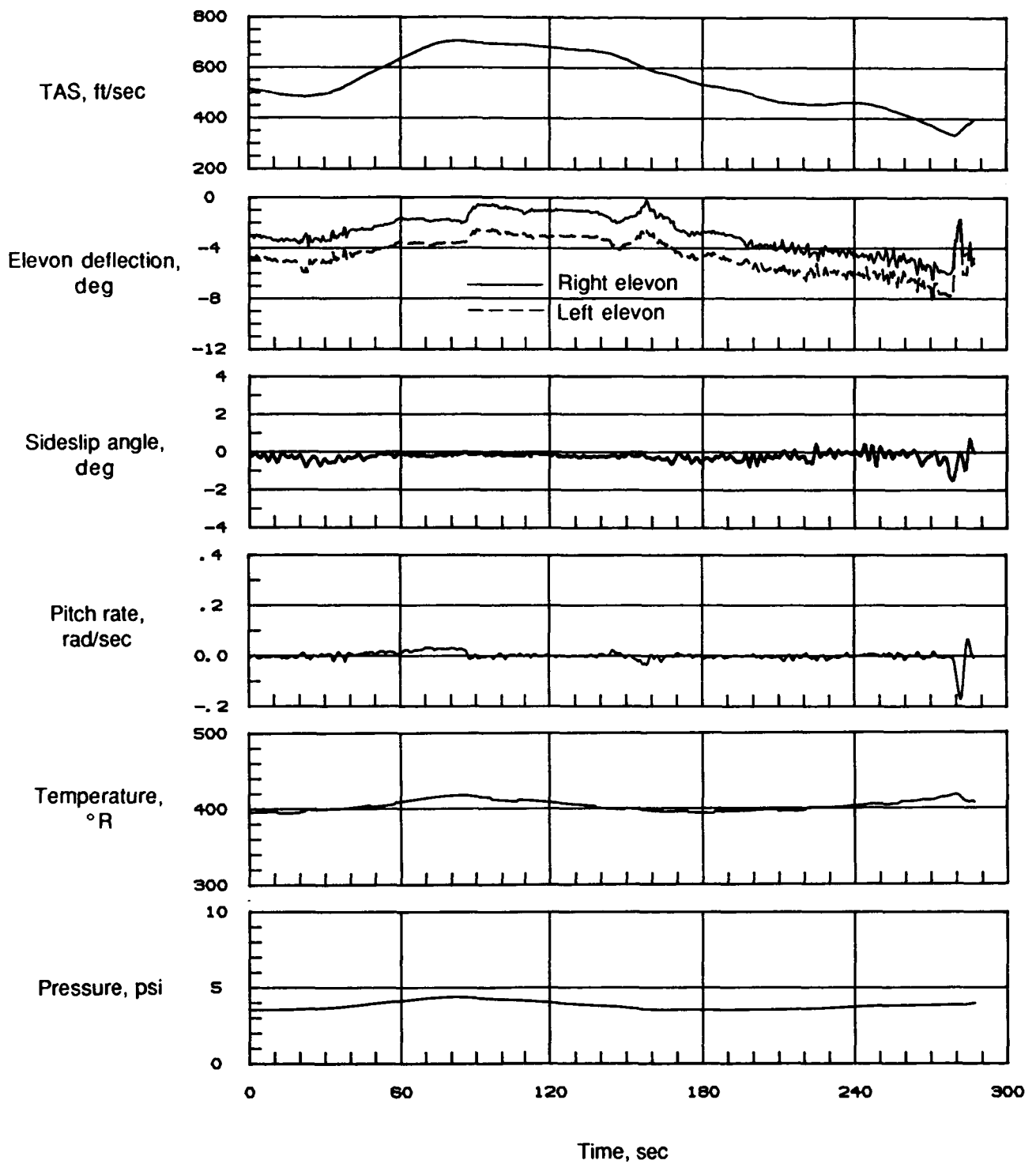


Figure 38. Concluded.

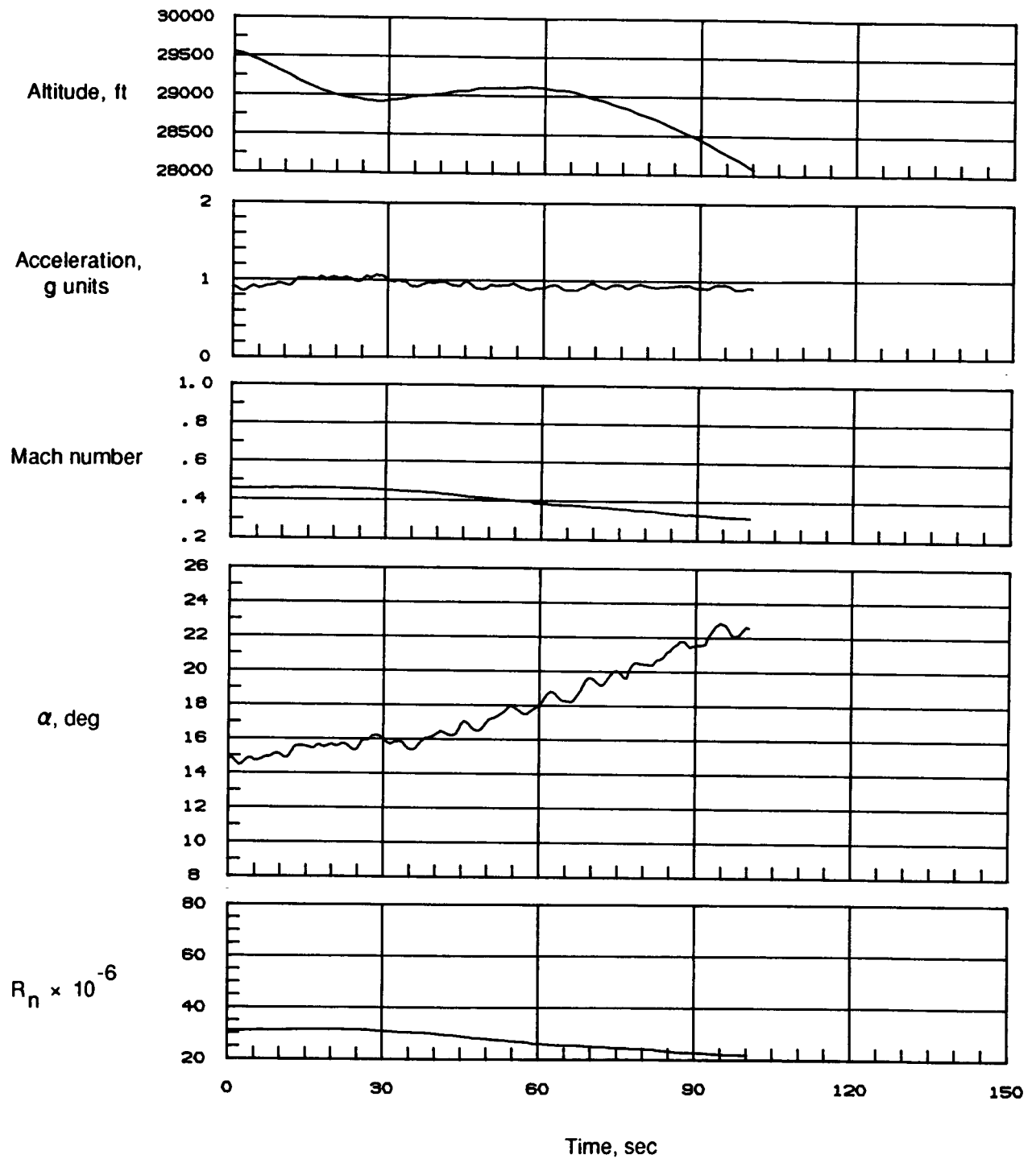


Figure 39. Time history of selected flight parameters for 1g deceleration at 30 000 ft (85-012/05).

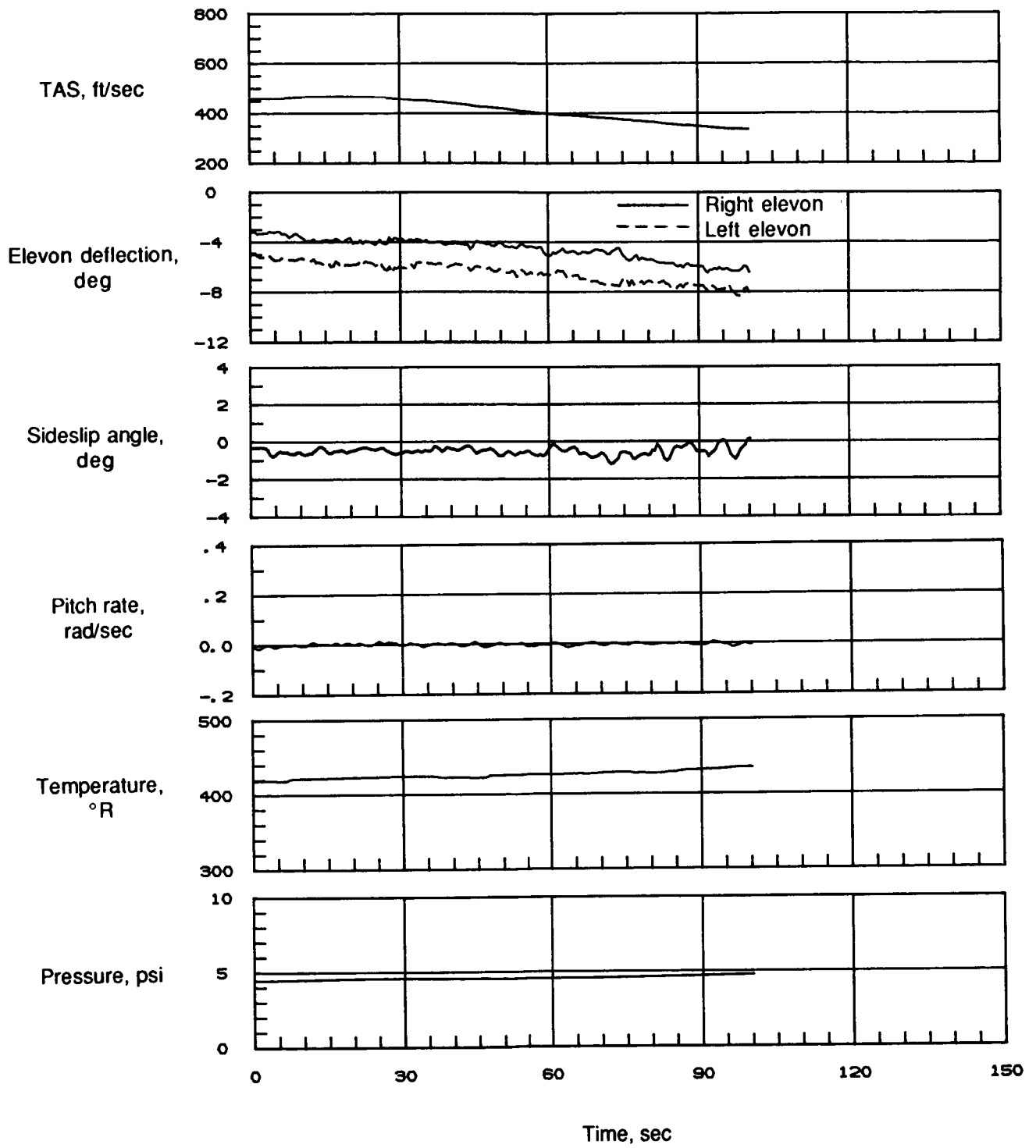


Figure 39. Concluded.

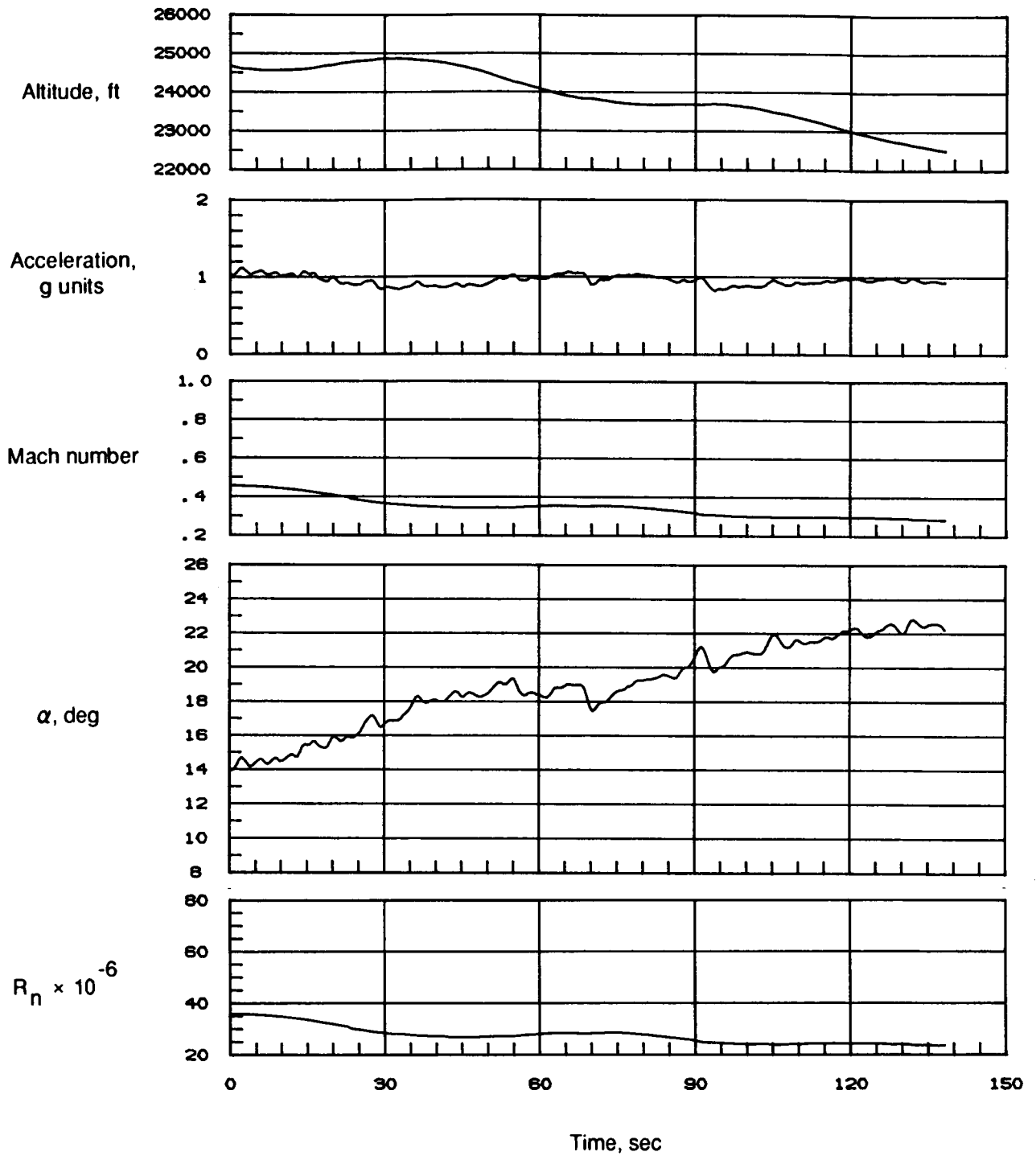


Figure 40. Time history of selected flight parameters for 1g deceleration at 25 000 ft (85-012/06).

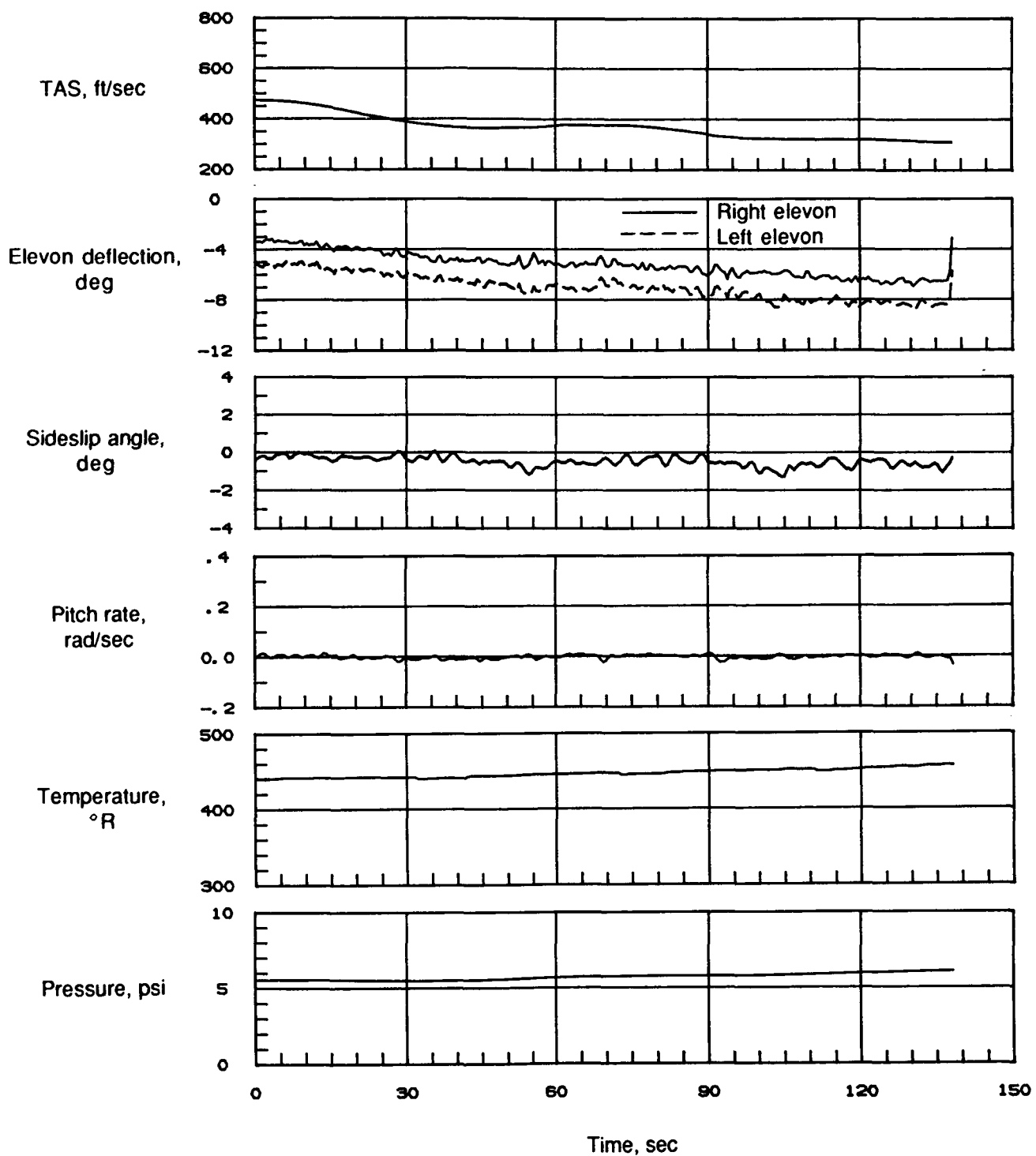


Figure 40. Concluded.

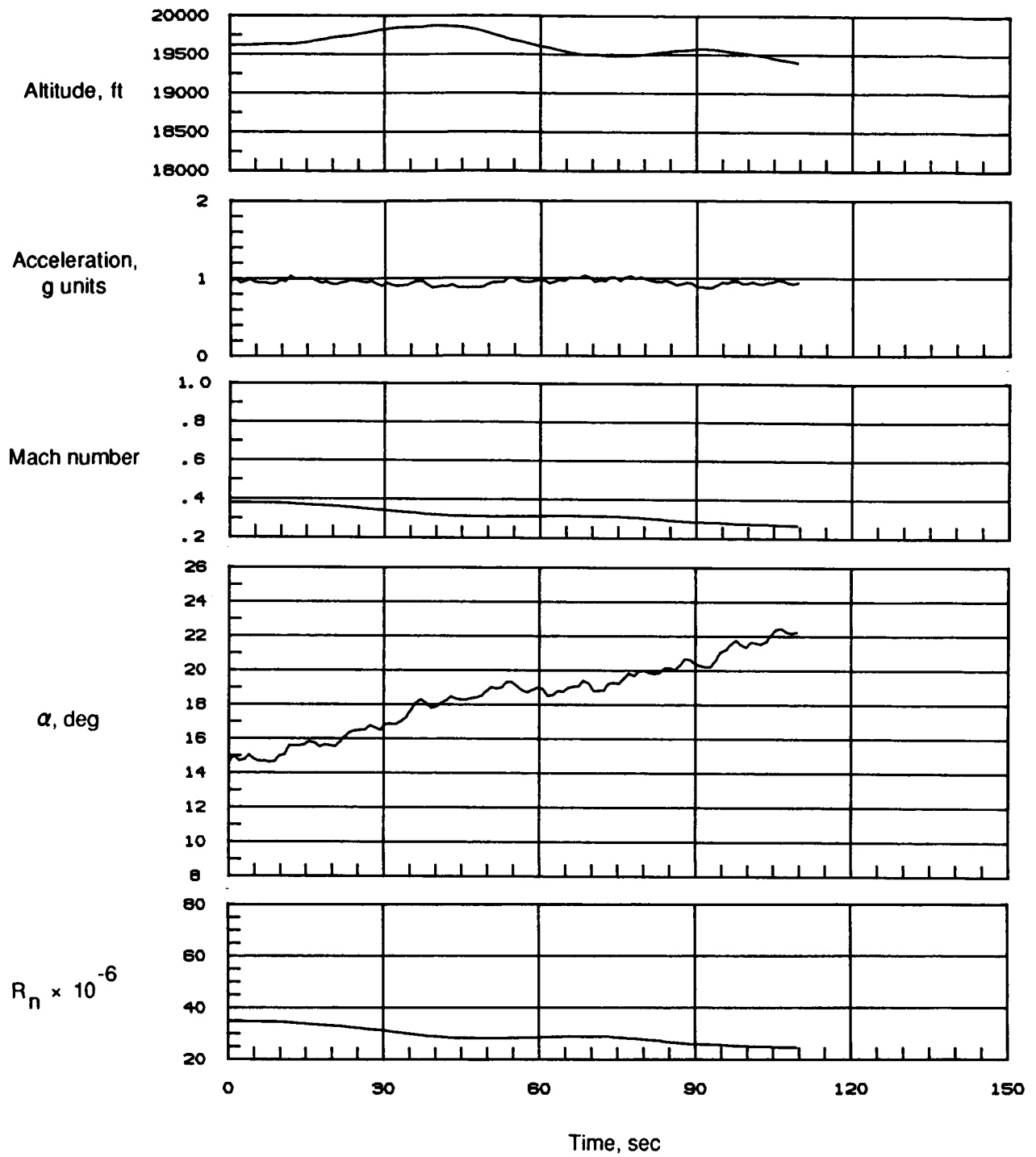


Figure 41. Time history of selected flight parameters for 1g deceleration at 20 000 ft (85-012/07).

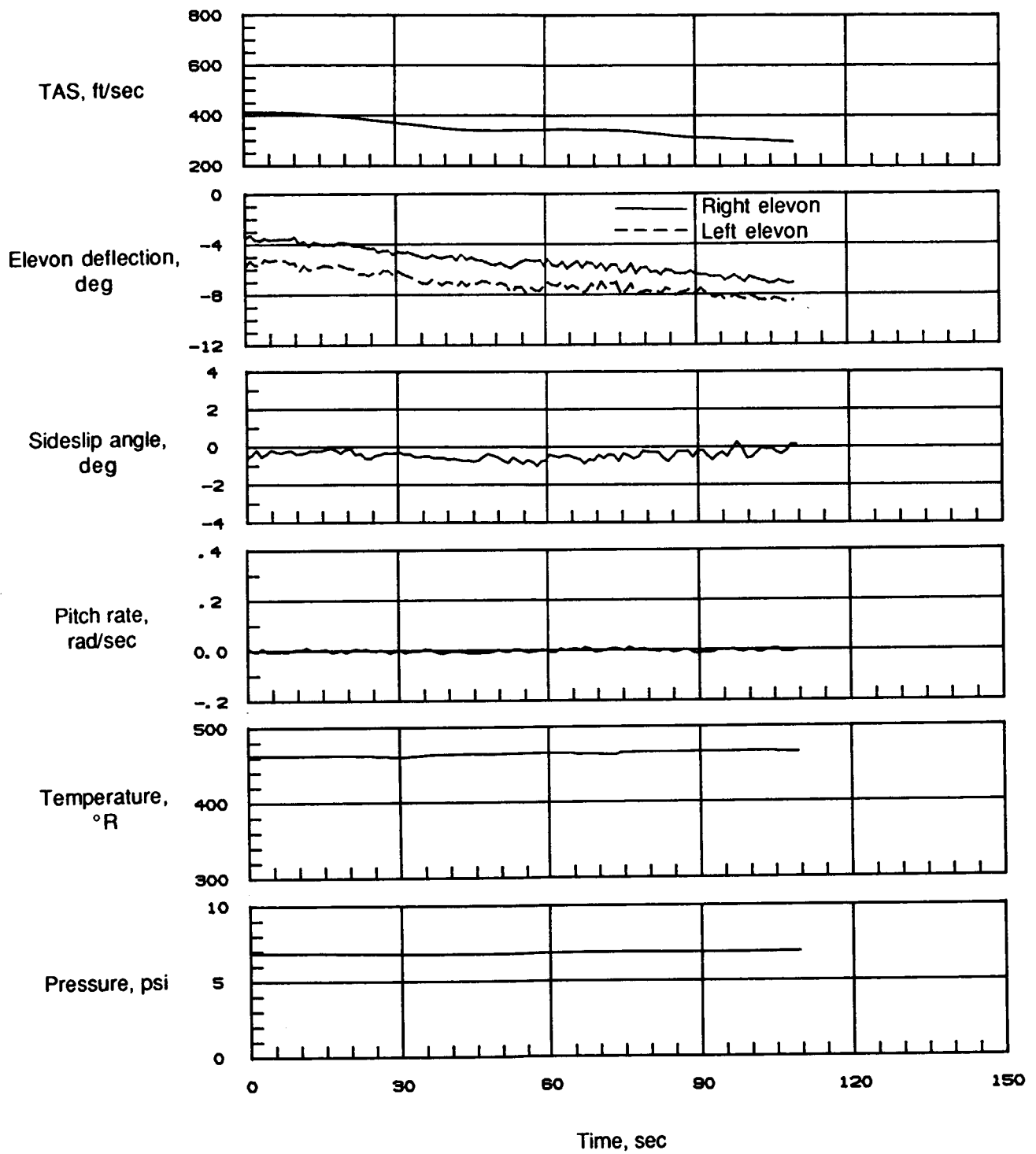


Figure 41. Concluded.

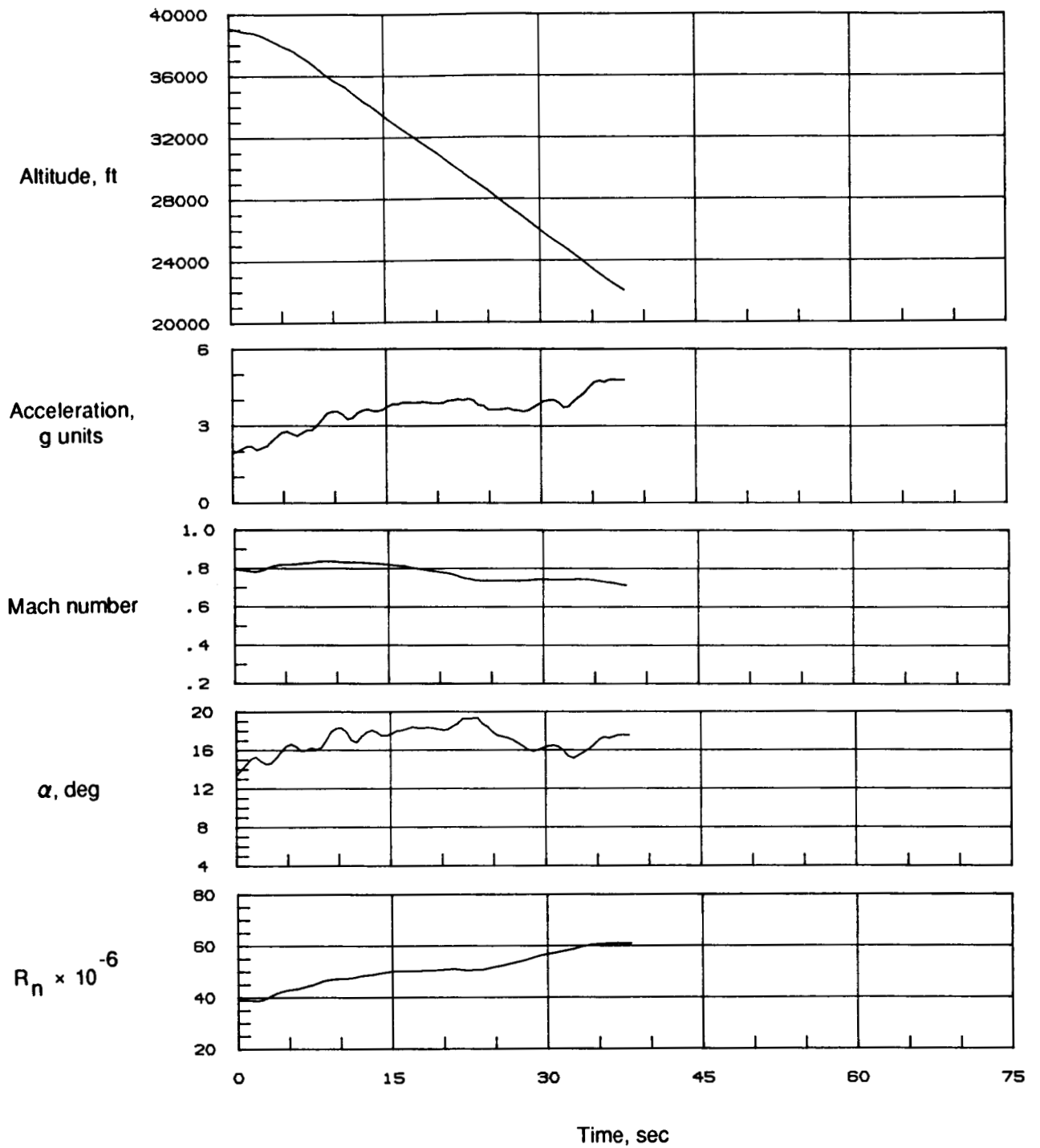


Figure 42. Time history of selected flight parameters at high-g during left spiral descent (85-012/09).

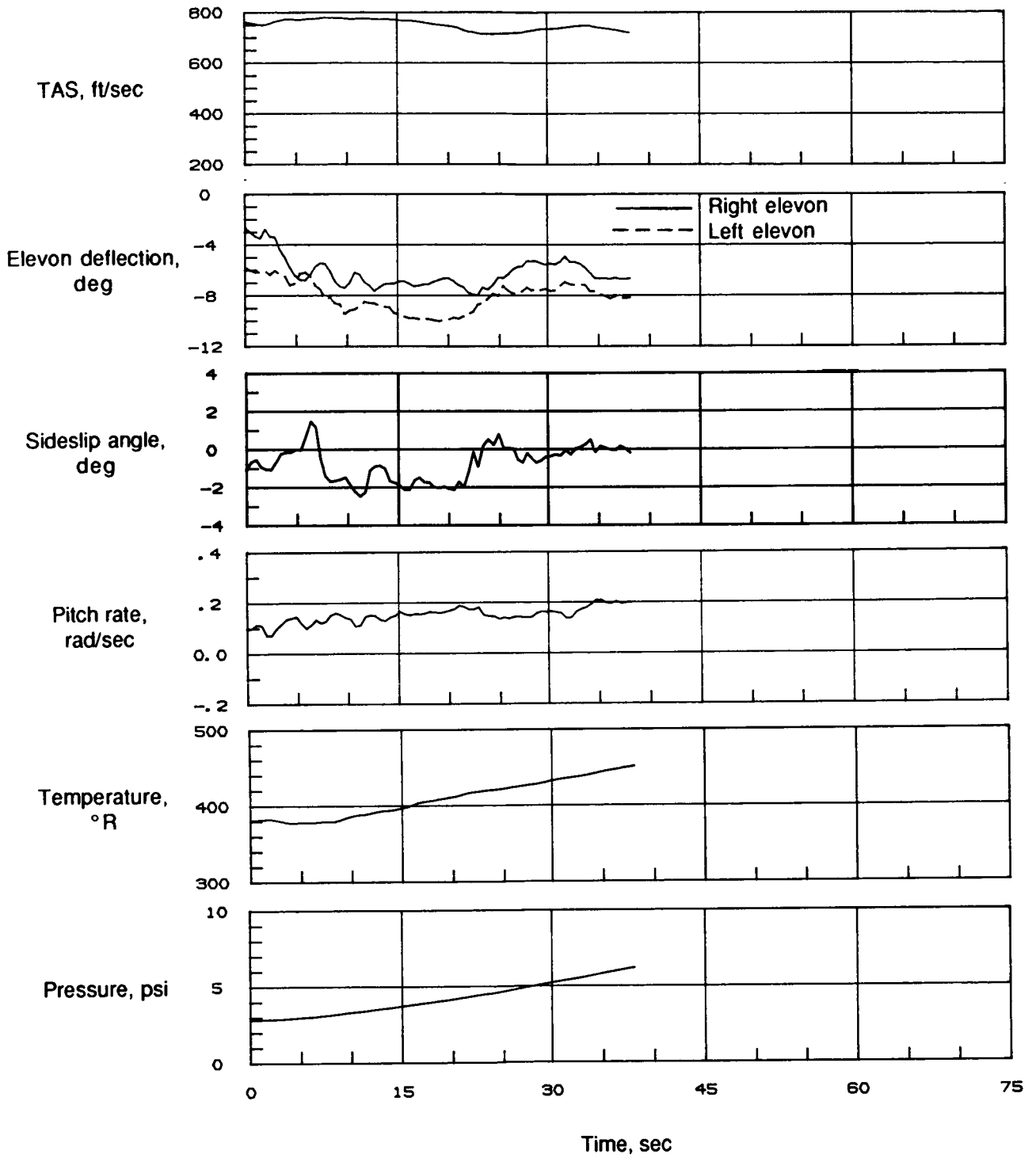
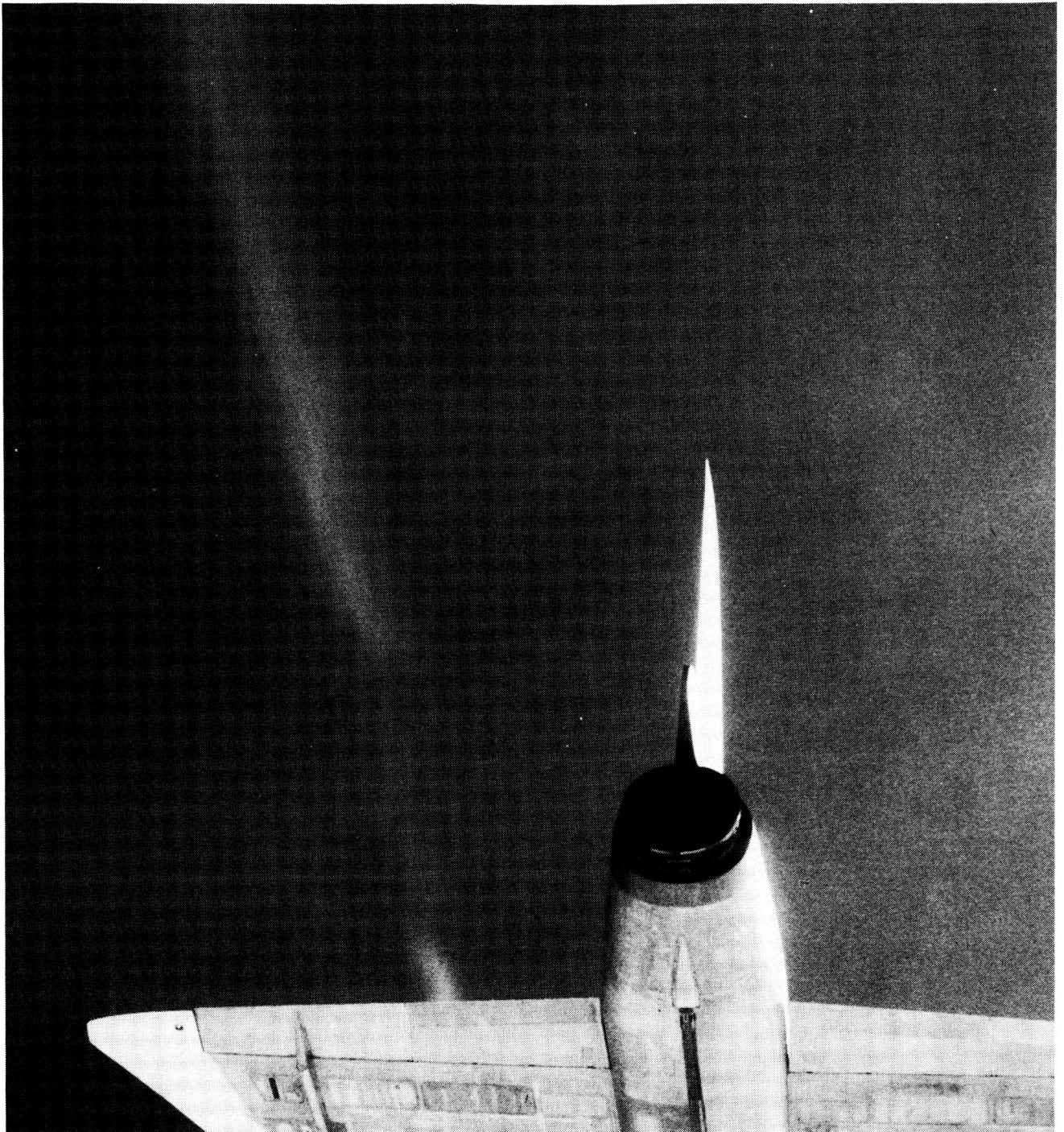


Figure 42. Concluded.

ORIGINAL PAGE IS
OF POOR QUALITY



L-87-588

Figure 43. Persistence of propylene glycol "smoke."



Report Documentation Page

1. Report No. NASA TM-4004	2. Government Accession No.	3. Recipient's Catalog No.	
4. Title and Subtitle Operational Performance of Vapor-Screen Systems for In-Flight Visualization of Leading-Edge Vortices on the F-106B Aircraft		5. Report Date September 1987	6. Performing Organization Code
		8. Performing Organization Report No. L-16306	
7. Author(s) John E. Lamar, Philip W. Brown, Robert A. Bruce, Joseph D. Pride, Jr., Ronald H. Smith, and Thomas D. Johnson, Jr.		10. Work Unit No. 505-61-71-03	
		11. Contract or Grant No.	
9. Performing Organization Name and Address NASA Langley Research Center Hampton, VA 23665-5225		13. Type of Report and Period Covered Technical Memorandum	
		14. Sponsoring Agency Code	
12. Sponsoring Agency Name and Address National Aeronautics and Space Administration Washington, DC 20546-0001		15. Supplementary Notes John E. Lamar, Philip W. Brown, Robert A. Bruce, Joseph D. Pride, Jr., and Ronald H. Smith: Langley Research Center, Hampton, Virginia. Thomas D. Johnson, Jr.: PRC Kentron, Inc., Hampton, Virginia.	
16. Abstract A flight research program was undertaken at the NASA Langley Research to apply the vapor-screen technique, widely used in wind tunnels, to an aircraft. The purpose was to obtain qualitative and quantitative information about near-field vortex flows above the wings of fighter aircraft and ascertain the effects of Reynolds and Mach numbers over an angle-of-attack range. The hardware for the systems required for flight application of the vapor-screen technique was successfully developed and integrated. Details of each system, its operational performance on the F-106B aircraft, and pertinent aircraft and environmental data collected are presented.			
17. Key Words (Suggested by Authors(s)) Vapor screen Vortex flow Flight experiment F-106B aircraft		18. Distribution Statement Unclassified—Unlimited Subject Category 02	
19. Security Classif.(of this report) Unclassified	20. Security Classif.(of this page) Unclassified	21. No. of Pages 81	22. Price A05